



Submitted to: JHEP

CERN-EP-2016-193
31st October 2016

Measurements of $\psi(2S)$ and $X(3872) \rightarrow J/\psi\pi^+\pi^-$ production in pp collisions at $\sqrt{s} = 8$ TeV with the ATLAS detector

The ATLAS Collaboration

Differential cross sections are presented for the prompt and non-prompt production of the hidden-charm states $X(3872)$ and $\psi(2S)$, in the decay mode $J/\psi\pi^+\pi^-$, measured using 11.4 fb^{-1} of pp collisions at $\sqrt{s} = 8$ TeV by the ATLAS detector at the LHC. The ratio of cross-sections $X(3872)/\psi(2S)$ is also given, separately for prompt and non-prompt components, as well as the non-prompt fractions of $X(3872)$ and $\psi(2S)$. Assuming independent single effective lifetimes for non-prompt $X(3872)$ and $\psi(2S)$ production gives $R_B = \frac{\mathcal{B}(B \rightarrow X(3872) + \text{any})\mathcal{B}(X(3872) \rightarrow J/\psi\pi^+\pi^-)}{\mathcal{B}(B \rightarrow \psi(2S) + \text{any})\mathcal{B}(\psi(2S) \rightarrow J/\psi\pi^+\pi^-)} = (3.95 \pm 0.32(\text{stat}) \pm 0.08(\text{sys})) \times 10^{-2}$, while separating short- and long-lived contributions, assuming that the short-lived component is due to B_c decays, gives $R_B = (3.57 \pm 0.33(\text{stat}) \pm 0.11(\text{sys})) \times 10^{-2}$, with the fraction of non-prompt $X(3872)$ produced via B_c decays for $p_T(X(3872)) > 10$ GeV being $(25 \pm 13(\text{stat}) \pm 2(\text{sys}) \pm 5(\text{spin}))\%$. The distributions of the dipion invariant mass in the $X(3872)$ and $\psi(2S)$ decays are also measured and compared to theoretical predictions.

1 Introduction

The hidden-charm state $X(3872)$ was discovered by the Belle Collaboration in 2003 [1] through its decay to $J/\psi\pi^+\pi^-$ in the exclusive decay $B^\pm \rightarrow K^\pm J/\psi\pi^+\pi^-$. Its existence was subsequently confirmed by CDF [2] through its production in $p\bar{p}$ collisions, and its production was also observed by the BaBar [3] and D0 [4] experiments shortly after. CDF determined [5] that the only possible quantum numbers for $X(3872)$ were $J^{PC} = 1^{++}$ and 2^{-+} . At the LHC, the $X(3872)$ was first observed by the LHCb Collaboration [6], which finally confirmed its quantum numbers to be 1^{++} [7]. A particularly interesting aspect of the $X(3872)$ is the closeness of its mass, $3871.69 \pm 0.17\text{MeV}$ [8], to the $D^0\bar{D}^{*0}$ threshold, such that it was hypothesised to be a $D^0\bar{D}^{*0}$ molecule with a very small binding energy [9]. A cross-section measurement of promptly produced $X(3872)$ was performed by CMS [10] as a function of p_T , and showed the non-relativistic QCD (NRQCD) prediction [11] for prompt $X(3872)$ production, assuming a $D^0\bar{D}^{*0}$ molecule, to be too high, although the shape of the p_T dependence was described fairly well. A later interpretation of $X(3872)$ as a mixed $\chi_{c1}(2P)\text{--}D^0\bar{D}^{*0}$ state, where the $X(3872)$ is produced predominantly through its $\chi_{c1}(2P)$ component, was adopted in conjunction with the next-to-leading-order (NLO) NRQCD model and fitted to CMS data, showing good agreement [12].

ATLAS previously observed the $X(3872)$ state while measuring the cross section of prompt and non-prompt $\psi(2S)$ meson production in the $J/\psi\pi^+\pi^-$ decay channel with 2011 data at a centre-of-mass energy $\sqrt{s} = 7\text{TeV}$ [13]. ATLAS later performed cross-section measurements for J/ψ and $\psi(2S)$ decaying through the $\mu^+\mu^-$ channel at $\sqrt{s} = 7\text{TeV}$ and $\sqrt{s} = 8\text{TeV}$ [14].

In this analysis, a measurement of the differential cross sections for the production of $\psi(2S)$ and $X(3872)$ states in the decay channel $J/\psi\pi^+\pi^-$ is performed, using 11.4fb^{-1} of proton–proton collision data collected by the ATLAS experiment at the LHC at $\sqrt{s} = 8\text{TeV}$. The $J/\psi\pi^+\pi^-$ final state allows good invariant mass resolution through the use of a constrained fit, and provides a straightforward way of comparing the production characteristics of $\psi(2S)$ and $X(3872)$ states, which are fairly close in mass. The prompt and non-prompt contributions for $\psi(2S)$ and $X(3872)$ are separated, based on an analysis of the displacement of the production vertex. Non-prompt production fractions for $\psi(2S)$ and $X(3872)$ are measured, and the $X(3872)/\psi(2S)$ production ratios are measured separately for prompt and non-prompt components. The non-prompt results show that while the non-prompt $\psi(2S)$ data is readily described by a traditional single-effective-lifetime fit, there are indications in the non-prompt $X(3872)$ data which suggest introducing a two-lifetime fit with both a short-lived and long-lived component. Results are presented here based on both the single- and two-lifetime fit models. In the two-lifetime case, assuming that the short-lived non-prompt component of $X(3872)$ originates from the decays of B_c mesons, the best-fit fractional contribution of the B_c component is determined. The distributions of the dipion invariant mass in $\psi(2S) \rightarrow J/\psi\pi^+\pi^-$ and $X(3872) \rightarrow J/\psi\pi^+\pi^-$ decays are also measured. Comparisons are made with theoretical models and available experimental data.

2 The ATLAS detector

The ATLAS detector [15] is a cylindrical, forward-backward symmetric, general-purpose particle detector. The innermost part of the inner detector (ID) comprises pixel and silicon microstrip (SCT) tracking technology for high-precision measurements, complemented further outwards by the transition radiation

tracker (TRT). The inner detector spans the pseudorapidity¹ range $|\eta| < 2.5$ and is immersed in a 2 T axial magnetic field. Enclosing the ID and the solenoidal magnet are the electromagnetic and hadronic sampling calorimeters, which provide good containment of the electromagnetic and hadronic showers in order to limit punch-through into the muon spectrometer (MS). Surrounding the calorimeters, the MS covers the rapidity range $|\eta| < 2.7$ and utilises three air-core toroidal magnets, each consisting of eight coils, generating a magnetic field providing 1.5–7.5 T·m of bending power. The MS consists of fast-trigger detectors (thin-gap chambers and resistive plate chambers) as well as precision-measurement detectors (monitored drift tubes and cathode strip chambers).

The ATLAS detector uses a three-level trigger system in order to select 300 Hz of interesting events to be written out from the 20 MHz of proton bunch collisions. This analysis uses a dimuon trigger with the lowest available transverse momentum threshold of 4 GeV for each muon. The level-1 muon trigger finds regions-of-interest (RoIs) by searching for hit coincidences in layers of the muon trigger detectors inside predefined geometrical windows. The software-based two-stage high-level trigger (HLT) is seeded by the level-1 RoIs, and uses more precise MS and ID information to reconstruct the final muon trigger objects with a resolution comparable to the full offline reconstruction.

3 Event selection

Events used in this analysis are triggered by a pair of muons successfully fitted to a common vertex. The data sample corresponds to an integrated luminosity of 11.4 fb^{-1} [16], collected at a proton–proton collision energy $\sqrt{s} = 8\text{TeV}$. Each muon candidate reconstructed offline is required to have good spatial matching to a trigger object, satisfying $\Delta R \equiv \sqrt{(\Delta\eta)^2 + (\Delta\phi)^2} < 0.01$. Events where two oppositely charged muon candidates are reconstructed with pseudorapidity $|\eta^\mu| < 2.3$ and transverse momenta $p_T^\mu > 4\text{GeV}$ are kept for further analysis only if the invariant mass of the dimuon system falls within $\pm 120 \text{ MeV}$ of the mass of the J/ψ meson, $m(J/\psi) = 3096.916 \pm 0.011 \text{ MeV}$ [8].

The two muon tracks are fitted to a common vertex with a loose cut on fit quality, $\chi^2 < 200$. The dimuon invariant mass is then constrained to the J/ψ mass, and the four-track vertex fit of the two muon tracks and pairs of non-muon tracks is performed to find $J/\psi\pi^+\pi^-$ candidates. The two non-muon tracks are assigned pion masses, and are required to have opposite charges and to satisfy the conditions $p_T^\pi > 0.6 \text{ GeV}$, $|\eta^\pi| < 2.4$. Four-track candidates with fit χ^2 probability $P(\chi^2) < 4\%$ are discarded.

Only $J/\psi\pi^+\pi^-$ combinations with rapidity y within the range $|y| < 0.75$ are considered in this analysis, with most of the contributing tracks measured within the barrel part of the detector $|\eta| \lesssim 1$ where the tracking resolution is optimal. Then the transverse momenta of the $J/\psi\pi^+\pi^-$ candidates are required to be within the range $10 \text{ GeV} < p_T < 70 \text{ GeV}$.

Further selection requirements are applied to the remaining $J/\psi\pi^+\pi^-$ combinations:

$$\Delta R(J/\psi, \pi^\pm) < 0.5, \quad Q < 0.3\text{GeV}, \quad (1)$$

¹ ATLAS uses a right-handed coordinate system with its origin at the nominal interaction point (IP) in the centre of the detector and the z -axis along the beam pipe. The x -axis points from the IP to the centre of the LHC ring, and the y -axis points upward. Polar coordinates (r, ϕ) are used in the transverse plane, ϕ being the azimuthal angle around the z -axis. The pseudorapidity η is defined in terms of the polar angle θ as $\eta = -\ln \tan(\theta/2)$, and the transverse momentum p_T is defined as $p_T = p \sin \theta$. The rapidity y is defined as $y = 0.5 \ln[(E + p_z)/(E - p_z)]$, where E and $p_z = p \cos \theta$ refer to energy and longitudinal momentum, respectively.

where $\Delta R(J/\psi, \pi^\pm)$ is the angular distance between the momenta of the dimuon system and each pion candidate, while $Q \equiv m(J/\psi\pi^+\pi^-) - m(J/\psi) - m(\pi^+\pi^-)$. Here $m(J/\psi\pi^+\pi^-)$ and $m(\pi^+\pi^-)$ are the fitted invariant masses of the $\mu^+\mu^-\pi^+\pi^-$ and the dipion system, respectively. These requirements are found to be $> 90\%$ efficient for the signal from $\psi(2S)$ and $X(3872)$ decays, while significantly suppressing the combinatorial background.

The invariant mass distribution of the dimuons contributing to the selected $J/\psi\pi^+\pi^-$ combinations is shown in Figure 1(a) between the dashed vertical lines. The distribution is fitted with the sum of a second-order polynomial background and a double-Gaussian function, which contains about 3.6 M J/ψ candidates. The invariant mass distribution of the $J/\psi\pi^+\pi^-$ candidates selected for further analysis is presented in Figure 1(b). The fitted function is the sum of a fourth-order polynomial background and two double-Gaussian functions. The double-Gaussian functions for $\psi(2S)$ and $X(3872)$ contain about 470 k and 30 k candidates, respectively.

Monte Carlo (MC) simulation is used to study the selection and reconstruction efficiencies. The MC samples with b -hadron production and decays are generated with PYTHIA 6.4 [17], complemented, where necessary, with a dedicated extension for B_c production based on calculations from Refs. [18–21]. The decays of b -hadrons are then simulated with EvtGen [22]. The generated events are passed through a full simulation of the detector using the ATLAS simulation framework [23] based on GEANT4 [24, 25] and processed with the same software as that used for the data.

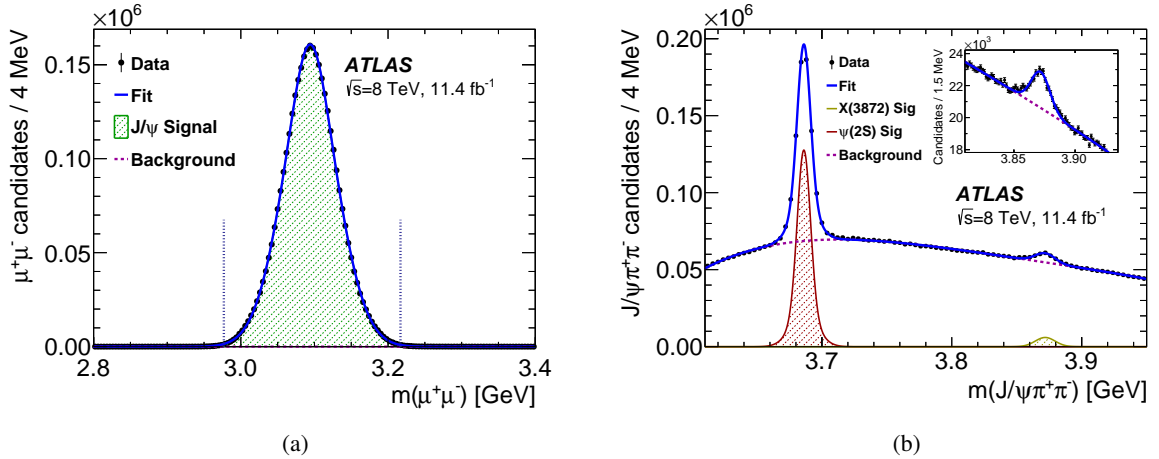


Figure 1: (a) The invariant mass distribution of the J/ψ candidates satisfying all selection criteria except the $\pm 120\text{MeV}$ J/ψ mass window requirement indicated here by the dotted vertical lines. The curve shows the result of a fit with a double-Gaussian function for signal and a second-order polynomial for background. (b) Invariant mass of the selected $J/\psi\pi^+\pi^-$ candidates collected over the full p_T range 10–70 GeV and the rapidity range $|y| < 0.75$ after selection requirements. The curve shows the results of the fit using double-Gaussian functions for the $\psi(2S)$ and $X(3872)$ peaks and a fourth-order polynomial for the background. The $X(3872)$ mass range is highlighted in the inset.

4 Analysis method

The production cross sections of the $\psi(2S)$ and $X(3872)$ states decaying to $J/\psi\pi^+\pi^-$ are measured in five bins of $J/\psi\pi^+\pi^-$ transverse momentum, with bin boundaries (10, 12, 16, 22, 40, 70) GeV.

The selected $J/\psi\pi^+\pi^-$ candidates are weighted in order to correct for signal loss at various stages of the selection process. Following previous similar analyses [13, 14] a per-candidate weight ω was calculated as

$$\omega = \left[\mathcal{A}(p_T, y) \cdot \epsilon_{\text{trig}}(p_T^{\mu^\pm}, \eta^{\mu^\pm}, y^{J/\psi}) \cdot \epsilon^\mu(p_T^{\mu^+}, \eta^{\mu^+}) \cdot \epsilon^\mu(p_T^{\mu^-}, \eta^{\mu^-}) \cdot \epsilon^\pi(p_T^{\pi^+}, \eta^{\pi^+}) \cdot \epsilon^\pi(p_T^{\pi^-}, \eta^{\pi^-}) \right]^{-1}. \quad (2)$$

Here, p_T and y stand for the transverse momentum and rapidity of the $J/\psi\pi^+\pi^-$ candidate, $y^{J/\psi}$ is the rapidity of the J/ψ candidate, while $p_T^{\pi^\pm}$, $p_T^{\mu^\pm}$, η^{π^\pm} and η^{μ^\pm} are transverse momenta and pseudorapidities of the respective pions and muons. The trigger efficiency ϵ_{trig} and the muon reconstruction efficiency ϵ^μ were obtained using data-driven tag-and-probe methods described in Refs. [14, 26]. The pion reconstruction efficiency ϵ^π is obtained through MC simulations using the method described in Ref. [13].

The acceptance $\mathcal{A}(p_T, y)$ is defined as the probability that the muons and pions comprising a $J/\psi\pi^+\pi^-$ candidate with transverse momentum p_T and rapidity y fall within the fiducial limits described in Section 3. The acceptance map is created using generator-level simulation, with small reconstruction-level corrections applied at a later stage (see Ref. [14] for more details). The different quantum numbers of the $\psi(2S)$ and $X(3872)$ ($J^{PC} = 1^{--}$ and 1^{++} , respectively) cause a difference in the expected dependence of the acceptance on the spin-alignments of the two states. The cross sections measured in this paper are obtained assuming no spin-alignment, but appropriate sets of correction factors for a number of extreme spin-alignment scenarios are calculated and presented in Appendix A for each p_T bin, separately for $\psi(2S)$ and $X(3872)$.

The efficiencies of the reconstruction-quality requirements and the background-suppression requirements described in Section 3 are determined using MC simulations, and the corrections are applied in each of the p_T bins, separately for $\psi(2S)$ and $X(3872)$. These efficiencies are found to vary between 84% and 95%. The simulated distributions are reweighted to match the data, and values with and without reweighting are used to estimate systematic uncertainties (see Section 6).

In order to separate prompt production of the $\psi(2S)$ and $X(3872)$ states from the non-prompt production occurring via the decays of long-lived particles such as b -hadrons, the data sample in each p_T bin is further divided into intervals of pseudo-proper lifetime τ , defined as

$$\tau = \frac{L_{xy} m}{c p_T}, \quad (3)$$

where m is the invariant mass, p_T is the transverse momentum and L_{xy} is the transverse decay length of the $J/\psi\pi^+\pi^-$ candidate. L_{xy} is defined as

$$L_{xy} = \frac{\vec{L} \cdot \vec{p}_T}{p_T}, \quad (4)$$

where \vec{L} is the vector pointing from the primary pp collision vertex to the $J/\psi\pi^+\pi^-$ vertex, while \vec{p}_T is the transverse momentum vector of the $J/\psi\pi^+\pi^-$ system. The coordinates of the primary vertices (PV) are obtained from charged-particle tracks with $p_T > 0.4$ GeV not used in the decay vertices, and are transversely constrained to the luminous region of the colliding beams. The matching of a $J/\psi\pi^+\pi^-$

candidate to a PV is made by finding the one with the smallest three-dimensional impact parameter, calculated between the $J/\psi\pi^+\pi^-$ momentum and each PV.

Based on an analysis of the lifetime resolution and lifetime dependence of the signal, four lifetime intervals were defined:

$$w_0 : -0.3 \text{ ps} < \tau(J/\psi\pi\pi) < 0.025 \text{ ps},$$

$$w_1 : 0.025 \text{ ps} < \tau(J/\psi\pi\pi) < 0.3 \text{ ps},$$

$$w_2 : 0.3 \text{ ps} < \tau(J/\psi\pi\pi) < 1.5 \text{ ps},$$

$$w_3 : 1.5 \text{ ps} < \tau(J/\psi\pi\pi) < 15.0 \text{ ps}.$$

In each of these intervals, and for each p_T bin, the invariant mass distribution of the $J/\psi\pi^+\pi^-$ system is built using fully corrected weighted events. These distributions are shown in Figure 2 for representative p_T bins.

In order to determine the yields of the $\psi(2S)$ and $X(3872)$ signals, the distributions are fitted in each lifetime interval to the function:

$$f(m) = Y^\psi \left(f_1 G_1^\psi(m) + (1 - f_1) G_2^\psi(m) \right) + Y^X \left(f_1 G_1^X(m) + (1 - f_1) G_2^X(m) \right) + N(m - m_{\text{th}})^{p_1} e^{p_2(m - m_{\text{th}})} P(m - m_{\text{th}}), \quad (5)$$

where the threshold mass $m_{\text{th}} = m_{J/\psi} + 2m_\pi = 3376.06$ MeV. The $\psi(2S)$ and $X(3872)$ signal yields Y^ψ and Y^X , coefficients of the second-order polynomial P , parameters p_1 and p_2 , and the normalisation of the background term N , are determined from the fits. Signal peaks for $\psi(2S)$ and $X(3872)$ are described by normalised double-Gaussian functions with common means: $G_1^\psi(m)$ and $G_1^X(m)$ are the narrower Gaussian functions with respective widths σ_ψ and σ_X , while $G_2^\psi(m)$ and $G_2^X(m)$ are wider Gaussian functions with widths $2\sigma_\psi$ and $2\sigma_X$. The fraction of the narrower Gaussian function f_1 is assumed to be the same for $\psi(2S)$ and $X(3872)$, while the widths σ_ψ and σ_X are related by $\sigma_X = \kappa\sigma_\psi$. The parameters f_1 and κ are fixed for the main fits to the values $f_1 = 0.76 \pm 0.04$, $\kappa = 1.52 \pm 0.05$ as determined from a fit applied in the range $16 \text{ GeV} < p_T < 70 \text{ GeV}$, which offers a better signal-to-background ratio than the full range, and is varied within these errors in the systematic uncertainty studies. The fit quality is found to be good throughout the range of transverse momenta and lifetimes. The yields extracted from the fits are shown in Table 1 for the $\psi(2S)$ and Table 2 for the $X(3872)$.

τ window	Corrected yields of $\psi(2S)$ [$\times 10^5$] vs. p_T [GeV]				
	10–12	12–16	16–22	22–40	40–70
w_0	17.48 ± 0.36	11.03 ± 0.11	3.53 ± 0.03	1.14 ± 0.01	0.078 ± 0.004
w_1	14.07 ± 0.37	9.04 ± 0.10	2.94 ± 0.03	1.01 ± 0.01	0.071 ± 0.003
w_2	9.13 ± 0.29	7.04 ± 0.09	2.97 ± 0.03	1.27 ± 0.01	0.104 ± 0.004
w_3	6.74 ± 0.16	5.21 ± 0.06	2.22 ± 0.02	0.94 ± 0.01	0.081 ± 0.003

Table 1: Fitted yields of $\psi(2S)$ in bins of pseudo-proper lifetime and p_T . Uncertainties are statistical only.

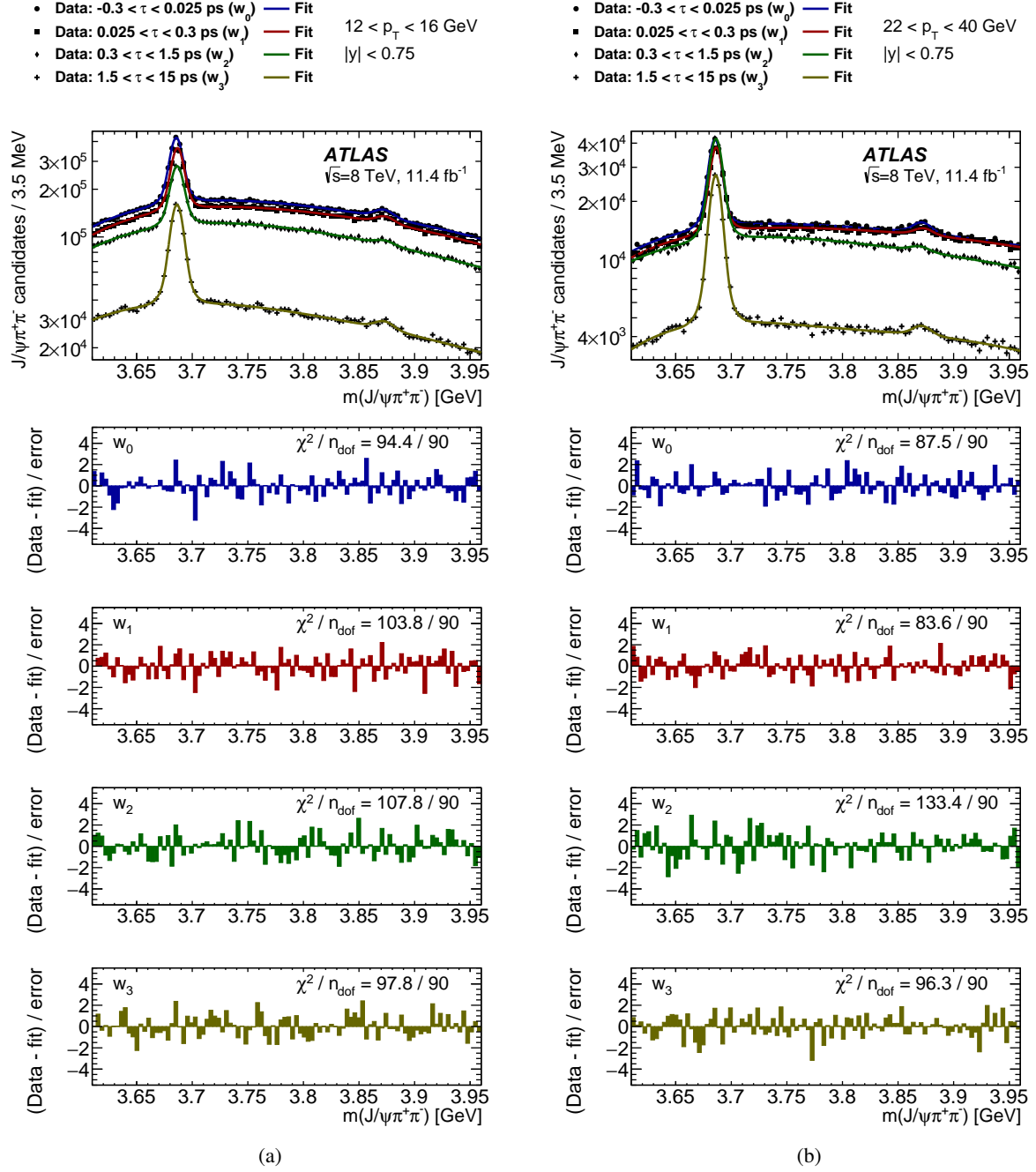


Figure 2: The invariant mass spectra of the $J/\psi\pi^+\pi^-$ candidates to extract $\psi(2S)$ and $X(3872)$ signal for each pseudo-proper lifetime window in the p_T bin (a) [12, 16]GeV and (b) [22, 40]GeV. Shown underneath the fits are the corresponding pull distributions, with respective values of χ^2 per degree of freedom for each fit.

τ window	Corrected yields of $X(3872)$ [$\times 10^4$] vs. p_T [GeV]				
	10–12	12–16	16–22	22–40	40–70
w_0	10.8 ± 2.3	10.55 ± 0.76	3.53 ± 0.26	1.19 ± 0.11	0.093 ± 0.030
w_1	9.3 ± 2.7	8.21 ± 0.71	2.60 ± 0.24	0.72 ± 0.11	0.039 ± 0.023
w_2	4.1 ± 1.7	3.83 ± 0.63	1.29 ± 0.21	0.45 ± 0.10	0.036 ± 0.023
w_3	2.06 ± 0.81	2.09 ± 0.34	0.98 ± 0.13	0.30 ± 0.06	0.020 ± 0.014

Table 2: Fitted yields of $X(3872)$ in bins of pseudo-proper lifetime and p_T . Uncertainties are statistical only.

Once the corrected yields Y^ψ and Y^X are determined in each p_T bin, the double differential cross sections (times the product of the relevant branching fractions) can be calculated:

$$\mathcal{B}(i \rightarrow J/\psi \pi^+ \pi^-) \mathcal{B}(J/\psi \rightarrow \mu^+ \mu^-) \frac{d^2 \sigma(i)}{dp_T dy} = \frac{Y^i}{\Delta p_T \Delta y \int \mathcal{L} dt}, \quad (6)$$

where i stands for $\psi(2S)$ or $X(3872)$, $\int \mathcal{L} dt$ is the integrated luminosity, while Δp_T and Δy are widths of the relevant transverse momentum and rapidity bins, with $\Delta y = 1.5$. $\mathcal{B}(i \rightarrow J/\psi \pi^+ \pi^-)$ and $\mathcal{B}(J/\psi \rightarrow \mu^+ \mu^-)$ are the branching fractions of these respective decays.

5 Lifetime fits

The probability density function (PDF) describing the dependence of $\psi(2S)$ and $X(3872)$ signal yields on the pseudo-proper lifetime τ is a superposition of prompt (P) and non-prompt (NP) components:

$$F^i(\tau) = (1 - f_{\text{NP}}^i) F_{\text{P}}^i(\tau) + f_{\text{NP}}^i F_{\text{NP}}^i(\tau), \quad (7)$$

where f_{NP} is the non-prompt fraction, while i stands for either $\psi(2S)$ or $X(3872)$. The prompt components of $\psi(2S)$ and $X(3872)$ production should not have any observable decay length, and hence $F_{\text{P}}(\tau)$ is effectively described by the lifetime resolution function $F_{\text{res}}(\tau)$, assumed to be the same for $\psi(2S)$ and $X(3872)$ signals. This was verified with simulated data samples. The resolution function $F_{\text{res}}(\tau)$ is parameterised as a weighted sum of three normalised Gaussian functions with a common mean, with respective width parameters $\sigma_1 = \sigma_\tau$, $\sigma_2 = 2\sigma_\tau$ and $\sigma_3 = 4\sigma_\tau$. The resolution parameter σ_τ and the relative weights of the three Gaussian functions are determined separately for each analysis p_T bin, using two-dimensional mass–lifetime unbinned maximum-likelihood fits on the subset of data which contains a narrow range of masses around the $\psi(2S)$ peak. The fitted values for σ_τ are within the range of 32–52 fs, with the weight of the narrowest Gaussian function steadily increasing with p_T from 6% to about 50%.

The simplest description of the non-prompt components of the signal PDF is given by a single one-sided exponential smeared with the resolution function, with the effective lifetime τ_{eff} determined from the fit. This model, referred to as a ‘single-lifetime fit’, is applied to the $\psi(2S)$ and $X(3872)$ yields from Tables 1 and 2, and the results of the corresponding binned minimum- χ^2 fits are shown in Figure 3.

Figure 3(a) shows the effective pseudo-proper lifetimes τ_{eff} for non-prompt $\psi(2S)$ and $X(3872)$ signals in bins of p_T (see also Table 3). While for $\psi(2S)$ the fitted values of τ_{eff} are measured to be around 1.45 ps

p_T bin [GeV]	$\tau_{\text{eff}}(\psi(2S))$ [ps]	$\tau_{\text{eff}}(X(3872))$ [ps]
10–12	1.44 ± 0.04	1.12 ± 0.40
12–16	1.43 ± 0.02	1.18 ± 0.17
16–22	1.43 ± 0.01	1.45 ± 0.21
22–40	1.41 ± 0.01	1.37 ± 0.26
40–70	1.44 ± 0.04	1.27 ± 0.62

Table 3: Effective pseudo-proper lifetimes for non-prompt $\psi(2S)$ and $X(3872)$ obtained with the single-lifetime fit model.

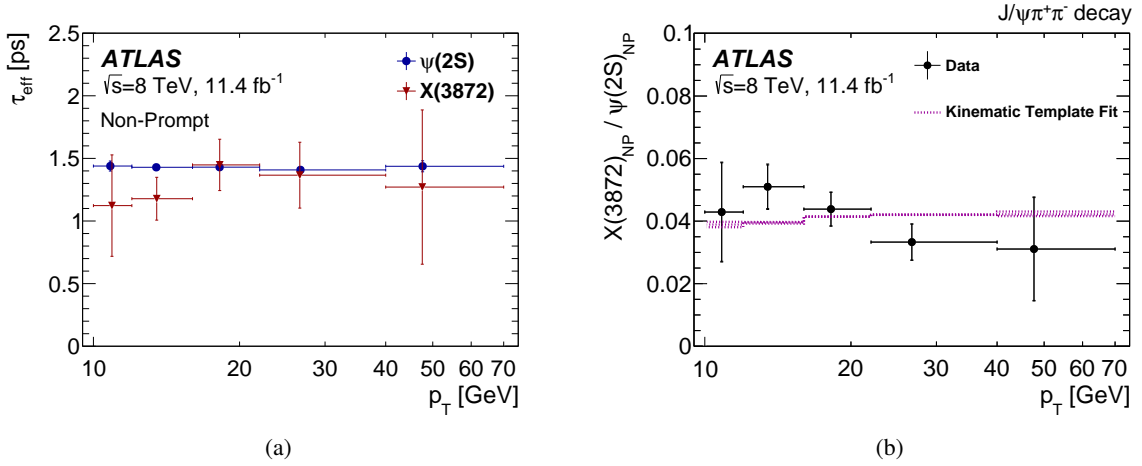


Figure 3: (a) Measured effective pseudo-proper lifetimes for non-prompt $X(3872)$ and $\psi(2S)$. (b) Ratio of non-prompt production cross sections times branching fractions, $X(3872)/\psi(2S)$, in the single-lifetime fit model. The measured distribution is fitted to the kinematic template described in the text.

in all p_T bins, the signal from $X(3872)$ at low p_T tends to have shorter lifetimes, possibly hinting at a different production mechanism at low p_T .

In Figure 3(b) the ratio of non-prompt production cross sections of $X(3872)$ and $\psi(2S)$, times respective branching fractions, for the single-lifetime fit is plotted as a function of transverse momentum. The measured distribution is compared to the kinematic template, which is calculated as a ratio of the simulated p_T distributions of non-prompt $X(3872)$ and non-prompt $\psi(2S)$, assuming that the same mix of the parent b -hadrons contributes to both signals. The shape of the template reflects the kinematics of the decay of a b -hadron into $\psi(2S)$ or $X(3872)$, with the width of the band showing the range of variation for extreme values of the invariant mass of the recoiling hadronic system. A fit of the measured ratio to this template allows determination of the ratio of the average branching fractions:

$$R_B^{\text{IL}} = \frac{\mathcal{B}(B \rightarrow X(3872) + \text{any})\mathcal{B}(X(3872) \rightarrow J/\psi\pi^+\pi^-)}{\mathcal{B}(B \rightarrow \psi(2S) + \text{any})\mathcal{B}(\psi(2S) \rightarrow J/\psi\pi^+\pi^-)} = (3.95 \pm 0.32(\text{stat}) \pm 0.08(\text{sys})) \times 10^{-2}, \quad (8)$$

where the systematic uncertainty reflects the variation of the kinematic template. The χ^2 of the fit is 5.4 for the four degrees of freedom (dof).

An alternative lifetime model, also implemented in this analysis, allows for two non-prompt contributions with distinctly different effective lifetimes (the ‘two-lifetime fit’). The statistical power of the data sample is insufficient for determining two free lifetimes, especially in the case of $X(3872)$ production, so in this fit model the non-prompt PDFs are represented in each p_T bin by a sum of two contributions with different fixed lifetimes, and a relative weight determined by the fit:

$$F_{\text{NP}}^i(\tau) = (1 - f_{\text{SL}}^i)F_{\text{LL}}(\tau) + f_{\text{SL}}^i F_{\text{SL}}(\tau). \quad (9)$$

Here, the labels SL and LL refer to short-lived and long-lived non-prompt components, respectively, and f_{SL}^i are the short-lived non-prompt fractions for $i = \psi(2S), X(3872)$. The PDFs $F_{\text{SL}}(\tau)$ and $F_{\text{LL}}(\tau)$ are parameterised as single one-sided exponential functions with fixed lifetimes, smeared with the lifetime resolution function $F_{\text{res}}(\tau)$ described above. Any long-lived part of the non-prompt contribution is assumed to originate from the usual mix of B^\pm, B^0, B_s mesons and b -baryons, while any short-lived part would be due to the contribution of B_c^\pm mesons.

Simulations show that the observed effective pseudo-proper lifetime of $\psi(2S)$ or $X(3872)$ from B_c decays depends on the invariant mass of the hadronic system recoiling from the hidden-charm state. Within the kinematic range of this measurement, it varies from about 0.3 ps for small masses of the recoiling system to about 0.5 ps for the largest ones. The majority of the decays are expected to have masses of the recoiling system between these values, therefore τ_{SL} is taken as the mean of the two extremes, 0.40 ± 0.05 ps.

The effective pseudo-proper lifetime of the long-lived component, τ_{LL} , is determined from the two-lifetime test fits to the $\psi(2S)$ mass range, with τ_{LL} free and allowing for an unknown contribution of a short-lived component with lifetime τ_{SL} . Across the p_T bins, τ_{LL} is found to be within the range 1.45 ± 0.05 ps. The effective pseudo-proper lifetimes τ_{LL} and τ_{SL} are fixed to the above values for the main fits, and are varied within the quoted errors during systematic uncertainty studies.

Figure 4 shows the p_T dependence of the ratio of $X(3872)$ to $\psi(2S)$ cross sections (times respective branching fractions), separately for prompt and non-prompt production contributions. The non-prompt production cross section of $X(3872)$ is further split into short-lived and long-lived components. The short-lived contribution to non-prompt $\psi(2S)$ production is found to be not significant (see Table 6 below). The measured ratio of long-lived $X(3872)$ to long-lived $\psi(2S)$, shown in Figure 4(b) with blue triangles, is fitted with the MC kinematic template described before to obtain

$$R_B^{2\text{L}} = \frac{\mathcal{B}(B \rightarrow X(3872) + \text{any})\mathcal{B}(X(3872) \rightarrow J/\psi\pi^+\pi^-)}{\mathcal{B}(B \rightarrow \psi(2S) + \text{any})\mathcal{B}(\psi(2S) \rightarrow J/\psi\pi^+\pi^-)} = (3.57 \pm 0.33(\text{stat}) \pm 0.11(\text{sys})) \times 10^{-2}, \quad (10)$$

with $\chi^2/\text{dof} = 2.3/4$. This value of R_B is somewhat lower than the corresponding result in Equation (8) obtained from the same data with the single-lifetime fit model. Either is significantly smaller than the value 0.18 ± 0.08 obtained by using the estimate for the numerator, $(1.9 \pm 0.8) \times 10^{-4}$ [11], obtained from the Tevatron data, and the world average values for the branching fractions in the denominator: $\mathcal{B}(B \rightarrow \psi(2S)) = (3.07 \pm 0.21) \times 10^{-3}$, $\mathcal{B}(\psi(2S) \rightarrow J/\psi\pi^+\pi^-) = (34.46 \pm 0.30)\%$.

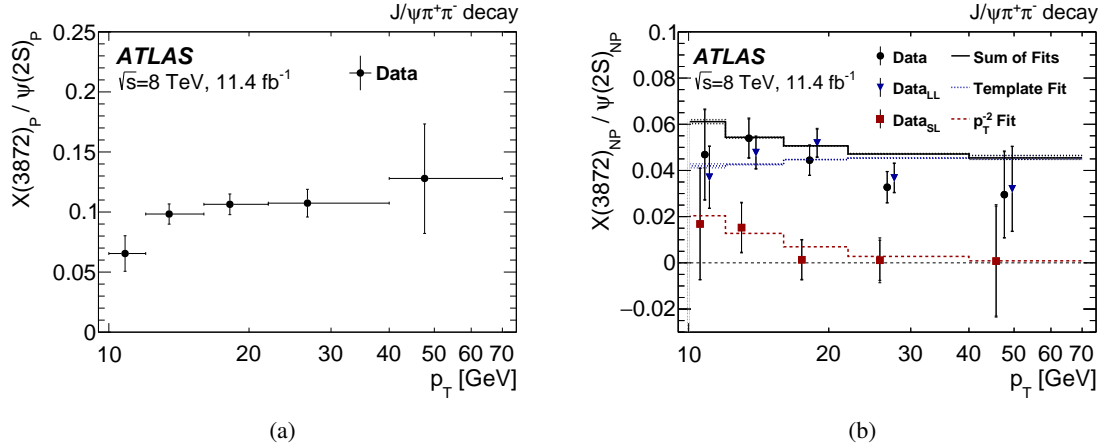


Figure 4: Ratio of cross sections times branching fractions, $X(3872)/\psi(2S)$, for (a) prompt and (b) non-prompt production, in the two-lifetime fit model. In (b), the total non-prompt ratio (black circles) is separated into short-lived (red squares) and long-lived (blue triangles) components for the $X(3872)$, shown with respective fits described in the text. The data points are slightly shifted horizontally for visibility.

Production of B_c mesons in high-energy hadronic collisions at low transverse momentum is expected to be dominated by non-fragmentation processes [27]. These processes are expected to have p_T dependence $\propto p_T^{-2}$ relative to the fragmentation contribution, while it is the fragmentation contribution which dominates the production of long-lived b -hadrons [28].

So the ratio of short-lived non-prompt $X(3872)$ to non-prompt $\psi(2S)$, shown in Figure 4(b) with red squares, is fitted with a function a/p_T^2 to find $a = 2.04 \pm 1.43(\text{stat}) \pm 0.34(\text{sys})\text{GeV}^2$, with $\chi^2/\text{dof} = 0.43/4$. This value of a , and the measured non-prompt yields of $X(3872)$ and $\psi(2S)$ states, are used to determine the fraction of non-prompt $X(3872)$ from short-lived sources, integrated over the p_T range ($p_T > 10\text{GeV}$) covered in this measurement, giving:

$$\frac{\sigma(pp \rightarrow B_c)\mathcal{B}(B_c \rightarrow X(3872))}{\sigma(pp \rightarrow \text{non-prompt } X(3872))} = (25 \pm 13(\text{stat}) \pm 2(\text{sys}) \pm 5(\text{spin}))\%, \quad (11)$$

where the last uncertainty comes from varying the spin-alignment of $X(3872)$ over the extreme scenarios discussed in Appendix A. Since B_c production is only small fraction of the inclusive beauty production, this value of the ratio would mean that the production of $X(3872)$ in B_c decays is strongly enhanced compared to its production in the decays of other b -hadrons.

The two-lifetime fits are used for $\psi(2S)$ and $X(3872)$ to obtain all subsequent results in this paper, unless specified otherwise, with the relatively small differences between the results of the single-lifetime and two-lifetime fits being highlighted alongside all other sources of systematic uncertainty.

6 Systematic uncertainties

The sources of various uncertainties and their smallest (Min), median (Med) and largest (Max) values across the p_T bins are summarised in Table 4 for the differential cross sections of $X(3872)$ and $\psi(2S)$ states, and in Table 5 for the measured fractions.

Source of uncertainty	$\psi(2S)$ [%]			$X(3872)$ [%]		
	Min	Med	Max	Min	Med	Max
Statistical	0.9	1.4	5.4	7.3	9.9	63
Trigger eff.	1.0	1.3	2.5	1.1	1.3	2.6
Muon tracking	2.0	2.0	2.0	2.0	2.0	2.0
Muon reconstruction eff.	0.2	0.2	0.3	0.2	0.2	0.4
Pion reconstruction eff.	2.5	2.5	2.5	2.5	2.5	2.5
Bkgd suppression req.	0.8	0.8	3.0	2.0	3.0	6.0
Mass fit model variation	0.6	0.8	1.2	0.9	1.6	2.6
Short-lifetime variation	0.1	0.2	0.3	0.2	0.7	1.7
Long-lifetime variation	0.6	1.0	1.2	0.3	0.6	0.9
Lifetime resolution model	0.4	1.5	4.0	0.6	2.6	3.4
Total systematic	3.5	3.6	6.4	4.1	4.9	7.5
(2L-fit – 1L-fit) / 2L-fit (prompt)	–0.1	–0.4	–0.6	–0.3	–0.5	–3.4
(2L-fit – 1L-fit) / 2L-fit (non-prompt)	+0.1	+0.4	+0.7	+0.1	+1.4	+9.8

Table 4: Summary of relative uncertainties for the $\psi(2S)$ and $X(3872)$ cross-section measurements showing the smallest (Min), median (Med) and largest (Max) values across the p_T bins. The last two rows are described in the text. The uncertainty of the integrated luminosity (1.9%) is not included.

Uncertainties in the trigger efficiency, and in the muon and pion reconstruction efficiencies are determined using the procedures adopted in Ref. [13]. Additional uncertainty of $\pm 2\%$ [14] is assigned to the tracking efficiency of the two muons within the ID, primarily due to its dependence on the total number of pp collisions per event. The uncertainties in matching generator-level particles to reconstruction-level particles, and in the detector material simulation within the barrel part of the inner detector are found to be the main contributions to the systematic uncertainty of the pion reconstruction efficiency, estimated to be $\pm 2.5\%$. Such efficiency uncertainties largely cancel in the various non-prompt fractions (Table 5).

The uncertainties in the efficiency of the background suppression requirements (see Section 4), obtained by combining MC statistical errors and systematic errors in quadrature, are in the range 1%–6%. The uncertainties in the mass fits are estimated by varying the values of parameters that were fixed during the main fit, and by increasing the order of the polynomial P in the background parameterisation (see Equation (5)). Similarly, the systematic uncertainties of the lifetime fits are determined by varying the values of the fixed lifetimes and the parameters of the lifetime resolution function within their predetermined ranges.

The statistical and individual systematic uncertainties are added in quadrature to form the total error shown in the tables. In general, the results for $X(3872)$ are dominated by statistical errors, while for $\psi(2S)$ statistical and systematic uncertainties are of comparable size.

The last rows in Tables 4 and 5 show the relative differences between the values obtained using the single- and two-lifetime fits, labelled as ‘1L-fit’ and ‘2L-fit’, respectively. For the quantities listed in Tables 4 and 5, these differences were found to be generally fairly small, compared to the combined systematic uncertainty from other sources.

Source of uncertainty	Absolute uncertainty [%]								
	f_{NP}^{ψ}			f_{NP}^X			f_{SL}^X		
	Min	Med	Max	Min	Med	Max	Min	Med	Max
Statistical	0.4	0.5	1.4	4.2	5.8	17.8	16.4	25.8	63
Trigger eff.	0.1	0.1	0.3	0.1	0.1	0.4	0.0	0.1	0.1
Muon tracking eff.	0.0	0.0	0.0	0.0	0.0	0.0	0.0	0.0	0.0
Muon reconstruction eff.	0.0	0.0	0.1	0.0	0.0	0.1	0.0	0.0	0.1
Pion reconstruction eff.	0.4	0.5	0.7	0.3	0.3	0.4	0.0	0.3	0.4
Bkgd suppression req.	0.8	1.1	1.4	0.6	0.7	0.7	0.1	0.1	0.7
Mass fit model variation	0.1	0.1	0.2	0.2	0.6	1.8	1.0	1.3	2.4
Lifetime resolution variation	0.2	0.7	1.7	0.4	1.0	2.9	1.8	3.6	12.1
Short-lifetime variation	0.0	0.1	0.1	0.1	0.4	0.8	0.3	0.7	2.8
Long-lifetime variation	0.3	0.4	0.4	0.2	0.2	0.3	3.3	4.0	4.4
Total systematic	1.3	1.5	2.4	1.0	1.4	3.6	4.1	4.9	13.5
(2L-fit – 1L-fit) / 2L-fit	+0.4	+0.6	+0.9	+0.9	+3.1	+9.1	–	–	–

Table 5: Summary of uncertainties for $\psi(2S)$ and $X(3872)$ non-prompt fractions, and short-lived non-prompt fraction for $X(3872)$ production, showing the smallest (Min), median (Med) and largest (Max) values across the p_T bins. The last row is described in the text.

7 Results and discussion

The measured differential cross section (times the product of the relevant branching fractions) for prompt production of $\psi(2S)$ is shown in Figure 5(a). It is described fairly well by the NLO NRQCD model [29] with long-distance matrix elements (LDMEs) determined from the Tevatron data, although some overestimation is observed at the highest p_T values. The k_T factorisation model [30], which includes the colour-octet (CO) contributions tuned to 7TeV CMS data [31] in addition to colour-singlet (CS) production, describes ATLAS data fairly well, with a slight underestimation at higher p_T . The NNLO* Colour-Singlet Model (CSM) predictions [32] are close to the data points at low p_T , but significantly underestimate them at higher p_T values. The measured differential cross section for non-prompt $\psi(2S)$ production is presented in Figure 5(b), compared with the predictions of the FONLL calculation [28]. The calculation describes the data well over the whole range of transverse momenta.

Similarly, the differential cross section for prompt production of $X(3872)$ is shown in Figure 6(a). It is described within the theoretical uncertainty by the prediction of the NRQCD model which, in this case, considers $X(3872)$ to be a mixture of $\chi_{c1}(2P)$ and a $D^0\bar{D}^{*0}$ molecular state [12], with the production being dominated by the $\chi_{c1}(2P)$ component and the normalisation fixed through the fit to CMS data [10]. The measured differential cross section for non-prompt production of $X(3872)$ is shown in Figure 6(b). This is compared to a calculation based on the FONLL model prediction for $\psi(2S)$, recalculated for $X(3872)$ using the kinematic template for the non-prompt $X(3872)/\psi(2S)$ ratio shown in Figure 3(b) and the effective value of the product of the branching fractions $\mathcal{B}(B \rightarrow X(3872))\mathcal{B}(X(3872) \rightarrow J/\psi\pi^+\pi^-) = (1.9 \pm 0.8) \times 10^{-4}$ estimated in Ref. [11] based on the Tevatron data [33]. This calculation overestimates the data by a factor increasing with p_T from about four to about eight over the p_T range of this measurement.

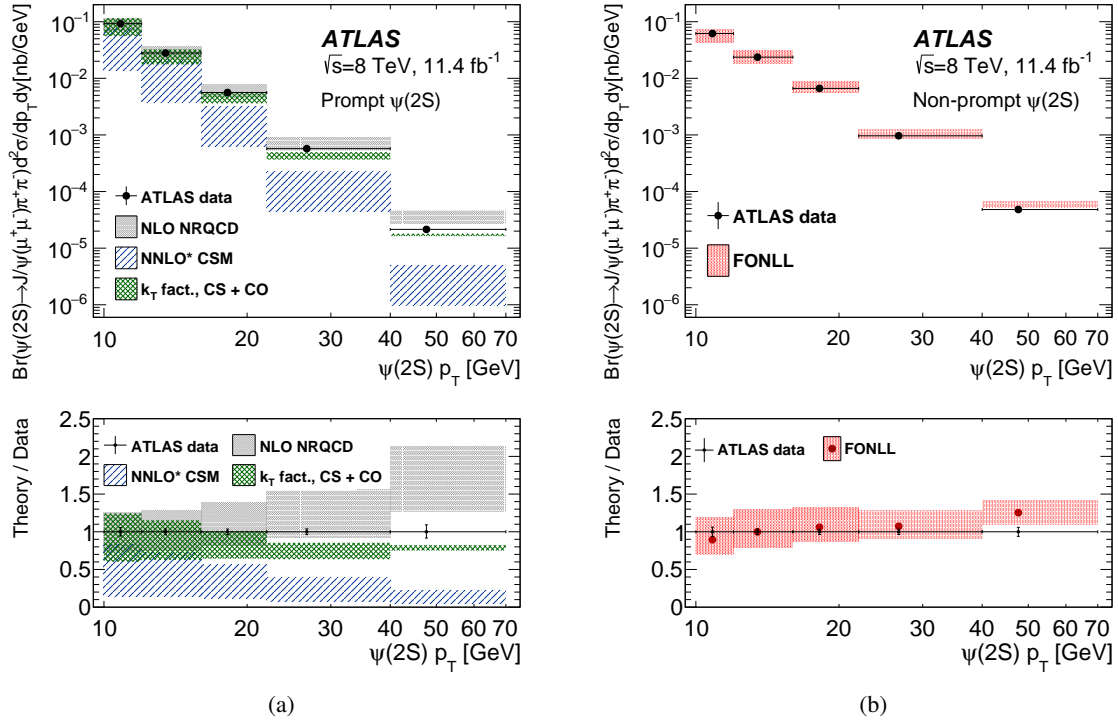


Figure 5: Measured cross section times branching fractions as a function of p_T for (a) prompt $\psi(2S)$ production compared to NLO NRQCD [29], the k_T factorisation model [30] and the NNLO* CSM [32], and (b) non-prompt $\psi(2S)$ production compared to FONLL [28] predictions.

The non-prompt fractions of $\psi(2S)$ and $X(3872)$ production are shown in Figure 7. In the case of $\psi(2S)$, f_{NP} increases with p_T , in good agreement with measurements obtained with dimuon decays of $\psi(2S)$ from ATLAS [14] and CMS [34]. The non-prompt fraction of $X(3872)$ shows no sizeable dependence on p_T . This measurement agrees within errors with the CMS result obtained at $\sqrt{s} = 7$ TeV [10].

The numerical values of all cross sections and fractions shown in Figures 4–7 are presented in Table 6.

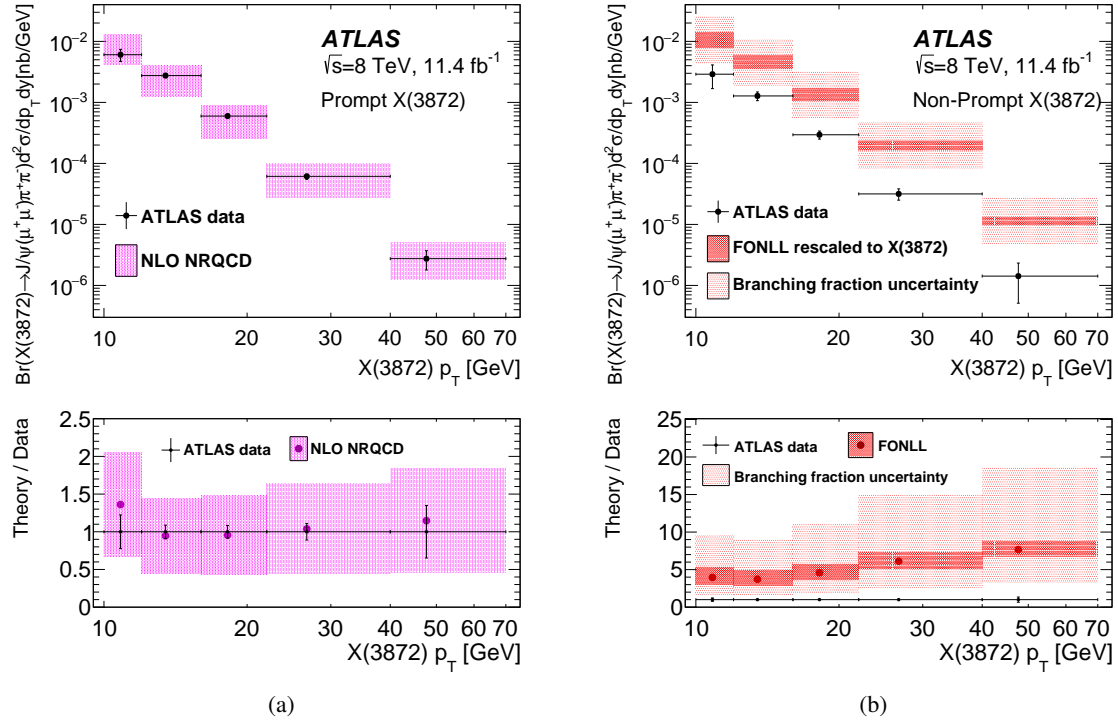


Figure 6: Measured cross section times branching fractions as a function of p_T for (a) prompt $X(3872)$ compared to NLO NRQCD predictions with the $X(3872)$ modelled as a mixture of $\chi_{c1}(2P)$ and a $D^0\bar{D}^{*0}$ molecular state [12], and (b) non-prompt $X(3872)$ compared to the FONLL [28] model prediction, recalculated using the branching fraction estimate from Ref. [11] as described in the text.

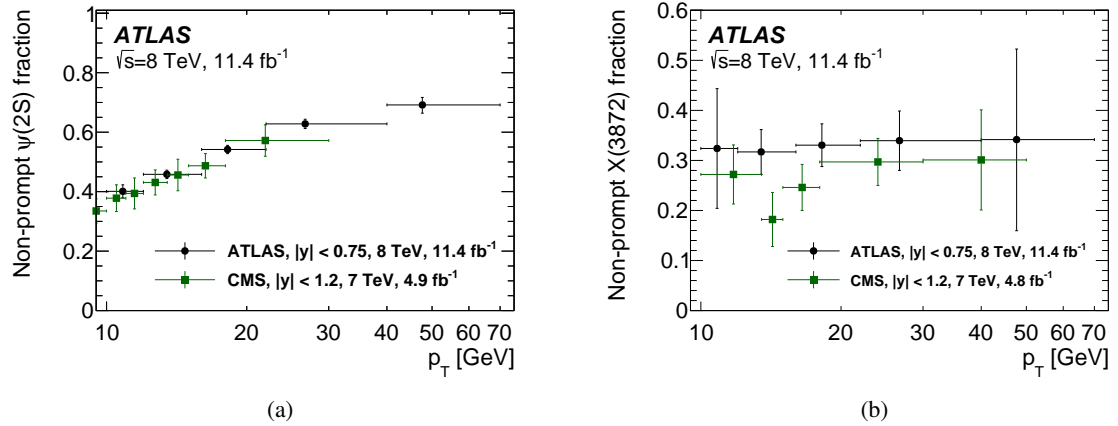


Figure 7: Measured non-prompt fractions for (a) $\psi(2S)$ and (b) $X(3872)$ production, compared to CMS results at $\sqrt{s} = 7$ TeV. The blue circles are the results shown in this paper, while the green squares show CMS results [10, 34].

	p_T range [GeV]			
	10–12	12–16	16–22	22–40
	Cross sections times branching fractions [pb / GeV]			
$\psi(2S)_P$	$92.4 \pm 1.9 \pm 4.8$	$27.97 \pm 0.27 \pm 1.02$	$5.61 \pm 0.06 \pm 0.19$	$0.57 \pm 0.01 \pm 0.02$
$\psi(2S)_{NP}$	$61.9 \pm 1.9 \pm 3.4$	$23.66 \pm 0.27 \pm 0.85$	$6.63 \pm 0.06 \pm 0.22$	$0.97 \pm 0.01 \pm 0.03$
$\psi(2S)_{NP}^{LL}$	$60.8 \pm 1.6 \pm 4.0$	$23.09 \pm 0.27 \pm 1.46$	$6.53 \pm 0.06 \pm 0.41$	$0.93 \pm 0.01 \pm 0.06$
$\psi(2S)_{NP}^{SL}$	$1.1 \pm 2.4 \pm 3.9$	$0.56 \pm 0.37 \pm 1.14$	$0.11 \pm 0.08 \pm 0.29$	$0.04 \pm 0.01 \pm 0.04$
$X(3872)_P$	$6.05 \pm 1.30 \pm 0.38$	$2.75 \pm 0.20 \pm 0.13$	$0.60 \pm 0.04 \pm 0.02$	$0.06 \pm 0.01 \pm 0.00$
$X(3872)_{NP}$	$2.90 \pm 1.20 \pm 0.21$	$1.28 \pm 0.20 \pm 0.07$	$0.29 \pm 0.04 \pm 0.01$	$0.03 \pm 0.01 \pm 0.00$
$X(3872)_{NP}^{LL}$	$1.87 \pm 0.82 \pm 0.14$	$0.92 \pm 0.16 \pm 0.06$	$0.29 \pm 0.04 \pm 0.02$	$0.03 \pm 0.01 \pm 0.00$
$X(3872)_{NP}^{SL}$	$1.02 \pm 1.49 \pm 0.20$	$0.35 \pm 0.25 \pm 0.06$	$0.01 \pm 0.06 \pm 0.02$	$0.00 \pm 0.01 \pm 0.00$
	Fractions			
$F_{NP}^{\psi(2S)}$	$0.40 \pm 0.01 \pm 0.02$	$0.46 \pm 0.00 \pm 0.01$	$0.54 \pm 0.00 \pm 0.01$	$0.63 \pm 0.00 \pm 0.01$
$F_{SL}^{\psi(2S)}$	$0.02 \pm 0.04 \pm 0.06$	$0.02 \pm 0.02 \pm 0.05$	$0.02 \pm 0.01 \pm 0.04$	$0.04 \pm 0.01 \pm 0.04$
$F_{NP}^{X(3872)}$	$0.32 \pm 0.12 \pm 0.02$	$0.32 \pm 0.04 \pm 0.01$	$0.33 \pm 0.04 \pm 0.01$	$0.34 \pm 0.06 \pm 0.01$
$F_{SL}^{X(3872)}$	$0.35 \pm 0.39 \pm 0.05$	$0.28 \pm 0.16 \pm 0.04$	$0.03 \pm 0.19 \pm 0.05$	$0.03 \pm 0.26 \pm 0.05$
	Ratios			
$X(3872)_P/\psi(2S)_P$	$0.065 \pm 0.014 \pm 0.004$	$0.098 \pm 0.007 \pm 0.004$	$0.106 \pm 0.008 \pm 0.004$	$0.107 \pm 0.011 \pm 0.004$
$X(3872)_{NP}/\psi(2S)_{NP}$	$0.047 \pm 0.019 \pm 0.004$	$0.054 \pm 0.008 \pm 0.003$	$0.044 \pm 0.006 \pm 0.002$	$0.033 \pm 0.007 \pm 0.001$
$X(3872)_{NP}^{LL}/\psi(2S)_{NP}^{LL}$	$0.031 \pm 0.014 \pm 0.002$	$0.040 \pm 0.007 \pm 0.003$	$0.044 \pm 0.006 \pm 0.003$	$0.033 \pm 0.006 \pm 0.002$
$X(3872)_{NP}^{SL}/\psi(2S)_{NP}^{SL}$	$0.016 \pm 0.024 \pm 0.003$	$0.015 \pm 0.011 \pm 0.003$	$0.001 \pm 0.008 \pm 0.002$	$0.001 \pm 0.009 \pm 0.004$

Table 6: Summary of $\psi(2S)$ and $X(3872)$ cross-section measurements, fractions and ratios. The subscripts P and NP denote prompt and non-prompt components, while the labels SL and LL stand for short-lived and long-lived non-prompt components, respectively. The first uncertainty is statistical, the second is systematic. Uncertainties from integrated luminosity (1.9%) and those due to unknown spin-alignment are not included.

8 Dipion invariant mass spectra

The distributions of the dipion invariant mass $m_{\pi\pi}$ in the $\psi(2S) \rightarrow J/\psi\pi^+\pi^-$ and $X(3872) \rightarrow J/\psi\pi^+\pi^-$ decays are measured by determining the corrected yields of $\psi(2S)$ and $X(3872)$ signals in narrow bins of $m_{\pi\pi}$. The two additional selection requirements (Equation (1)) used specifically to reduce combinatorial background in the cross-section measurement, are found to bias the $m_{\pi\pi}$ distributions and are therefore replaced for this study by requirements on the pseudo-proper lifetime significance, $\tau/\Delta\tau < 2.5$, and the transverse momentum of the $J/\psi\pi^+\pi^-$ candidates, $p_T > 12$ GeV.

The invariant mass distributions of the corrected $J/\psi\pi^+\pi^-$ candidates selected for this analysis are shown in Figure 8(a) for the mass range around $\psi(2S)$ peak and in Figure 8(b) for $X(3872)$.

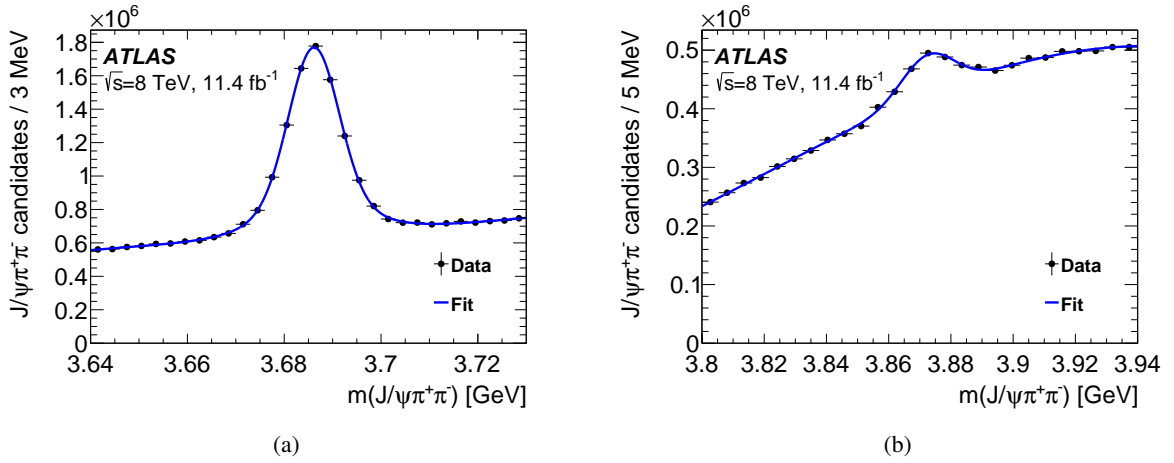


Figure 8: The invariant mass distributions of the $J/\psi\pi^+\pi^-$ candidates to extract (a) $\psi(2S)$ and (b) $X(3872)$ signal integrated over a wide range of $m_{\pi\pi}$.

The interval of allowed $m_{\pi\pi}$ values is subdivided into 21 and 11 bins for $\psi(2S)$ and $X(3872)$, respectively. In each $m_{\pi\pi}$ bin, the signal yield is extracted using a fit to the function

$$f(m) = Y[f_1 G_1(m) + (1 - f_1)G_2(m)] + N_{\text{bkg}} \left(\frac{m - p_0}{m_0 - p_0} \right)^{p_1} e^{-p_2(m-p_0) - p_3(m-p_0)^2}, \quad (12)$$

where m is the invariant mass of the $J/\psi\pi^+\pi^-$ system, Y is the yield of the parent resonance, N_{bkg} is the normalisation factor of the background PDF, m_0 is the world average mass [8] of the parent resonance, and $p_{0,1,2,3}$ are free parameters. The signals are described by the same double-Gaussian PDFs $f_1 G_1(m) + (1 - f_1)G_2(m)$ as the ones used in the cross-section analysis described in Section 4. In most $m_{\pi\pi}$ bins the position of the signal peak is determined from the fit; however, in some bins with small signal yields it is necessary to fix the centre and the width of the signal peak to the values obtained from the fits over the whole $m_{\pi\pi}$ range shown in Figure 8(b). As in the cross-section analysis, the fraction of the narrow Gaussian function f_1 is fixed to 0.76 ± 0.04 , varied within the range of ± 0.04 during systematic uncertainty studies. In another variation a first-order polynomial is added as a factor multiplying the PDF in Equation (12). For both the $\psi(2S)$ and $X(3872)$ samples, the errors from the fits in $m_{\pi\pi}$ bins are found to be statistically dominated.

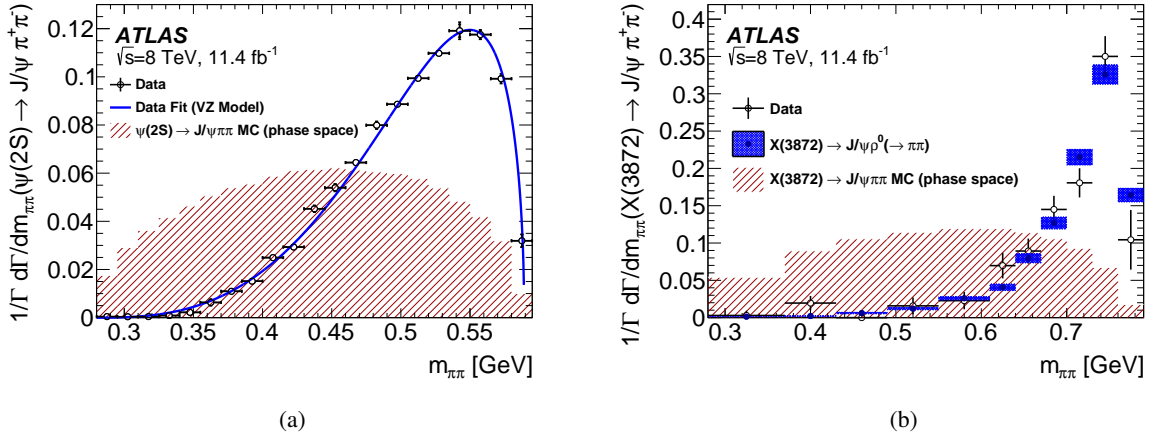


Figure 9: (a) Normalised differential decay width of $\psi(2S) \rightarrow J/\psi(\rightarrow \mu^+\mu^-)\pi^+\pi^-$ in bins of dipion invariant mass over the range $0.280\text{GeV} < m_{\pi\pi} < 0.595\text{GeV}$, fitted with the Voloshin–Zakharov model. Also shown is the normalised $m_{\pi\pi}$ phase-space distribution (red shaded histogram). (b) Normalised differential decay width of $X(3872) \rightarrow J/\psi(\rightarrow \mu^+\mu^-)\pi^+\pi^-$ in bins of dipion invariant mass over the range $0.28\text{GeV} < m_{\pi\pi} < 0.79\text{GeV}$. Also shown is the MC prediction for the decay $X(3872) \rightarrow J/\psi(\rightarrow \mu^+\mu^-)\rho^0(\rightarrow \pi^+\pi^-)$ (blue histogram) and the normalised distribution of $m_{\pi\pi}$ phase-space (red shaded histogram).

The resulting normalised differential distributions in $m_{\pi\pi}$ are shown in Figure 9(a) for $\psi(2S) \rightarrow J/\psi\pi^+\pi^-$ and in Figure 9(b) for $X(3872) \rightarrow J/\psi\pi^+\pi^-$ decays. The solid blue curve in Figure 9(a) represents a fit to the data points with the Voloshin–Zakharov distribution [35]

$$\frac{1}{\Gamma} \frac{d\Gamma}{dm_{\pi\pi}} \propto (m_{\pi\pi}^2 - \lambda m_{\pi}^2)^2 \times \text{PS}, \quad (13)$$

where PS stands for the dipion phase-space. The fitted value of the parameter λ is found to be $\lambda = 4.16 \pm 0.06(\text{stat}) \pm 0.03(\text{sys})$, in agreement with $\lambda = 4.35 \pm 0.18$ measured by BES [36], and $\lambda = 4.46 \pm 0.25$ measured by LHCb [37]. The shaded blue histogram in Figure 9(b) is obtained from straightforward simulations, assuming the dipion system in the decay $X(3872) \rightarrow J/\psi\pi^+\pi^-$ is produced purely via the ρ^0 meson, and appears to be in good agreement with the data. In both decays the measured $m_{\pi\pi}$ spectrum strongly disfavours the dipion phase-space distribution (shown in Figures 9(a) and 9(b) by the red shaded area), with the data clearly preferring higher masses in either case.

9 Summary

The measurement of the differential production cross section of $\psi(2S)$ and $X(3872)$ states in the $J/\psi\pi^+\pi^-$ final state is carried out using 11.4 fb^{-1} of $\sqrt{s} = 8 \text{ TeV}$ pp collision data recorded by the ATLAS detector at the LHC. The prompt and non-prompt production of $\psi(2S)$ and $X(3872)$ is studied separately, as a function of transverse momentum in the rapidity region $|y| < 0.75$ and transverse momentum range $10\text{GeV} < p_T < 70\text{GeV}$.

The $\psi(2S)$ cross-section measurements show good consistency with the theoretical predictions based on NLO NRQCD and FONLL for prompt and non-prompt production, respectively. The predictions from

the k_T factorisation model with the colour-octet component tuned to 7 TeV CMS data describe the prompt $\psi(2S)$ measurement fairly well, while NNLO* colour-singlet model calculations underestimate the data, especially at higher transverse momenta.

The prompt $X(3872)$ cross-section measurement shows good agreement with the CMS result for transverse momenta $10\text{GeV} < p_T < 30\text{GeV}$ where they overlap, and extends the range of transverse momenta up to 70GeV . Good agreement is found with theoretical predictions within the model based on NLO NRQCD, which considers $X(3872)$ to be a mixture of $\chi_{c1}(2P)$ and a $D^0\bar{D}^{*0}$ molecular state, with the production being dominated by the $\chi_{c1}(2P)$ component and the normalisation fixed through the fit to CMS data.

The non-prompt production of $\psi(2S)$ is described by the FONLL predictions within the uncertainties. But the same predictions, recalculated for $X(3872)$ using the branching fraction extracted from the Tevatron data, overestimate the non-prompt production of $X(3872)$, especially at large transverse momenta.

Two models of lifetime dependence of the non-prompt production are considered: a model with a single effective lifetime, and an alternative model with two distinctly different effective lifetimes. The two models give compatible results for the prompt and non-prompt differential cross sections of $\psi(2S)$ and $X(3872)$.

Within the single-lifetime model, assuming that non-prompt $\psi(2S)$ and $X(3872)$ originate from the same mix of parent b -hadrons, the following result is obtained for the ratio of the branching fractions:

$$R_B^{1L} = \frac{\mathcal{B}(B \rightarrow X(3872) + \text{any})\mathcal{B}(X(3872) \rightarrow J/\psi\pi^+\pi^-)}{\mathcal{B}(B \rightarrow \psi(2S) + \text{any})\mathcal{B}(\psi(2S) \rightarrow J/\psi\pi^+\pi^-)} = (3.95 \pm 0.32(\text{stat}) \pm 0.08(\text{sys})) \times 10^{-2}. \quad (14)$$

In the two-lifetime model, the two lifetimes are fixed to expected values for $X(3872)$ originating from the decays of B_c and from long-lived b -hadrons, respectively, with their relative weight determined from the fits to the data. The ratio of the branching fractions R_B is determined from the long-lived component alone:

$$R_B^{2L} = \frac{\mathcal{B}(B \rightarrow X(3872) + \text{any})\mathcal{B}(X(3872) \rightarrow J/\psi\pi^+\pi^-)}{\mathcal{B}(B \rightarrow \psi(2S) + \text{any})\mathcal{B}(\psi(2S) \rightarrow J/\psi\pi^+\pi^-)} = (3.57 \pm 0.33(\text{stat}) \pm 0.11(\text{sys})) \times 10^{-2}. \quad (15)$$

In the two-lifetime model, the fraction of the short-lived non-prompt component in $X(3872)$ production, for $p_T > 10\text{ GeV}$, is found to be

$$\frac{\sigma(pp \rightarrow B_c + \text{any})\mathcal{B}(B_c \rightarrow X(3872) + \text{any})}{\sigma(pp \rightarrow \text{non-prompt } X(3872) + \text{any})} = (25 \pm 13(\text{stat}) \pm 2(\text{sys}) \pm 5(\text{spin}))\%. \quad (16)$$

The invariant mass distributions of the dipion system in $\psi(2S) \rightarrow J/\psi\pi^+\pi^-$ and $X(3872) \rightarrow J/\psi\pi^+\pi^-$ decays are also measured. The results disfavour a phase-space distribution in both cases, and point strongly to the dominance of the $X(3872) \rightarrow J/\psi\rho^0$ mode in $X(3872)$ decays.

Acknowledgements

We thank CERN for the very successful operation of the LHC, as well as the support staff from our institutions without whom ATLAS could not be operated efficiently.

We acknowledge the support of ANPCyT, Argentina; YerPhI, Armenia; ARC, Australia; BMWFW and FWF, Austria; ANAS, Azerbaijan; SSTC, Belarus; CNPq and FAPESP, Brazil; NSERC, NRC and CFI, Canada; CERN; CONICYT, Chile; CAS, MOST and NSFC, China; COLCIENCIAS, Colombia; MSMT CR, MPO CR and VSC CR, Czech Republic; DNRF and DNSRC, Denmark; IN2P3-CNRS, CEA-DSM/IRFU, France; GNSF, Georgia; BMBF, HGF, and MPG, Germany; GSRT, Greece; RGC, Hong Kong SAR, China; ISF, I-CORE and Benoziyo Center, Israel; INFN, Italy; MEXT and JSPS, Japan; CNRST, Morocco; FOM and NWO, Netherlands; RCN, Norway; MNiSW and NCN, Poland; FCT, Portugal; MNE/IFA, Romania; MES of Russia and NRC KI, Russian Federation; JINR; MESTD, Serbia; MSSR, Slovakia; ARRS and MIZŠ, Slovenia; DST/NRF, South Africa; MINECO, Spain; SRC and Wallenberg Foundation, Sweden; SERI, SNSF and Cantons of Bern and Geneva, Switzerland; MOST, Taiwan; TAEK, Turkey; STFC, United Kingdom; DOE and NSF, United States of America. In addition, individual groups and members have received support from BCKDF, the Canada Council, CANARIE, CRC, Compute Canada, FQRNT, and the Ontario Innovation Trust, Canada; EPLANET, ERC, FP7, Horizon 2020 and Marie Skłodowska-Curie Actions, European Union; Investissements d’Avenir Labex and Idex, ANR, Région Auvergne and Fondation Partager le Savoir, France; DFG and AvH Foundation, Germany; Herakleitos, Thales and Aristeia programmes co-financed by EU-ESF and the Greek NSRF; BSF, GIF and Minerva, Israel; BRF, Norway; Generalitat de Catalunya, Generalitat Valenciana, Spain; the Royal Society and Leverhulme Trust, United Kingdom.

The crucial computing support from all WLCG partners is acknowledged gratefully, in particular from CERN, the ATLAS Tier-1 facilities at TRIUMF (Canada), NDGF (Denmark, Norway, Sweden), CC-IN2P3 (France), KIT/GridKA (Germany), INFN-CNAF (Italy), NL-T1 (Netherlands), PIC (Spain), ASGC (Taiwan), RAL (UK) and BNL (USA), the Tier-2 facilities worldwide and large non-WLCG resource providers. Major contributors of computing resources are listed in Ref. [38].

Appendix

A Spin-alignment

The acceptance of the $\mu^+\mu^-\pi^+\pi^-$ final state depends on the spin-alignment of the parent state. Several polarisation hypotheses were considered, based on the measured quantum numbers of the hidden-charm states ($J^P = 1^-$ for $\psi(2S)$ and J/ψ [8], 1^+ for $X(3872)$ [7]) and of the dipion system (0^+ in $\psi(2S) \rightarrow J/\psi\pi^+\pi^-$ decay [36], 1^- in $X(3872) \rightarrow J/\psi\pi^+\pi^-$ [7]). In both decays, the dipion system is assumed to be in S -wave with respect to the J/ψ .

The spin-alignment scenarios considered in this paper were derived using the helicity formalism [39–41], and are conveniently classified in terms of the various helicity amplitudes of the parent state, A_m , with $m = -1, 0, +1$:

- *Unpolarised* - an incoherent superposition of $A_- = 1, A_0 = 1$ and $A_+ = 1$, which is labelled UNPOL. This is used as the central hypothesis.
- *Transversely* polarised with either $A_+ = +1, A_0 = 0, A_- = 0$, or $A_+ = 0, A_0 = 0, A_- = +1$, which is labelled T_{+0} .
- *Transversely* polarised with $A_+ = +1/\sqrt{2}, A_0 = 0, A_- = +1/\sqrt{2}$, which is labelled T_{++} .
- *Transversely* polarised with $A_+ = -1/\sqrt{2}, A_0 = 0, A_- = +1/\sqrt{2}$, which is labelled T_{+-} .
- *Longitudinally* polarised with $A_+ = 0, A_0 = +1, A_- = 0$, which is labelled LONG.
- *Off-Plane Positive* - with $A_+ = -\sqrt{6}/3, A_0 = +\sqrt{3}/3, A_- = 0$, which is labelled OFFP+.
- *Off-Plane Negative* - with $A_+ = +\sqrt{6}/3, A_0 = +\sqrt{3}/3, A_- = 0$, which is labelled OFFP-.

Average acceptance weights are calculated for each of these scenarios in each of the analysis p_T bins. The ratios of the average weights for each polarisation scenario to those of the unpolarised case are shown in Figure 10(a) for $\psi(2S)$ and Figure 10(b) for $X(3872)$, with the values tabulated in Tables 7 and 8, respectively.

No individual production process can lead to an unpolarised vector state, but an unpolarised vector state can be observed due to a superposition of several production subprocesses with different spin-alignments [42]. The polarisation of prompt $\psi(2S)$ has been measured by CMS [43] and LHCb [44] and it was found that the angular dependence was close to isotropic, justifying the choice of unpolarised production for the central hypothesis. The non-prompt $\psi(2S)$ and $X(3872)$ are unlikely to show significant spin-alignment, since they are produced from a large number of different incoherent exclusive decays of parent b -hadrons.

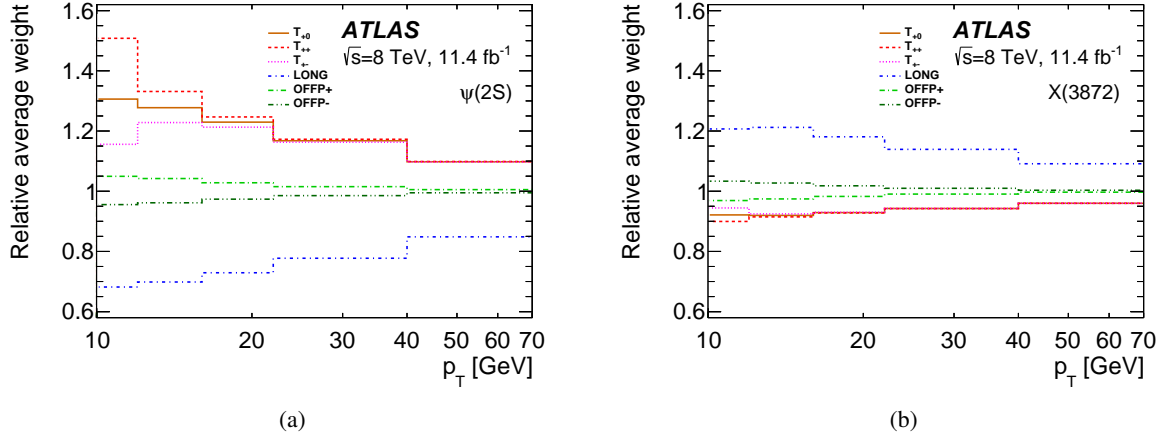


Figure 10: Correction factors for the (a) $\psi(2S)$ and (b) $X(3872)$ yields for various polarisation hypotheses.

Polarisation hypothesis	p_T [GeV]				
	10–12	12–16	16–22	22–40	40–70
T_{+0}	1.306	1.277	1.229	1.168	1.098
T_{++}	1.508	1.331	1.247	1.173	1.099
T_{+-}	1.156	1.228	1.213	1.163	1.097
LONG	0.682	0.698	0.729	0.777	0.848
OFFP+	1.049	1.042	1.028	1.015	1.005
OFFP–	0.956	0.962	0.974	0.985	0.995

Table 7: Correction factors for various polarisation hypotheses in p_T bins for $\psi(2S)$ production.

Polarisation hypothesis	p_T [GeV]				
	10–12	12–16	16–22	22–40	40–70
T_{+0}	0.921	0.920	0.929	0.943	0.960
T_{++}	0.900	0.915	0.928	0.942	0.960
T_{+-}	0.944	0.925	0.930	0.943	0.960
LONG	1.207	1.212	1.181	1.139	1.091
OFFP+	0.969	0.974	0.983	0.990	0.997
OFFP–	1.033	1.027	1.018	1.010	1.003

Table 8: Correction factors for various polarisation hypotheses in p_T bins for $X(3872)$ production.

References

- [1] Belle Collaboration, S. K. Choi et al., *Observation of a narrow charmonium - like state in exclusive $B^+ \rightarrow K^+\pi^+\pi^- J/\psi$ decays*, *Phys. Rev. Lett.* **91** (2003) 262001, arXiv:[hep-ex/0309032](#).
- [2] CDF Collaboration, D. Acosta et al., *Observation of the narrow state $X(3872) \rightarrow J/\psi\pi^+\pi^-$ in $\bar{p}p$ collisions at $\sqrt{s} = 1.96$ TeV*, *Phys. Rev. Lett.* **93** (2004) 072001, arXiv:[hep-ex/0312021](#).
- [3] BaBar Collaboration, B. Aubert et al., *Study of the $B \rightarrow J/\psi K^-\pi^+\pi^-$ decay and measurement of the $B \rightarrow X(3872)K^-$ branching fraction*, *Phys. Rev. D* **71** (2005) 071103, arXiv:[hep-ex/0406022](#).
- [4] D0 Collaboration, V. M. Abazov et al., *Observation and properties of the $X(3872)$ decaying to $J/\psi\pi^+\pi^-$ in $p\bar{p}$ collisions at $\sqrt{s} = 1.96$ TeV*, *Phys. Rev. Lett.* **93** (2004) 162002, arXiv:[hep-ex/0405004](#).
- [5] CDF Collaboration, A. Abulencia et al., *Analysis of the quantum numbers J^{PC} of the $X(3872)$* , *Phys. Rev. Lett.* **98** (2007) 132002, arXiv:[hep-ex/0612053](#).
- [6] LHCb Collaboration, R. Aaij et al., *Observation of $X(3872)$ production in pp collisions at $\sqrt{s} = 7$ TeV*, *Eur. Phys. J. C* **72** (2012) 1972, arXiv:[1112.5310](#) [[hep-ex](#)].
- [7] LHCb Collaboration, R. Aaij et al., *Quantum numbers of the $X(3872)$ state and orbital angular momentum in its $\rho^0 J/\psi$ decay*, *Phys. Rev. D* **92** (2015) 011102, arXiv:[1504.06339](#) [[hep-ex](#)].
- [8] K. A. Olive et al., *Review of Particle Physics*, *Chin. Phys. C* **38** (2014) 090001.
- [9] A. Tomaradze et al., *Precision Measurement of the Mass of the D^{*0} Meson and the Binding Energy of the $X(3872)$ Meson as a $D^0\bar{D}^{*0}$ Molecule*, *Phys. Rev. D* **91** (2015) 011102, arXiv:[1501.01658](#) [[hep-ex](#)].
- [10] CMS Collaboration, *Measurement of the $X(3872)$ production cross section via decays to $J/\psi\pi\pi$ in pp collisions at $\sqrt{s} = 7$ TeV*, *JHEP* **04** (2013) 154, arXiv:[1302.3968](#) [[hep-ex](#)].
- [11] P. Artoisenet and E. Braaten, *Production of the $X(3872)$ at the Tevatron and the LHC*, *Phys. Rev. D* **81** (2010) 114018, arXiv:[0911.2016](#) [[hep-ph](#)].
- [12] C. Meng, H. Han and K.-T. Chao, *$X(3872)$ and its production at hadron colliders*, (2013), arXiv:[1304.6710](#) [[hep-ph](#)].
- [13] ATLAS Collaboration, *Measurement of the production cross-section of $\psi(2S) \rightarrow J/\psi(\rightarrow \mu^+\mu^-)\pi^+\pi^-$ in pp collisions at $\sqrt{s} = 7$ TeV at ATLAS*, *JHEP* **09** (2014) 079, arXiv:[1407.5532](#) [[hep-ex](#)].
- [14] ATLAS Collaboration, *Measurement of the differential cross-sections of prompt and non-prompt production of J/ψ and $\psi(2S)$ in pp collisions at $\sqrt{s} = 7$ and 8 TeV with the ATLAS detector*, *Eur. Phys. J. C* **76** (2016) 283, arXiv:[1512.03657](#) [[hep-ex](#)].
- [15] ATLAS Collaboration, *The ATLAS Experiment at the CERN Large Hadron Collider*, *JINST* **3** (2008) S08003.

- [16] ATLAS Collaboration, *Luminosity determination in pp collisions at $\sqrt{s} = 8$ TeV using the ATLAS detector at the LHC*, (2016), arXiv:[1608.03953 \[hep-ex\]](#).
- [17] T. Sjöstrand, S. Mrenna and P. Z. Skands, *PYTHIA 6.4 Physics and Manual*, *JHEP* **05** (2006) 026, arXiv:[hep-ph/0603175](#).
- [18] A. V. Berezhnoy, A. K. Likhoded and O. P. Yushchenko, *Some features of the hadronic B_c^* meson production at large p_T* , *Phys. Atom. Nucl.* **59** (1996) 709–713, arXiv:[hep-ph/9504302](#).
- [19] A. V. Berezhnoy, V. V. Kiselev and A. K. Likhoded, *Hadronic production of S and P wave states of $\bar{b}c$ quarkonium*, *Z. Phys. A* **356** (1996) 79–87, arXiv:[hep-ph/9602347](#).
- [20] A. V. Berezhnoy et al., *B_c meson at LHC*, *Phys. Atom. Nucl.* **60** (1997) 1729–1740, arXiv:[hep-ph/9703341](#).
- [21] A. V. Berezhnoy, *Color flows for the process $gg \rightarrow B_c + c + \bar{b}$* , *Phys. Atom. Nucl.* **68** (2005) 1866–1872, arXiv:[hep-ph/0407315](#).
- [22] D. J. Lange, *The EvtGen particle decay simulation package*, *Nucl. Instrum. Meth. A* **462** (2001) 152–155.
- [23] ATLAS Collaboration, *The ATLAS Simulation Infrastructure*, *Eur. Phys. J. C* **70** (2010) 823, arXiv:[1005.4568 \[hep-ex\]](#).
- [24] S. Agostinelli et al., *GEANT4: A Simulation toolkit*, *Nucl. Instrum. Meth. A* **506** (2003) 250–303.
- [25] J. Allison et al., *Geant4 developments and applications*, *IEEE Trans. Nucl. Sci.* **53** (2006) 270.
- [26] ATLAS Collaboration, *Measurement of Upsilon production in 7 TeV pp collisions at ATLAS*, *Phys. Rev. D* **87** (2013) 052004, arXiv:[1211.7255 \[hep-ex\]](#).
- [27] A. V. Berezhnoy and A. K. Likhoded, *The relative yields of heavy hadrons as function of transverse momentum at LHC experiments*, (2013), arXiv:[1309.1979 \[hep-ph\]](#).
- [28] M. Cacciari et al., *Theoretical predictions for charm and bottom production at the LHC*, *JHEP* **10** (2012) 137, arXiv:[1205.6344 \[hep-ph\]](#).
- [29] ATLAS Collaboration, *Flavour tagged time-dependent angular analysis of the $B_s^0 \rightarrow J/\psi\phi$ decay and extraction of $\Delta\Gamma_s$ and the weak phase ϕ_s in ATLAS*, *Phys. Rev. D* **90** (2014) 052007, arXiv:[1407.1796 \[hep-ex\]](#).
- [30] S. P. Baranov, A. V. Lipatov and N. P. Zotov, *Prompt charmonia production and polarization at LHC in the NRQCD with k_T -factorization. Part I: $\psi(2S)$ meson*, *Eur. Phys. J. C* **75** (2015) 455, arXiv:[1508.05480 \[hep-ph\]](#).
- [31] CMS Collaboration, *Measurement of J/ψ and $\psi(2S)$ Prompt Double-Differential Cross Sections in pp Collisions at $\sqrt{s} = 7$ TeV*, *Phys. Rev. Lett.* **114** (2015) 191802, arXiv:[1502.04155 \[hep-ex\]](#).
- [32] J. P. Lansberg, *On the mechanisms of heavy-quarkonium hadroproduction*, *Eur. Phys. J. C* **61** (2009) 693–703, arXiv:[0811.4005 \[hep-ph\]](#).
- [33] G. Bauer, *The X(3872) at CDF II*, *Int. J. Mod. Phys. A* **20** (2005) 3765–3767, arXiv:[hep-ex/0409052](#).

- [34] CMS Collaboration, *J/ψ and ψ(2S) production in pp collisions at $\sqrt{s} = 7$ TeV*, *JHEP* **02** (2012) 011, arXiv:1111.1557 [hep-ex].
- [35] M. B. Voloshin and V. I. Zakharov, *Measuring QCD Anomalies in Hadronic Transitions Between Onium States*, *Phys. Rev. Lett.* **45** (1980) 688.
- [36] BES Collaboration, J. Z. Bai et al., *ψ(2S) → π⁺π⁻J/ψ decay distributions*, *Phys. Rev. D* **62** (2000) 032002, arXiv:hep-ex/9909038.
- [37] LHCb Collaboration, R. Aaij et al., *Measurement of ψ(2S) meson production in pp collisions at $\sqrt{s}=7$ TeV*, *Eur. Phys. J. C* **72** (2012) 2100, arXiv:1204.1258 [hep-ex].
- [38] ATLAS Collaboration, *ATLAS Computing Acknowledgements 2016–2017*, ATL-GEN-PUB-2016-002, 2016, URL: <https://cds.cern.ch/record/2202407>.
- [39] M. Jacob and G. C. Wick, *On the general theory of collisions for particles with spin*, *Annals Phys.* **7** (1959) 404–428, [Annals Phys.281,774(2000)].
- [40] J. D. Richman, *An Experimenter’s Guide to the Helicity Formalism*, CALT-68-1148, (1984).
- [41] S. U. Chung, *A General formulation of covariant helicity coupling amplitudes*, *Phys. Rev. D* **57** (1998) 431–442.
- [42] P. Faccioli et al., *Towards the experimental clarification of quarkonium polarization*, *Eur. Phys. J. C* **69** (2010) 657–673, arXiv:1006.2738 [hep-ph].
- [43] CMS Collaboration, *Measurement of the prompt J/ψ and ψ(2S) polarizations in pp collisions at $\sqrt{s} = 7$ TeV*, *Phys. Lett. B* **727** (2013) 381–402, arXiv:1307.6070 [hep-ex].
- [44] LHCb Collaboration, R. Aaij et al., *Measurement of ψ(2S) polarisation in pp collisions at $\sqrt{s} = 7$ TeV*, *Eur. Phys. J. C* **74** (2014) 2872, arXiv:1403.1339 [hep-ex].

The ATLAS Collaboration

M. Aaboud^{136d}, G. Aad⁸⁷, B. Abbott¹¹⁴, J. Abdallah⁸, O. Abidinov¹², B. Abeloos¹¹⁸, R. Aben¹⁰⁸, O.S. AbouZeid¹³⁸, N.L. Abraham¹⁵², H. Abramowicz¹⁵⁶, H. Abreu¹⁵⁵, R. Abreu¹¹⁷, Y. Abulaiti^{149a,149b}, B.S. Acharya^{168a,168b,a}, S. Adachi¹⁵⁸, L. Adamczyk^{40a}, D.L. Adams²⁷, J. Adelman¹⁰⁹, S. Adomeit¹⁰¹, T. Adye¹³², A.A. Affolder⁷⁶, T. Agatonovic-Jovin¹⁴, J. Agricola⁵⁶, J.A. Aguilar-Saavedra^{127a,127f}, S.P. Ahlen²⁴, F. Ahmadov^{67,b}, G. Aielli^{134a,134b}, H. Akerstedt^{149a,149b}, T.P.A. Åkesson⁸³, A.V. Akimov⁹⁷, G.L. Alberghi^{22a,22b}, J. Albert¹⁷³, S. Albrand⁵⁷, M.J. Alconada Verzini⁷³, M. Aleksa³², I.N. Aleksandrov⁶⁷, C. Alexa^{28b}, G. Alexander¹⁵⁶, T. Alexopoulos¹⁰, M. Alhroob¹¹⁴, B. Ali¹²⁹, M. Aliev^{75a,75b}, G. Alimonti^{93a}, J. Alison³³, S.P. Alkire³⁷, B.M.M. Allbrooke¹⁵², B.W. Allen¹¹⁷, P.P. Allport¹⁹, A. Aloisio^{105a,105b}, A. Alonso³⁸, F. Alonso⁷³, C. Alpigiani¹³⁹, A.A. Alshehri⁵⁵, M. Alstady⁸⁷, B. Alvarez Gonzalez³², D. Álvarez Piqueras¹⁷¹, M.G. Alviggi^{105a,105b}, B.T. Amadio¹⁶, K. Amako⁶⁸, Y. Amaral Coutinho^{26a}, C. Amelung²⁵, D. Amidei⁹¹, S.P. Amor Dos Santos^{127a,127c}, A. Amorim^{127a,127b}, S. Amoroso³², G. Amundsen²⁵, C. Anastopoulos¹⁴², L.S. Ancu⁵¹, N. Andari¹⁹, T. Andeen¹¹, C.F. Anders^{60b}, G. Anders³², J.K. Anders⁷⁶, K.J. Anderson³³, A. Andreazza^{93a,93b}, V. Andrei^{60a}, S. Angelidakis⁹, I. Angelozzi¹⁰⁸, P. Anger⁴⁶, A. Angerami³⁷, F. Anghinolfi³², A.V. Anisenkov^{110,c}, N. Anjos¹³, A. Annovi^{125a,125b}, C. Antel^{60a}, M. Antonelli⁴⁹, A. Antonov^{99,*}, F. Anulli^{133a}, M. Aoki⁶⁸, L. Aperio Bella¹⁹, G. Arabidze⁹², Y. Arai⁶⁸, J.P. Araque^{127a}, A.T.H. Arce⁴⁷, F.A. Arduh⁷³, J-F. Arguin⁹⁶, S. Argyropoulos⁶⁵, M. Arik^{20a}, A.J. Armbruster¹⁴⁶, L.J. Armitage⁷⁸, O. Arnaez³², H. Arnold⁵⁰, M. Arratia³⁰, O. Arslan²³, A. Artamonov⁹⁸, G. Artoni¹²¹, S. Artz⁸⁵, S. Asai¹⁵⁸, N. Asbah⁴⁴, A. Ashkenazi¹⁵⁶, B. Åsman^{149a,149b}, L. Asquith¹⁵², K. Assamagan²⁷, R. Astalos^{147a}, M. Atkinson¹⁷⁰, N.B. Atlay¹⁴⁴, K. Augsten¹²⁹, G. Avolio³², B. Axen¹⁶, M.K. Ayoub¹¹⁸, G. Azuelos^{96,d}, M.A. Baak³², A.E. Baas^{60a}, M.J. Baca¹⁹, H. Bachacou¹³⁷, K. Bachas^{75a,75b}, M. Backes¹²¹, M. Backhaus³², P. Bagiacchi^{133a,133b}, P. Bagnaia^{133a,133b}, Y. Bai^{35a}, J.T. Baines¹³², O.K. Baker¹⁸⁰, E.M. Baldin^{110,c}, P. Balek¹⁷⁶, T. Balestri¹⁵¹, F. Balli¹³⁷, W.K. Balunas¹²³, E. Banas⁴¹, Sw. Banerjee^{177,e}, A.A.E. Bannoura¹⁷⁹, L. Barak³², E.L. Barberio⁹⁰, D. Barberis^{52a,52b}, M. Barbero⁸⁷, T. Barillari¹⁰², M-S Barisits³², T. Barklow¹⁴⁶, N. Barlow³⁰, S.L. Barnes⁸⁶, B.M. Barnett¹³², R.M. Barnett¹⁶, Z. Barnovska-Blenessy⁵, A. Baroncelli^{135a}, G. Barone²⁵, A.J. Barr¹²¹, L. Barranco Navarro¹⁷¹, F. Barreiro⁸⁴, J. Barreiro Guimarães da Costa^{35a}, R. Bartoldus¹⁴⁶, A.E. Barton⁷⁴, P. Bartos^{147a}, A. Basalae¹²⁴, A. Bassalat^{118,f}, R.L. Bates⁵⁵, S.J. Batista¹⁶², J.R. Batley³⁰, M. Battaglia¹³⁸, M. Bauge^{133a,133b}, F. Bauer¹³⁷, H.S. Bawa^{146,g}, J.B. Beacham¹¹², M.D. Beattie⁷⁴, T. Beau⁸², P.H. Beauchemin¹⁶⁶, P. Bechtel²³, H.P. Beck^{18,h}, K. Becker¹²¹, M. Becker⁸⁵, M. Beckingham¹⁷⁴, C. Becot¹¹¹, A.J. Beddall^{20e}, A. Beddall^{20b}, V.A. Bednyakov⁶⁷, M. Bedognetti¹⁰⁸, C.P. Bee¹⁵¹, L.J. Beemster¹⁰⁸, T.A. Beermann³², M. Begel²⁷, J.K. Behr⁴⁴, C. Belanger-Champagne⁸⁹, A.S. Bell⁸⁰, G. Bella¹⁵⁶, L. Bellagamba^{22a}, A. Bellerive³¹, M. Bellomo⁸⁸, K. Belotskiy⁹⁹, O. Beltramello³², N.L. Belyaev⁹⁹, O. Benary^{156,*}, D. Benchekroun^{136a}, M. Bender¹⁰¹, K. Bendtz^{149a,149b}, N. Benekos¹⁰, Y. Benhammou¹⁵⁶, E. Benhar Noccioli¹⁸⁰, J. Benitez⁶⁵, D.P. Benjamin⁴⁷, J.R. Bensinger²⁵, S. Bentvelsen¹⁰⁸, L. Beresford¹²¹, M. Beretta⁴⁹, D. Berge¹⁰⁸, E. Bergeas Kuutmann¹⁶⁹, N. Berger⁵, J. Beringer¹⁶, S. Berlendis⁵⁷, N.R. Bernard⁸⁸, C. Bernius¹¹¹, F.U. Bernlochner²³, T. Berry⁷⁹, P. Berta¹³⁰, C. Bertella⁸⁵, G. Bertoli^{149a,149b}, F. Bertolucci^{125a,125b}, I.A. Bertram⁷⁴, C. Bertsche⁴⁴, D. Bertsche¹¹⁴, G.J. Besjes³⁸, O. Bessidskaia Bylund^{149a,149b}, M. Bessner⁴⁴, N. Besson¹³⁷, C. Betancourt⁵⁰, A. Bethani⁵⁷, S. Bethke¹⁰², A.J. Bevan⁷⁸, R.M. Bianchi¹²⁶, L. Bianchini²⁵, M. Bianco³², O. Biebel¹⁰¹, D. Biedermann¹⁷, R. Bielski⁸⁶, N.V. Biesuz^{125a,125b}, M. Biglietti^{135a}, J. Bilbao De Mendizabal⁵¹, T.R.V. Billoud⁹⁶, H. Bilokon⁴⁹, M. Bindi⁵⁶, S. Binet¹¹⁸, A. Bingul^{20b}, C. Bini^{133a,133b}, S. Biondi^{22a,22b}, T. Bisanz⁵⁶, D.M. Bjergaard⁴⁷, C.W. Black¹⁵³, J.E. Black¹⁴⁶, K.M. Black²⁴, D. Blackburn¹³⁹, R.E. Blair⁶, J.-B. Blanchard¹³⁷, T. Blazek^{147a}, I. Bloch⁴⁴,

C. Blocker²⁵, A. Blue⁵⁵, W. Blum^{85,*}, U. Blumenschein⁵⁶, S. Blunier^{34a}, G.J. Bobbink¹⁰⁸, V.S. Bobrovnikov^{110,c}, S.S. Bocchetta⁸³, A. Bocci⁴⁷, C. Bock¹⁰¹, M. Boehler⁵⁰, D. Boerner¹⁷⁹, J.A. Bogaerts³², D. Bogavac¹⁴, A.G. Bogdanchikov¹¹⁰, C. Bohm^{149a}, V. Boisvert⁷⁹, P. Bokan¹⁴, T. Bold^{40a}, A.S. Boldyrev^{168a,168c}, M. Bomben⁸², M. Bona⁷⁸, M. Boonekamp¹³⁷, A. Borisov¹³¹, G. Borissov⁷⁴, J. Bortfeldt³², D. Bortoletto¹²¹, V. Bortolotto^{62a,62b,62c}, K. Bos¹⁰⁸, D. Boscherini^{22a}, M. Bosman¹³, J.D. Bossio Sola²⁹, J. Boudreau¹²⁶, J. Bouffard², E.V. Bouhova-Thacker⁷⁴, D. Boumediene³⁶, C. Bourdarios¹¹⁸, S.K. Boutle⁵⁵, A. Boveia³², J. Boyd³², I.R. Boyko⁶⁷, J. Bracinik¹⁹, A. Brandt⁸, G. Brandt⁵⁶, O. Brandt^{60a}, U. Bratzler¹⁵⁹, B. Brau⁸⁸, J.E. Brau¹¹⁷, W.D. Breaden Madden⁵⁵, K. Brendlinger¹²³, A.J. Brennan⁹⁰, L. Brenner¹⁰⁸, R. Brenner¹⁶⁹, S. Bressler¹⁷⁶, T.M. Bristow⁴⁸, D. Britton⁵⁵, D. Britzger⁴⁴, F.M. Brochu³⁰, I. Brock²³, R. Brock⁹², G. Brooijmans³⁷, T. Brooks⁷⁹, W.K. Brooks^{34b}, J. Brosamer¹⁶, E. Brost¹⁰⁹, J.H. Broughton¹⁹, P.A. Bruckman de Renstrom⁴¹, D. Bruncko^{147b}, R. Bruneliere⁵⁰, A. Bruni^{22a}, G. Bruni^{22a}, L.S. Bruni¹⁰⁸, B.H. Brunt³⁰, M. Bruschi^{22a}, N. Bruscinò²³, P. Bryant³³, L. Bryngemark⁸³, T. Buanes¹⁵, Q. Buat¹⁴⁵, P. Buchholz¹⁴⁴, A.G. Buckley⁵⁵, I.A. Budagov⁶⁷, F. Buehrer⁵⁰, M.K. Bugge¹²⁰, O. Bulekov⁹⁹, D. Bullock⁸, H. Burckhart³², S. Burdina⁷⁶, C.D. Burgard⁵⁰, B. Burghgrave¹⁰⁹, K. Burka⁴¹, S. Burke¹³², I. Burmeister⁴⁵, J.T.P. Burr¹²¹, E. Busato³⁶, D. Büscher⁵⁰, V. Büscher⁸⁵, P. Bussey⁵⁵, J.M. Butler²⁴, C.M. Buttar⁵⁵, J.M. Butterworth⁸⁰, P. Butti¹⁰⁸, W. Buttinger²⁷, A. Buzatu⁵⁵, A.R. Buzykaev^{110,c}, S. Cabrera Urbán¹⁷¹, D. Caforio¹²⁹, V.M. Cairo^{39a,39b}, O. Cakir^{4a}, N. Calace⁵¹, P. Calafiura¹⁶, A. Calandri⁸⁷, G. Calderini⁸², P. Calfayan¹⁰¹, G. Callea^{39a,39b}, L.P. Caloba^{26a}, S. Calvente Lopez⁸⁴, D. Calvet³⁶, S. Calvet³⁶, T.P. Calvet⁸⁷, R. Camacho Toro³³, S. Camarda³², P. Camarri^{134a,134b}, D. Cameron¹²⁰, R. Caminal Armadans¹⁷⁰, C. Camincher⁵⁷, S. Campana³², M. Campanelli⁸⁰, A. Camplani^{93a,93b}, A. Campoverde¹⁴⁴, V. Canale^{105a,105b}, A. Canepa^{164a}, M. Cano Bret¹⁴¹, J. Cantero¹¹⁵, T. Cao⁴², M.D.M. Capeans Garrido³², I. Caprini^{28b}, M. Caprini^{28b}, M. Capua^{39a,39b}, R.M. Carbone³⁷, R. Cardarelli^{134a}, F. Cardillo⁵⁰, I. Carli¹³⁰, T. Carli³², G. Carlino^{105a}, L. Carminati^{93a,93b}, S. Caron¹⁰⁷, E. Carquin^{34b}, G.D. Carrillo-Montoya³², J.R. Carter³⁰, J. Carvalho^{127a,127c}, D. Casadei¹⁹, M.P. Casado^{13,i}, M. Casolino¹³, D.W. Casper¹⁶⁷, E. Castaneda-Miranda^{148a}, R. Castelijns¹⁰⁸, A. Castelli¹⁰⁸, V. Castillo Gimenez¹⁷¹, N.F. Castro^{127a,j}, A. Catinaccio³², J.R. Catmore¹²⁰, A. Cattai³², J. Caudron²³, V. Cavaliere¹⁷⁰, E. Cavallaro¹³, D. Cavalli^{93a}, M. Cavalli-Sforza¹³, V. Cavasinni^{125a,125b}, F. Ceradini^{135a,135b}, L. Cerda Alberich¹⁷¹, B.C. Cerio⁴⁷, A.S. Cerqueira^{26b}, A. Cerri¹⁵², L. Cerrito^{134a,134b}, F. Cerutti¹⁶, M. Cerv³², A. Cervelli¹⁸, S.A. Cetin^{20d}, A. Chafaq^{136a}, D. Chakraborty¹⁰⁹, S.K. Chan⁵⁸, Y.L. Chan^{62a}, P. Chang¹⁷⁰, J.D. Chapman³⁰, D.G. Charlton¹⁹, A. Chatterjee⁵¹, C.C. Chau¹⁶², C.A. Chavez Barajas¹⁵², S. Che¹¹², S. Cheatham^{168a,168c}, A. Chegwidan⁹², S. Chekanov⁶, S.V. Chekulaev^{164a}, G.A. Chelkov^{67,k}, M.A. Chelstowska⁹¹, C. Chen⁶⁶, H. Chen²⁷, K. Chen¹⁵¹, S. Chen^{35b}, S. Chen¹⁵⁸, X. Chen^{35c}, Y. Chen⁶⁹, H.C. Cheng⁹¹, H.J. Cheng^{35a}, Y. Cheng³³, A. Cheplakov⁶⁷, E. Cheremushkina¹³¹, R. Cherkaoui El Moursli^{136e}, V. Chernyatin^{27,*}, E. Cheu⁷, L. Chevalier¹³⁷, V. Chiarella⁴⁹, G. Chiarelli^{125a,125b}, G. Chiodini^{75a}, A.S. Chisholm³², A. Chitan^{28b}, M.V. Chizhov⁶⁷, K. Choi⁶³, A.R. Chomont³⁶, S. Chouridou⁹, B.K.B. Chow¹⁰¹, V. Christodoulou⁸⁰, D. Chromek-Burckhart³², J. Chudoba¹²⁸, A.J. Chuinard⁸⁹, J.J. Chwastowski⁴¹, L. Chytka¹¹⁶, G. Ciapetti^{133a,133b}, A.K. Ciftci^{4a}, D. Cinca⁴⁵, V. Cindro⁷⁷, I.A. Cioara²³, C. Ciocca^{22a,22b}, A. Ciocio¹⁶, F. Ciotto^{105a,105b}, Z.H. Citron¹⁷⁶, M. Citterio^{93a}, M. Ciubancan^{28b}, A. Clark⁵¹, B.L. Clark⁵⁸, M.R. Clark³⁷, P.J. Clark⁴⁸, R.N. Clarke¹⁶, C. Clement^{149a,149b}, Y. Coadou⁸⁷, M. Cokal^{168a,168c}, A. Coccaro⁵¹, J. Cochran⁶⁶, L. Colasurdo¹⁰⁷, B. Cole³⁷, A.P. Colijn¹⁰⁸, J. Collot⁵⁷, T. Colombo¹⁶⁷, G. Compostella¹⁰², P. Conde Muiño^{127a,127b}, E. Coniavitis⁵⁰, S.H. Connell^{148b}, I.A. Connelly⁷⁹, V. Consorti⁵⁰, S. Constantinescu^{28b}, G. Conti³², F. Conventi^{105a,l}, M. Cooke¹⁶, B.D. Cooper⁸⁰, A.M. Cooper-Sarkar¹²¹, K.J.R. Cormier¹⁶², T. Cornelissen¹⁷⁹, M. Corradi^{133a,133b}, F. Corriveau^{89,m}, A. Corso-Radu¹⁶⁷, A. Cortes-Gonzalez³², G. Cortiana¹⁰², G. Costa^{93a}, M.J. Costa¹⁷¹, D. Costanzo¹⁴², G. Cottin³⁰, G. Cowan⁷⁹, B.E. Cox⁸⁶, K. Cranmer¹¹¹, S.J. Crawley⁵⁵, G. Cree³¹, S. Crépe- Renaudin⁵⁷, F. Crescioli⁸², W.A. Cribbs^{149a,149b},

M. Crispin Ortuzar¹²¹, M. Cristinziani²³, V. Croft¹⁰⁷, G. Crosetti^{39a,39b}, A. Cueto⁸⁴,
T. Cuhadar Donszelmann¹⁴², J. Cummings¹⁸⁰, M. Curatolo⁴⁹, J. Cúth⁸⁵, H. Czirr¹⁴⁴, P. Czodrowski³,
G. D'amen^{22a,22b}, S. D'Auria⁵⁵, M. D'Onofrio⁷⁶, M.J. Da Cunha Sargedas De Sousa^{127a,127b},
C. Da Via⁸⁶, W. Dabrowski^{40a}, T. Dado^{147a}, T. Dai⁹¹, O. Dale¹⁵, F. Dallaire⁹⁶, C. Dallapiccola⁸⁸,
M. Dam³⁸, J.R. Dandoy³³, N.P. Dang⁵⁰, A.C. Daniells¹⁹, N.S. Dann⁸⁶, M. Danninger¹⁷²,
M. Dano Hoffmann¹³⁷, V. Dao⁵⁰, G. Darbo^{52a}, S. Darmora⁸, J. Dassoulas³, A. Dattagupta¹¹⁷,
W. Davey²³, C. David¹⁷³, T. Davidek¹³⁰, M. Davies¹⁵⁶, P. Davison⁸⁰, E. Dawe⁹⁰, I. Dawson¹⁴², K. De⁸,
R. de Asmundis^{105a}, A. De Benedetti¹¹⁴, S. De Castro^{22a,22b}, S. De Cecco⁸², N. De Groot¹⁰⁷,
P. de Jong¹⁰⁸, H. De la Torre⁹², F. De Lorenzi⁶⁶, A. De Maria⁵⁶, D. De Pedis^{133a}, A. De Salvo^{133a},
U. De Sanctis¹⁵², A. De Santo¹⁵², J.B. De Vivie De Regie¹¹⁸, W.J. Dearnaley⁷⁴, R. Debbe²⁷,
C. Debenedetti¹³⁸, D.V. Dedovich⁶⁷, N. Dehghanian³, I. Deigaard¹⁰⁸, M. Del Gaudio^{39a,39b},
J. Del Peso⁸⁴, T. Del Prete^{125a,125b}, D. Delgove¹¹⁸, F. Deliot¹³⁷, C.M. Delitzsch⁵¹, A. Dell'Acqua³²,
L. Dell'Asta²⁴, M. Dell'Orso^{125a,125b}, M. Della Pietra^{105a,l}, D. della Volpe⁵¹, M. Delmastro⁵,
P.A. Delsart⁵⁷, D.A. DeMarco¹⁶², S. Demers¹⁸⁰, M. Demichev⁶⁷, A. Demilly⁸², S.P. Denisov¹³¹,
D. Denysiuk¹³⁷, D. Derendarz⁴¹, J.E. Derkaoui^{136d}, F. Derue⁸², P. Dervan⁷⁶, K. Desch²³, C. Deterre⁴⁴,
K. Dette⁴⁵, P.O. Deviveiros³², A. Dewhurst¹³², S. Dhaliwal²⁵, A. Di Ciaccio^{134a,134b}, L. Di Ciaccio⁵,
W.K. Di Clemente¹²³, C. Di Donato^{133a,133b}, A. Di Girolamo³², B. Di Girolamo³², B. Di Micco^{135a,135b},
R. Di Nardo³², A. Di Simone⁵⁰, R. Di Sipio¹⁶², D. Di Valentino³¹, C. Diaconu⁸⁷, M. Diamond¹⁶²,
F.A. Dias⁴⁸, M.A. Diaz^{34a}, E.B. Diehl⁹¹, J. Dietrich¹⁷, S. Díez Cornell⁴⁴, A. Dimitrievska¹⁴,
J. Dingfelder²³, P. Dita^{28b}, S. Dita^{28b}, F. Dittus³², F. Djama⁸⁷, T. Djobava^{53b}, J.I. Djuvsland^{60a},
M.A.B. do Vale^{26c}, D. Dobos³², M. Dobre^{28b}, C. Doglioni⁸³, J. Dolejsi¹³⁰, Z. Dolezal¹³⁰,
M. Donadelli^{26d}, S. Donati^{125a,125b}, P. Dondero^{122a,122b}, J. Donini³⁶, J. Dopke¹³², A. Doria^{105a},
M.T. Dova⁷³, A.T. Doyle⁵⁵, E. Drechsler⁵⁶, M. Dris¹⁰, Y. Du¹⁴⁰, J. Duarte-Campderros¹⁵⁶,
E. Duchovni¹⁷⁶, G. Duckeck¹⁰¹, O.A. Ducu^{96,n}, D. Duda¹⁰⁸, A. Dudarev³², A.Ch. Dudder⁸⁵,
E.M. Duffield¹⁶, L. Dufлот¹¹⁸, M. Dührssen³², M. Dumancic¹⁷⁶, M. Dunford^{60a}, H. Duran Yildiz^{4a},
M. Düren⁵⁴, A. Durglishvili^{53b}, D. Duschinger⁴⁶, B. Dutta⁴⁴, M. Dyndal⁴⁴, C. Eckardt⁴⁴, K.M. Ecker¹⁰²,
R.C. Edgar⁹¹, N.C. Edwards⁴⁸, T. Eifert³², G. Eigen¹⁵, K. Einsweiler¹⁶, T. Ekelof¹⁶⁹, M. El Kacimi^{136c},
V. Ellajosyula⁸⁷, M. Ellert¹⁶⁹, S. Elles⁵, F. Ellinghaus¹⁷⁹, A.A. Elliot¹⁷³, N. Ellis³², J. Elmsheuser²⁷,
M. Elsing³², D. Emelianov¹³², Y. Enari¹⁵⁸, O.C. Endner⁸⁵, J.S. Ennis¹⁷⁴, J. Erdmann⁴⁵, A. Ereditato¹⁸,
G. Ernis¹⁷⁹, J. Ernst², M. Ernst²⁷, S. Errede¹⁷⁰, E. Ertel⁸⁵, M. Escalier¹¹⁸, H. Esch⁴⁵, C. Escobar¹²⁶,
B. Esposito⁴⁹, A.I. Etienne¹³⁷, E. Etzion¹⁵⁶, H. Evans⁶³, A. Ezhilov¹²⁴, M. Ezzi^{136e}, F. Fabbri^{22a,22b},
L. Fabbri^{22a,22b}, G. Facini³³, R.M. Fakhruddinov¹³¹, S. Falciano^{133a}, R.J. Falla⁸⁰, J. Faltova³², Y. Fang^{35a},
M. Fanti^{93a,93b}, A. Farbin⁸, A. Farilla^{135a}, C. Farina¹²⁶, E.M. Farina^{122a,122b}, T. Farooque¹³, S. Farrell¹⁶,
S.M. Farrington¹⁷⁴, P. Farthouat³², F. Fassi^{136e}, P. Fassnacht³², D. Fassouliotis⁹, M. Fauci Giannelli⁷⁹,
A. Favareto^{52a,52b}, W.J. Fawcett¹²¹, L. Fayard¹¹⁸, O.L. Fedin^{124,o}, W. Fedorko¹⁷², S. Feigl¹²⁰,
L. Feligioni⁸⁷, C. Feng¹⁴⁰, E.J. Feng³², H. Feng⁹¹, A.B. Fenyuk¹³¹, L. Feremenga⁸,
P. Fernandez Martinez¹⁷¹, S. Fernandez Perez¹³, J. Ferrando⁴⁴, A. Ferrari¹⁶⁹, P. Ferrari¹⁰⁸, R. Ferrari^{122a},
D.E. Ferreira de Lima^{60b}, A. Ferrer¹⁷¹, D. Ferrere⁵¹, C. Ferretti⁹¹, A. Ferretto Parodi^{52a,52b}, F. Fiedler⁸⁵,
A. Filipčić⁷⁷, M. Filipuzzi⁴⁴, F. Filthaut¹⁰⁷, M. Fincke-Keeler¹⁷³, K.D. Finelli¹⁵³,
M.C.N. Fiolhais^{127a,127c}, L. Fiorini¹⁷¹, A. Firan⁴², A. Fischer², C. Fischer¹³, J. Fischer¹⁷⁹, W.C. Fisher⁹²,
N. Flaschel⁴⁴, I. Fleck¹⁴⁴, P. Fleischmann⁹¹, G.T. Fletcher¹⁴², R.R.M. Fletcher¹²³, T. Flick¹⁷⁹,
L.R. Flores Castillo^{62a}, M.J. Flowerdew¹⁰², G.T. Forcolin⁸⁶, A. Formica¹³⁷, A. Forti⁸⁶, A.G. Foster¹⁹,
D. Fournier¹¹⁸, H. Fox⁷⁴, S. Fracchia¹³, P. Francavilla⁸², M. Franchini^{22a,22b}, D. Francis³²,
L. Franconi¹²⁰, M. Franklin⁵⁸, M. Frate¹⁶⁷, M. Fraternali^{122a,122b}, D. Freeborn⁸⁰,
S.M. Fressard-Batraneanu³², F. Friedrich⁴⁶, D. Froidevaux³², J.A. Frost¹²¹, C. Fukunaga¹⁵⁹,
E. Fullana Torregrosa⁸⁵, T. Fusayasu¹⁰³, J. Fuster¹⁷¹, C. Gabaldon⁵⁷, O. Gabizon¹⁷⁹, A. Gabrielli^{22a,22b},
A. Gabrielli¹⁶, G.P. Gach^{40a}, S. Gadatsch³², S. Gadomski⁷⁹, G. Gagliardi^{52a,52b}, L.G. Gagnon⁹⁶,

P. Gagnon⁶³, C. Galea¹⁰⁷, B. Galhardo^{127a,127c}, E.J. Gallas¹²¹, B.J. Gallop¹³², P. Gallus¹²⁹, G. Galster³⁸,
 K.K. Gan¹¹², J. Gao⁵⁹, Y. Gao⁴⁸, Y.S. Gao^{146,g}, F.M. Garay Walls⁴⁸, C. García¹⁷¹,
 J.E. García Navarro¹⁷¹, M. Garcia-Sciveres¹⁶, R.W. Gardner³³, N. Garelli¹⁴⁶, V. Garonne¹²⁰,
 A. Gascon Bravo⁴⁴, K. Gasnikova⁴⁴, C. Gatti⁴⁹, A. Gaudiello^{52a,52b}, G. Gaudio^{122a}, L. Gauthier⁹⁶,
 I.L. Gavrilenko⁹⁷, C. Gay¹⁷², G. Gaycken²³, E.N. Gazis¹⁰, Z. Gecse¹⁷², C.N.P. Gee¹³²,
 Ch. Geich-Gimbel²³, M. Geisen⁸⁵, M.P. Geisler^{60a}, K. Gellerstedt^{149a,149b}, C. Gemme^{52a},
 M.H. Genest⁵⁷, C. Geng^{59,p}, S. Gentile^{133a,133b}, C. Gentsos¹⁵⁷, S. George⁷⁹, D. Gerbaudo¹³,
 A. Gershon¹⁵⁶, S. Ghasemi¹⁴⁴, M. Ghneimat²³, B. Giacobbe^{22a}, S. Giagu^{133a,133b}, P. Giannetti^{125a,125b},
 B. Gibbard²⁷, S.M. Gibson⁷⁹, M. Gignac¹⁷², M. Gilchriese¹⁶, T.P.S. Gillam³⁰, D. Gillberg³¹,
 G. Gilles¹⁷⁹, D.M. Gingrich^{3,d}, N. Giokaris⁹, M.P. Giordani^{168a,168c}, F.M. Giorgi^{22a}, F.M. Giorgi¹⁷,
 P.F. Giraud¹³⁷, P. Giromini⁵⁸, D. Giugni^{93a}, F. Giuli¹²¹, C. Giuliani¹⁰², M. Giulini^{60b}, B.K. Gjølsten¹²⁰,
 S. Gkaitatzis¹⁵⁷, I. Gkialas¹⁵⁷, E.L. Gkougkousis¹¹⁸, L.K. Gladilin¹⁰⁰, C. Glasman⁸⁴, J. Glatzer⁵⁰,
 P.C.F. Glaysheer⁴⁸, A. Glazov⁴⁴, M. Goblirsch-Kolb²⁵, J. Godlewski⁴¹, S. Goldfarb⁹⁰, T. Golling⁵¹,
 D. Golubkov¹³¹, A. Gomes^{127a,127b,127d}, R. Gonçalves^{127a}, J. Goncalves Pinto Firmino Da Costa¹³⁷,
 G. Gonella⁵⁰, L. Gonella¹⁹, A. Gongadze⁶⁷, S. González de la Hoz¹⁷¹, G. Gonzalez Parra¹³,
 S. Gonzalez-Sevilla⁵¹, L. Goossens³², P.A. Gorbounov⁹⁸, H.A. Gordon²⁷, I. Gorelov¹⁰⁶, B. Gorini³²,
 E. Gorini^{75a,75b}, A. Gorišek⁷⁷, E. Gornicki⁴¹, A.T. Goshaw⁴⁷, C. Gössling⁴⁵, M.I. Gostkin⁶⁷,
 C.R. Goudet¹¹⁸, D. Goujdami^{136c}, A.G. Goussiou¹³⁹, N. Govender^{148b,q}, E. Gozani¹⁵⁵, L. Graber⁵⁶,
 I. Grabowska-Bold^{40a}, P.O.J. Gradin⁵⁷, P. Grafström^{22a,22b}, J. Gramling⁵¹, E. Gramstad¹²⁰,
 S. Grancagnolo¹⁷, V. Gratchev¹²⁴, P.M. Gravila^{28e}, H.M. Gray³², E. Graziani^{135a}, Z.D. Greenwood^{81,r},
 C. Grefe²³, K. Gregersen⁸⁰, I.M. Gregor⁴⁴, P. Grenier¹⁴⁶, K. Grevtsov⁵, J. Griffiths⁸, A.A. Grillo¹³⁸,
 K. Grimm⁷⁴, S. Grinstein^{13,s}, Ph. Gris³⁶, J.-F. Grivaz¹¹⁸, S. Groh⁸⁵, J.P. Grohs⁴⁶, E. Gross¹⁷⁶,
 J. Grosse-Knetter⁵⁶, G.C. Grossi⁸¹, Z.J. Grout⁸⁰, L. Guan⁹¹, W. Guan¹⁷⁷, J. Guenther⁶⁴, F. Guescini⁵¹,
 D. Guest¹⁶⁷, O. Gueta¹⁵⁶, E. Guido^{52a,52b}, T. Guillemin⁵, S. Guindon², U. Gul⁵⁵, C. Gumpert³²,
 J. Guo¹⁴¹, Y. Guo^{59,p}, R. Gupta⁴², S. Gupta¹²¹, G. Gustavino^{133a,133b}, P. Gutierrez¹¹⁴,
 N.G. Gutierrez Ortiz⁸⁰, C. Gutschow⁴⁶, C. Guyot¹³⁷, C. Gwenlan¹²¹, C.B. Gwilliam⁷⁶, A. Haas¹¹¹,
 C. Haber¹⁶, H.K. Hadavand⁸, N. Haddad^{136e}, A. Hadeef⁸⁷, S. Hageböck²³, M. Hagihara¹⁶⁵, Z. Hajduk⁴¹,
 H. Hakobyan^{181,*}, M. Haleem⁴⁴, J. Haley¹¹⁵, G. Halladjian⁹², G.D. Hallewell⁸⁷, K. Hamacher¹⁷⁹,
 P. Hamal¹¹⁶, K. Hamano¹⁷³, A. Hamilton^{148a}, G.N. Hamity¹⁴², P.G. Hamnett⁴⁴, L. Han⁵⁹,
 K. Hanagaki^{68,t}, K. Hanawa¹⁵⁸, M. Hance¹³⁸, B. Haney¹²³, P. Hanke^{60a}, R. Hanna¹³⁷, J.B. Hansen³⁸,
 J.D. Hansen³⁸, M.C. Hansen²³, P.H. Hansen³⁸, K. Hara¹⁶⁵, A.S. Hard¹⁷⁷, T. Harenberg¹⁷⁹, F. Hariri¹¹⁸,
 S. Harkusha⁹⁴, R.D. Harrington⁴⁸, P.F. Harrison¹⁷⁴, F. Hartjes¹⁰⁸, N.M. Hartmann¹⁰¹, M. Hasegawa⁶⁹,
 Y. Hasegawa¹⁴³, A. Hasib¹¹⁴, S. Hassani¹³⁷, S. Haug¹⁸, R. Hauser⁹², L. Hauswald⁴⁶, M. Havranek¹²⁸,
 C.M. Hawkes¹⁹, R.J. Hawkings³², D. Hayakawa¹⁶⁰, D. Hayden⁹², C.P. Hays¹²¹, J.M. Hays⁷⁸,
 H.S. Hayward⁷⁶, S.J. Haywood¹³², S.J. Head¹⁹, T. Heck⁸⁵, V. Hedberg⁸³, L. Heelan⁸, S. Heim¹²³,
 T. Heim¹⁶, B. Heinemann¹⁶, J.J. Heinrich¹⁰¹, L. Heinrich¹¹¹, C. Heinz⁵⁴, J. Hejbal¹²⁸, L. Helary³²,
 S. Hellman^{149a,149b}, C. Helsen³², J. Henderson¹²¹, R.C.W. Henderson⁷⁴, Y. Heng¹⁷⁷, S. Henkelmann¹⁷²,
 A.M. Henriques Correia³², S. Henrot-Versille¹¹⁸, G.H. Herbert¹⁷, H. Herde²⁵, V. Herget¹⁷⁸,
 Y. Hernández Jiménez¹⁷¹, G. Herten⁵⁰, R. Hertenberger¹⁰¹, L. Hervas³², G.G. Hesketh⁸⁰, N.P. Hessey¹⁰⁸,
 J.W. Hetherly⁴², R. Hickling⁷⁸, E. Higón-Rodríguez¹⁷¹, E. Hill¹⁷³, J.C. Hill³⁰, K.H. Hiller⁴⁴,
 S.J. Hillier¹⁹, I. Hinchliffe¹⁶, E. Hines¹²³, R.R. Hinman¹⁶, M. Hirose⁵⁰, D. Hirschbuehl¹⁷⁹, J. Hobbs¹⁵¹,
 N. Hod^{164a}, M.C. Hodgkinson¹⁴², P. Hodgson¹⁴², A. Hoecker³², M.R. Hoferkamp¹⁰⁶, F. Hoenig¹⁰¹,
 D. Hohn²³, T.R. Holmes¹⁶, M. Homann⁴⁵, T. Honda⁶⁸, T.M. Hong¹²⁶, B.H. Hooberman¹⁷⁰,
 W.H. Hopkins¹¹⁷, Y. Horii¹⁰⁴, A.J. Horton¹⁴⁵, J.-Y. Hostachy⁵⁷, S. Hou¹⁵⁴, A. Hoummada^{136a},
 J. Howarth⁴⁴, J. Hoya⁷³, M. Hrabovsky¹¹⁶, I. Hristova¹⁷, J. Hrivnac¹¹⁸, T. Hryn'ova⁵, A. Hrynevich⁹⁵,
 C. Hsu^{148c}, P.J. Hsu^{154,u}, S.-C. Hsu¹³⁹, Q. Hu⁵⁹, S. Hu¹⁴¹, Y. Huang⁴⁴, Z. Hubacek¹²⁹, F. Hubaut⁸⁷,
 F. Huegging²³, T.B. Huffman¹²¹, E.W. Hughes³⁷, G. Hughes⁷⁴, M. Huhtinen³², P. Huo¹⁵¹,

N. Huseynov^{67,b}, J. Huston⁹², J. Huth⁵⁸, G. Iacobucci⁵¹, G. Iakovidis²⁷, I. Ibragimov¹⁴⁴,
 L. Iconomidou-Fayard¹¹⁸, E. Ideal¹⁸⁰, Z. Idrissi^{136e}, P. Iengo³², O. Igonkina^{108,v}, T. Iizawa¹⁷⁵,
 Y. Ikegami⁶⁸, M. Ikeno⁶⁸, Y. Ilchenko^{11,w}, D. Iliadis¹⁵⁷, N. Ilic¹⁴⁶, T. Ince¹⁰², G. Introzzi^{122a,122b},
 P. Ioannou^{9,*}, M. Iodice^{135a}, K. Iordanidou³⁷, V. Ippolito⁵⁸, N. Ishijima¹¹⁹, M. Ishino¹⁵⁸, M. Ishitsuka¹⁶⁰,
 R. Ishmukhametov¹¹², C. Issever¹²¹, S. Istin^{20a}, F. Ito¹⁶⁵, J.M. Iturbe Ponce⁸⁶, R. Iuppa^{163a,163b},
 W. Iwanski⁶⁴, H. Iwasaki⁶⁸, J.M. Izen⁴³, V. Izzo^{105a}, S. Jabbar³, B. Jackson¹²³, P. Jackson¹, V. Jain²,
 K.B. Jakobi⁸⁵, K. Jakobs⁵⁰, S. Jakobsen³², T. Jakoubek¹²⁸, D.O. Jamin¹¹⁵, D.K. Jana⁸¹, R. Jansky⁶⁴,
 J. Janssen²³, M. Janus⁵⁶, G. Jarlskog⁸³, N. Javadov^{67,b}, T. Javůrek⁵⁰, F. Jeanneau¹³⁷, L. Jeanty¹⁶,
 G.-Y. Jeng¹⁵³, D. Jennens⁹⁰, P. Jenni^{50,x}, C. Jeske¹⁷⁴, S. Jézéquel⁵, H. Ji¹⁷⁷, J. Jia¹⁵¹, H. Jiang⁶⁶,
 Y. Jiang⁵⁹, S. Jiggins⁸⁰, J. Jimenez Pena¹⁷¹, S. Jin^{35a}, A. Jinaru^{28b}, O. Jinnouchi¹⁶⁰, H. Jivan^{148c},
 P. Johansson¹⁴², K.A. Johns⁷, W.J. Johnson¹³⁹, K. Jon-And^{149a,149b}, G. Jones¹⁷⁴, R.W.L. Jones⁷⁴,
 S. Jones⁷, T.J. Jones⁷⁶, J. Jongmanns^{60a}, P.M. Jorge^{127a,127b}, J. Jovicevic^{164a}, X. Ju¹⁷⁷, A. Juste Rozas^{13,s},
 M.K. Köhler¹⁷⁶, A. Kaczmarzka⁴¹, M. Kado¹¹⁸, H. Kagan¹¹², M. Kagan¹⁴⁶, S.J. Kahn⁸⁷, T. Kaji¹⁷⁵,
 E. Kajomovitz⁴⁷, C.W. Kalderon¹²¹, A. Kaluza⁸⁵, S. Kama⁴², A. Kamenshchikov¹³¹, N. Kanaya¹⁵⁸,
 S. Kaneti³⁰, L. Kanjir⁷⁷, V.A. Kantserov⁹⁹, J. Kanzaki⁶⁸, B. Kaplan¹¹¹, L.S. Kaplan¹⁷⁷, A. Kapliy³³,
 D. Kar^{148c}, K. Karakostas¹⁰, A. Karamaoun³, N. Karastathis¹⁰, M.J. Kareem⁵⁶, E. Karentzos¹⁰,
 M. Karnevskiy⁸⁵, S.N. Karpov⁶⁷, Z.M. Karpova⁶⁷, K. Karthik¹¹¹, V. Kartvelishvili⁷⁴,
 A.N. Karyukhin¹³¹, K. Kasahara¹⁶⁵, L. Kashif¹⁷⁷, R.D. Kass¹¹², A. Kastanas¹⁵, Y. Kataoka¹⁵⁸,
 C. Kato¹⁵⁸, A. Katre⁵¹, J. Katzy⁴⁴, K. Kawade¹⁰⁴, K. Kawagoe⁷², T. Kawamoto¹⁵⁸, G. Kawamura⁵⁶,
 V.F. Kazanin^{110,c}, R. Keeler¹⁷³, R. Kehoe⁴², J.S. Keller⁴⁴, J.J. Kempster⁷⁹, H. Keoshkerian¹⁶²,
 O. Kepka¹²⁸, B.P. Kerševan⁷⁷, S. Kersten¹⁷⁹, R.A. Keyes⁸⁹, M. Khader¹⁷⁰, F. Khalil-zada¹²,
 A. Khanov¹¹⁵, A.G. Kharlamov^{110,c}, T. Kharlamova¹¹⁰, T.J. Khoo⁵¹, V. Khovanskiy⁹⁸, E. Khramov⁶⁷,
 J. Khubua^{53b,y}, S. Kido⁶⁹, C.R. Kilby⁷⁹, H.Y. Kim⁸, S.H. Kim¹⁶⁵, Y.K. Kim³³, N. Kimura¹⁵⁷,
 O.M. Kind¹⁷, B.T. King⁷⁶, M. King¹⁷¹, J. Kirk¹³², A.E. Kiryunin¹⁰², T. Kishimoto¹⁵⁸, D. Kisielewska^{40a},
 F. Kiss⁵⁰, K. Kiuchi¹⁶⁵, O. Kivernyk¹³⁷, E. Kladiva^{147b}, M.H. Klein³⁷, M. Klein⁷⁶, U. Klein⁷⁶,
 K. Kleinknecht⁸⁵, P. Klimek¹⁰⁹, A. Klimentov²⁷, R. Klingenberg⁴⁵, J.A. Klinger¹⁴², T. Klioutchnikova³²,
 E.-E. Kluge^{60a}, P. Kluit¹⁰⁸, S. Kluth¹⁰², J. Knapik⁴¹, E. Kneringer⁶⁴, E.B.F.G. Knoops⁸⁷, A. Knue⁵⁵,
 A. Kobayashi¹⁵⁸, D. Kobayashi¹⁶⁰, T. Kobayashi¹⁵⁸, M. Kobel¹⁴⁶, M. Kocian¹⁴⁶, P. Kodys¹³⁰,
 N.M. Koehler¹⁰², T. Koffas³¹, E. Koffeman¹⁰⁸, T. Koi¹⁴⁶, H. Kolanoski¹⁷, M. Kolb^{60b}, I. Koletsou⁵,
 A.A. Komar^{97,*}, Y. Komori¹⁵⁸, T. Kondo⁶⁸, N. Kondrashova⁴⁴, K. Köneke⁵⁰, A.C. König¹⁰⁷,
 T. Kono^{68,z}, R. Konoplich^{111,aa}, N. Konstantinidis⁸⁰, R. Kopeliansky⁶³, S. Koperny^{40a}, L. Köpke⁸⁵,
 A.K. Kopp⁵⁰, K. Korcyl⁴¹, K. Kordas¹⁵⁷, A. Korn⁸⁰, A.A. Korol^{110,c}, I. Korolkov¹³, E.V. Korolkova¹⁴²,
 O. Kortner¹⁰², S. Kortner¹⁰², T. Kosek¹³⁰, V.V. Kostyukhin²³, A. Kotwal⁴⁷,
 A. Kourkoumeli-Charalampidi^{122a,122b}, C. Kourkoumelis⁹, V. Kouskoura²⁷, A.B. Kowalewska⁴¹,
 R. Kowalewski¹⁷³, T.Z. Kowalski^{40a}, C. Kozakai¹⁵⁸, W. Kozanecki¹³⁷, A.S. Kozhin¹³¹,
 V.A. Kramarenko¹⁰⁰, G. Kramberger⁷⁷, D. Krasnopevtsev⁹⁹, M.W. Krasny⁸², A. Krasznahorkay³²,
 A. Kravchenko²⁷, M. Kretz^{60c}, J. Kretzschmar⁷⁶, K. Kreutzfeldt⁵⁴, P. Krieger¹⁶², K. Krizka³³,
 K. Kroeninger⁴⁵, H. Kroha¹⁰², J. Kroll¹²³, J. Kroseberg²³, J. Krstic¹⁴, U. Kruchonak⁶⁷, H. Krüger²³,
 N. Krumnack⁶⁶, M.C. Kruse⁴⁷, M. Kruskal²⁴, T. Kubota⁹⁰, H. Kucuk⁸⁰, S. Kудay^{4b}, J.T. Kuechler¹⁷⁹,
 S. Kuehn⁵⁰, A. Kugel^{160c}, F. Kuger¹⁷⁸, A. Kuhl¹³⁸, T. Kuhl⁴⁴, V. Kukhtin⁶⁷, R. Kukla¹³⁷, Y. Kulchitsky⁹⁴,
 S. Kuleshov^{34b}, M. Kuna^{133a,133b}, T. Kunigo⁷⁰, A. Kupco¹²⁸, H. Kurashige⁶⁹, Y.A. Kurochkin⁹⁴,
 V. Kus¹²⁸, E.S. Kuwertz¹⁷³, M. Kuze¹⁶⁰, J. Kvitá¹¹⁶, T. Kwan¹⁷³, D. Kyriazopoulos¹⁴², A. La Rosa¹⁰²,
 J.L. La Rosa Navarro^{26d}, L. La Rotonda^{39a,39b}, C. Lacasta¹⁷¹, F. Lacava^{133a,133b}, J. Lacey³¹, H. Lacker¹⁷,
 D. Lacour⁸², V.R. Lacuesta¹⁷¹, E. Ladygin⁶⁷, R. Lafaye⁵, B. Laforge⁸², T. Lagouri¹⁸⁰, S. Lai⁵⁶,
 S. Lammers⁶³, W. Lampl⁷, E. Lançon¹³⁷, U. Landgraf⁵⁰, M.P.J. Landon⁷⁸, M.C. Lanfermann⁵¹,
 V.S. Lang^{60a}, J.C. Lange¹³, A.J. Lankford¹⁶⁷, F. Lanni²⁷, K. Lantzsck²³, A. Lanza^{122a}, S. Laplace⁸²,
 C. Lapoire³², J.F. Laporte¹³⁷, T. Lari^{93a}, F. Lasagni Manghi^{22a,22b}, M. Lassnig³², P. Laurelli⁴⁹,

W. Lavrijsen¹⁶, A.T. Law¹³⁸, P. Laycock⁷⁶, T. Lazovich⁵⁸, M. Lazzaroni^{93a,93b}, B. Le⁹⁰, O. Le Dortz⁸²,
 E. Le Guirriec⁸⁷, E.P. Le Quilleuc¹³⁷, M. LeBlanc¹⁷³, T. LeCompte⁶, F. Ledroit-Guillon⁵⁷, C.A. Lee²⁷,
 S.C. Lee¹⁵⁴, L. Lee¹, B. Lefebvre⁸⁹, G. Lefebvre⁸², M. Lefebvre¹⁷³, F. Legger¹⁰¹, C. Leggett¹⁶,
 A. Lehan⁷⁶, G. Lehmann Miotto³², X. Lei⁷, W.A. Leight³¹, A.G. Leister¹⁸⁰, M.A.L. Leite^{26d},
 R. Leitner¹³⁰, D. Lellouch¹⁷⁶, B. Lemmer⁵⁶, K.J.C. Leney⁸⁰, T. Lenz²³, B. Lenzi³², R. Leone⁷,
 S. Leone^{125a,125b}, C. Leonidopoulos⁴⁸, S. Leontsinis¹⁰, G. Lerner¹⁵², C. Leroy⁹⁶, A.A.J. Lesage¹³⁷,
 C.G. Lester³⁰, M. Levchenko¹²⁴, J. Levêque⁵, D. Levin⁹¹, L.J. Levinson¹⁷⁶, M. Levy¹⁹, D. Lewis⁷⁸,
 A.M. Leyko²³, M. Leyton⁴³, B. Li^{59,p}, C. Li⁵⁹, H. Li¹⁵¹, H.L. Li³³, L. Li⁴⁷, L. Li¹⁴¹, Q. Li^{35a}, S. Li⁴⁷,
 X. Li⁸⁶, Y. Li¹⁴⁴, Z. Liang^{35a}, B. Liberti^{134a}, A. Liblong¹⁶², P. Lichard³², K. Lie¹⁷⁰, J. Liebal²³,
 W. Liebig¹⁵, A. Limosani¹⁵³, S.C. Lin^{154,ab}, T.H. Lin⁸⁵, B.E. Lindquist¹⁵¹, A.E. Lioni⁵¹, E. Lipeles¹²³,
 A. Lipniacka¹⁵, M. Lisovyi^{60b}, T.M. Liss¹⁷⁰, A. Lister¹⁷², A.M. Litke¹³⁸, B. Liu^{154,ac}, D. Liu¹⁵⁴,
 H. Liu⁹¹, H. Liu²⁷, J. Liu⁸⁷, J.B. Liu⁵⁹, K. Liu⁸⁷, L. Liu¹⁷⁰, M. Liu⁴⁷, M. Liu⁵⁹, Y.L. Liu⁵⁹, Y. Liu⁵⁹,
 M. Livan^{122a,122b}, A. Lleres⁵⁷, J. Llorente Merino^{35a}, S.L. Lloyd⁷⁸, F. Lo Sterzo¹⁵⁴, E.M. Lobodzinska⁴⁴,
 P. Loch⁷, W.S. Lockman¹³⁸, F.K. Loebinger⁸⁶, A.E. Loevschall-Jensen³⁸, K.M. Loew²⁵,
 A. Loginov^{180,*}, T. Lohse¹⁷, K. Lohwasser⁴⁴, M. Lokajicek¹²⁸, B.A. Long²⁴, J.D. Long¹⁷⁰, R.E. Long⁷⁴,
 L. Longo^{75a,75b}, K.A. Looper¹¹², J.A. López^{34b}, D. Lopez Mateos⁵⁸, B. Lopez Paredes¹⁴²,
 I. Lopez Paz¹³, A. Lopez Solis⁸², J. Lorenz¹⁰¹, N. Lorenzo Martinez⁶³, M. Losada²¹, P.J. Lösel¹⁰¹,
 X. Lou^{35a}, A. Lounis¹¹⁸, J. Love⁶, P.A. Love⁷⁴, H. Lu^{62a}, N. Lu⁹¹, H.J. Lubatti¹³⁹, C. Luci^{133a,133b},
 A. Lucotte⁵⁷, C. Luedtke⁵⁰, F. Luehring⁶³, W. Lukas⁶⁴, L. Luminari^{133a}, O. Lundberg^{149a,149b},
 B. Lund-Jensen¹⁵⁰, P.M. Luzzi⁸², D. Lynn²⁷, R. Lysak¹²⁸, E. Lytken⁸³, V. Lyubushkin⁶⁷, H. Ma²⁷,
 L.L. Ma¹⁴⁰, Y. Ma¹⁴⁰, G. Maccarrone⁴⁹, A. Macchiolo¹⁰², C.M. Macdonald¹⁴², B. Maček⁷⁷,
 J. Machado Miguens^{123,127b}, D. Madaffari⁸⁷, R. Madar³⁶, H.J. Maddocks¹⁶⁹, W.F. Mader⁴⁶,
 A. Madsen⁴⁴, J. Maeda⁶⁹, S. Maeland¹⁵, T. Maeno²⁷, A. Maeviskiy¹⁰⁰, E. Magradze⁵⁶, J. Mahlstedt¹⁰⁸,
 C. Maiani¹¹⁸, C. Maidantchik^{26a}, A.A. Maier¹⁰², T. Maier¹⁰¹, A. Maio^{127a,127b,127d}, S. Majewski¹¹⁷,
 Y. Makida⁶⁸, N. Makovec¹¹⁸, B. Malaescu⁸², Pa. Malecki⁴¹, V.P. Maleev¹²⁴, F. Malek⁵⁷, U. Mallik⁶⁵,
 D. Malon⁶, C. Malone¹⁴⁶, C. Malone³⁰, S. Maltezos¹⁰, S. Malyukov³², J. Mamuzic¹⁷¹, G. Mancini⁴⁹,
 L. Mandelli^{93a}, I. Mandić⁷⁷, J. Maneira^{127a,127b}, L. Manhaes de Andrade Filho^{26b},
 J. Manjarres Ramos^{164b}, A. Mann¹⁰¹, A. Manousos³², B. Mansoulie¹³⁷, J.D. Mansour^{35a}, R. Mantifel⁸⁹,
 M. Mantoani⁵⁶, S. Manzoni^{93a,93b}, L. Mapelli³², G. Marceca²⁹, L. March⁵¹, G. Marchiori⁸²,
 M. Marcisovsky¹²⁸, M. Marjanovic¹⁴, D.E. Marley⁹¹, F. Marroquim^{26a}, S.P. Marsden⁸⁶, Z. Marshall¹⁶,
 S. Marti-Garcia¹⁷¹, B. Martin⁹², T.A. Martin¹⁷⁴, V.J. Martin⁴⁸, B. Martin dit Latour¹⁵, M. Martinez^{13,s},
 V.I. Martinez Outschoorn¹⁷⁰, S. Martin-Haugh¹³², V.S. Martoiu^{28b}, A.C. Martyniuk⁸⁰, M. Marx¹³⁹,
 A. Marzin³², L. Masetti⁸⁵, T. Mashimo¹⁵⁸, R. Mashinistov⁹⁷, J. Masik⁸⁶, A.L. Maslennikov^{110,c},
 I. Massa^{22a,22b}, L. Massa^{22a,22b}, P. Mastrandrea⁵, A. Mastroberardino^{39a,39b}, T. Masubuchi¹⁵⁸,
 P. Mättig¹⁷⁹, J. Mattmann⁸⁵, J. Maurer^{28b}, S.J. Maxfield⁷⁶, D.A. Maximov^{110,c}, R. Mazini¹⁵⁴,
 S.M. Mazza^{93a,93b}, N.C. Mc Fadden¹⁰⁶, G. Mc Goldrick¹⁶², S.P. Mc Kee⁹¹, A. McCarn⁹¹,
 R.L. McCarthy¹⁵¹, T.G. McCarthy¹⁰², L.I. McClymont⁸⁰, E.F. McDonald⁹⁰, J.A. McFayden⁸⁰,
 G. Mchedlidze⁵⁶, S.J. McMahon¹³², R.A. McPherson^{173,m}, M. Medinnis⁴⁴, S. Meehan¹³⁹,
 S. Mehlhase¹⁰¹, A. Mehta⁷⁶, K. Meier^{60a}, C. Meineck¹⁰¹, B. Meirose⁴³, D. Melini¹⁷¹,
 B.R. Mellado Garcia^{148c}, M. Melo^{147a}, F. Meloni¹⁸, A. Mengarelli^{22a,22b}, S. Menke¹⁰², E. Meoni¹⁶⁶,
 S. Mergelmeyer¹⁷, P. Mermod⁵¹, L. Merola^{105a,105b}, C. Meroni^{93a}, F.S. Merritt³³, A. Messina^{133a,133b},
 J. Metcalfe⁶, A.S. Mete¹⁶⁷, C. Meyer⁸⁵, C. Meyer¹²³, J-P. Meyer¹³⁷, J. Meyer¹⁰⁸,
 H. Meyer Zu Theenhausen^{60a}, F. Miano¹⁵², R.P. Middleton¹³², S. Miglioranzi^{52a,52b}, L. Mijović⁴⁸,
 G. Mikenberg¹⁷⁶, M. Mikestikova¹²⁸, M. Mikuž⁷⁷, M. Milesi⁹⁰, A. Milic⁶⁴, D.W. Miller³³, C. Mills⁴⁸,
 A. Milov¹⁷⁶, D.A. Milstead^{149a,149b}, A.A. Minaenko¹³¹, Y. Minami¹⁵⁸, I.A. Minashvili⁶⁷, A.I. Mincer¹¹¹,
 B. Mindur^{40a}, M. Mineev⁶⁷, Y. Minegishi¹⁵⁸, Y. Ming¹⁷⁷, L.M. Mir¹³, K.P. Mistry¹²³, T. Mitani¹⁷⁵,
 J. Mitrevski¹⁰¹, V.A. Mitsou¹⁷¹, A. Miucci¹⁸, P.S. Miyagawa¹⁴², J.U. Mjörnmark⁸³, M. Mlynarikova¹³⁰,

T. Moa^{149a,149b}, K. Mochizuki⁹⁶, S. Mohapatra³⁷, S. Molander^{149a,149b}, R. Moles-Valls²³, R. Monden⁷⁰, M.C. Mondragon⁹², K. Mönig⁴⁴, J. Monk³⁸, E. Monnier⁸⁷, A. Montalbano¹⁵¹, J. Montejo Berlingen³², F. Monticelli⁷³, S. Monzani^{93a,93b}, R.W. Moore³, N. Morange¹¹⁸, D. Moreno²¹, M. Moreno Llácer⁵⁶, P. Morettini^{52a}, S. Morgenstern³², D. Mori¹⁴⁵, T. Mori¹⁵⁸, M. Morii⁵⁸, M. Morinaga¹⁵⁸, V. Morisbak¹²⁰, S. Moritz⁸⁵, A.K. Morley¹⁵³, G. Mornacchi³², J.D. Morris⁷⁸, S.S. Mortensen³⁸, L. Morvaj¹⁵¹, M. Mosidze^{53b}, J. Moss^{146,ad}, K. Motohashi¹⁶⁰, R. Mount¹⁴⁶, E. Mountricha²⁷, E.J.W. Moyses⁸⁸, S. Muanza⁸⁷, R.D. Mudd¹⁹, F. Mueller¹⁰², J. Mueller¹²⁶, R.S.P. Mueller¹⁰¹, T. Mueller³⁰, D. Muenstermann⁷⁴, P. Mullen⁵⁵, G.A. Mullier¹⁸, F.J. Munoz Sanchez⁸⁶, J.A. Murillo Quijada¹⁹, W.J. Murray^{174,132}, H. Musheghyan⁵⁶, M. Muškinja⁷⁷, A.G. Myagkov^{131,ae}, M. Myska¹²⁹, B.P. Nachman¹⁴⁶, O. Nackenhorst⁵¹, K. Nagai¹²¹, R. Nagai^{68,z}, K. Nagano⁶⁸, Y. Nagasaka⁶¹, K. Nagata¹⁶⁵, M. Nagel⁵⁰, E. Nagy⁸⁷, A.M. Nairz³², Y. Nakahama¹⁰⁴, K. Nakamura⁶⁸, T. Nakamura¹⁵⁸, I. Nakano¹¹³, H. Namasivayam⁴³, R.F. Naranjo Garcia⁴⁴, R. Narayan¹¹, D.I. Narrias Villar^{60a}, I. Naryshkin¹²⁴, T. Naumann⁴⁴, G. Navarro²¹, R. Nayyar⁷, H.A. Neal⁹¹, P.Yu. Nechaeva⁹⁷, T.J. Neep⁸⁶, A. Negri^{122a,122b}, M. Negrini^{22a}, S. Nektarijevic¹⁰⁷, C. Nellist¹¹⁸, A. Nelson¹⁶⁷, S. Nemecek¹²⁸, P. Nemethy¹¹¹, A.A. Nepomuceno^{26a}, M. Nessi^{32,af}, M.S. Neubauer¹⁷⁰, M. Neumann¹⁷⁹, R.M. Neves¹¹¹, P. Nevski²⁷, P.R. Newman¹⁹, D.H. Nguyen⁶, T. Nguyen Manh⁹⁶, R.B. Nickerson¹²¹, R. Nicolaidou¹³⁷, J. Nielsen¹³⁸, A. Nikiforov¹⁷, V. Nikolaenko^{131,ae}, I. Nikolic-Audit⁸², K. Nikolopoulos¹⁹, J.K. Nilsen¹²⁰, P. Nilsson²⁷, Y. Ninomiya¹⁵⁸, A. Nisati^{133a}, R. Nisius¹⁰², T. Nobe¹⁵⁸, M. Nomachi¹¹⁹, I. Nomidis³¹, T. Nooney⁷⁸, S. Norberg¹¹⁴, M. Nordberg³², N. Norjoharuddeen¹²¹, O. Novgorodova⁴⁶, S. Nowak¹⁰², M. Nozaki⁶⁸, L. Nozka¹¹⁶, K. Ntekas¹⁶⁷, E. Nurse⁸⁰, F. Nuti⁹⁰, F. O'grady⁷, D.C. O'Neil¹⁴⁵, A.A. O'Rourke⁴⁴, V. O'Shea⁵⁵, F.G. Oakham^{31,d}, H. Oberlack¹⁰², T. Obermann²³, J. Ocariz⁸², A. Ochi⁶⁹, I. Ochoa³⁷, J.P. Ochoa-Ricoux^{34a}, S. Oda⁷², S. Odaka⁶⁸, H. Ogren⁶³, A. Oh⁸⁶, S.H. Oh⁴⁷, C.C. Ohm¹⁶, H. Ohman¹⁶⁹, H. Oide³², H. Okawa¹⁶⁵, Y. Okumura¹⁵⁸, T. Okuyama⁶⁸, A. Olariu^{28b}, L.F. Oleiro Seabra^{127a}, S.A. Olivares Pino⁴⁸, D. Oliveira Damazio²⁷, A. Olszewski⁴¹, J. Olszowska⁴¹, A. Onofre^{127a,127e}, K. Onogi¹⁰⁴, P.U.E. Onyisi^{11,w}, M.J. Oreglia³³, Y. Oren¹⁵⁶, D. Orestano^{135a,135b}, N. Orlando^{62b}, R.S. Ori¹⁶², B. Osculati^{52a,52b,*}, R. Ospanov⁸⁶, G. Otero y Garzon²⁹, H. Otono⁷², M. Ouchrif^{136d}, F. Ould-Saada¹²⁰, A. Ouraou¹³⁷, K.P. Oussoren¹⁰⁸, Q. Ouyang^{35a}, M. Owen⁵⁵, R.E. Owen¹⁹, V.E. Ozcan^{20a}, N. Ozturk⁸, K. Pachal¹⁴⁵, A. Pacheco Pages¹³, L. Pacheco Rodriguez¹³⁷, C. Padilla Aranda¹³, M. Pagáčová⁵⁰, S. Pagan Griso¹⁶, M. Paganini¹⁸⁰, F. Paige²⁷, P. Pais⁸⁸, K. Pajchel¹²⁰, G. Palacino^{164b}, S. Palazzo^{39a,39b}, S. Palestini³², M. Palka^{40b}, D. Pallin³⁶, E.St. Panagiotopoulou¹⁰, C.E. Pandini⁸², J.G. Panduro Vazquez⁷⁹, P. Pani^{149a,149b}, S. Panitkin²⁷, D. Pantea^{28b}, L. Paolozzi⁵¹, Th.D. Papadopoulou¹⁰, K. Papageorgiou¹⁵⁷, A. Paramonov⁶, D. Paredes Hernandez¹⁸⁰, A.J. Parker⁷⁴, M.A. Parker³⁰, K.A. Parker¹⁴², F. Parodi^{52a,52b}, J.A. Parsons³⁷, U. Parzefall⁵⁰, V.R. Pascuzzi¹⁶², E. Pasqualucci^{133a}, S. Passaggio^{52a}, Fr. Pastore⁷⁹, G. Pásztor^{31,ag}, S. Pataria¹⁷⁹, J.R. Pater⁸⁶, T. Pauly³², J. Pearce¹⁷³, B. Pearson¹¹⁴, L.E. Pedersen³⁸, M. Pedersen¹²⁰, S. Pedraza Lopez¹⁷¹, R. Pedro^{127a,127b}, S.V. Peleganchuk^{110,c}, O. Penc¹²⁸, C. Peng^{35a}, H. Peng⁵⁹, J. Penwell⁶³, B.S. Peralva^{26b}, M.M. Perego¹³⁷, D.V. Perepelitsa²⁷, E. Perez Codina^{164a}, L. Perini^{93a,93b}, H. Pernegger³², S. Perrella^{105a,105b}, R. Peschke⁴⁴, V.D. Peshekhonov⁶⁷, K. Peters⁴⁴, R.F.Y. Peters⁸⁶, B.A. Petersen³², T.C. Petersen³⁸, E. Petit⁵⁷, A. Petridis¹, C. Petridou¹⁵⁷, P. Petroff¹¹⁸, E. Petrolo^{133a}, M. Petrov¹²¹, F. Petrucci^{135a,135b}, N.E. Pettersson⁸⁸, A. Peyaud¹³⁷, R. Pezoa^{34b}, P.W. Phillips¹³², G. Piacquadio^{146,ah}, E. Pianori¹⁷⁴, A. Picazio⁸⁸, E. Piccaro⁷⁸, M. Piccinini^{22a,22b}, M.A. Pickering¹²¹, R. Piegaia²⁹, J.E. Pilcher³³, A.D. Pilkington⁸⁶, A.W.J. Pin⁸⁶, M. Pinamonti^{168a,168c,ai}, J.L. Pinfold³, A. Pingel³⁸, S. Pires⁸², H. Pirumov⁴⁴, M. Pitt¹⁷⁶, L. Plazak^{147a}, M.-A. Pleier²⁷, V. Pleskot⁸⁵, E. Plotnikova⁶⁷, P. Plucinski⁹², D. Pluth⁶⁶, R. Poettgen^{149a,149b}, L. Poggioli¹¹⁸, D. Pohl²³, G. Polesello^{122a}, A. Poley⁴⁴, A. Policicchio^{39a,39b}, R. Polifka¹⁶², A. Polini^{22a}, C.S. Pollard⁵⁵, V. Polychronakos²⁷, K. Pommès³², L. Pontecorvo^{133a}, B.G. Pope⁹², G.A. Popeneciu^{28c}, A. Poppleton³², S. Pospisil¹²⁹, K. Potamianos¹⁶, I.N. Potrap⁶⁷, C.J. Potter³⁰, C.T. Potter¹¹⁷, G. Poulard³², J. Poveda³²,

V. Pozdnyakov⁶⁷, M.E. Pozo Astigarraga³², P. Pralavorio⁸⁷, A. Pranko¹⁶, S. Prell⁶⁶, D. Price⁸⁶, L.E. Price⁶, M. Primavera^{75a}, S. Prince⁸⁹, K. Prokofiev^{62c}, F. Prokoshin^{34b}, S. Protopopescu²⁷, J. Proudfoot⁶, M. Przybycien^{40a}, D. Puddu^{135a,135b}, M. Purohit^{27,aj}, P. Puzo¹¹⁸, J. Qian⁹¹, G. Qin⁵⁵, Y. Qin⁸⁶, A. Quadt⁵⁶, W.B. Quayle^{168a,168b}, M. Queitsch-Maitland⁸⁶, D. Quilty⁵⁵, S. Raddum¹²⁰, V. Radeka²⁷, V. Radescu¹²¹, S.K. Radhakrishnan¹⁵¹, P. Radloff¹¹⁷, P. Rados⁹⁰, F. Ragusa^{93a,93b}, G. Rahal¹⁸², J.A. Raine⁸⁶, S. Rajagopalan²⁷, M. Rammensee³², C. Rangel-Smith¹⁶⁹, M.G. Ratti^{93a,93b}, F. Rauscher¹⁰¹, S. Rave⁸⁵, T. Ravenscroft⁵⁵, I. Ravinovich¹⁷⁶, M. Raymond³², A.L. Read¹²⁰, N.P. Readioff⁷⁶, M. Reale^{75a,75b}, D.M. Rebuffi^{122a,122b}, A. Redelbach¹⁷⁸, G. Redlinger²⁷, R. Reece¹³⁸, R.G. Reed^{148c}, K. Reeves⁴³, L. Rehnisch¹⁷, J. Reichert¹²³, A. Reiss⁸⁵, C. Rembser³², H. Ren^{35a}, M. Rescigno^{133a}, S. Resconi^{93a}, O.L. Rezanova^{110,c}, P. Reznicek¹³⁰, R. Rezvani⁹⁶, R. Richter¹⁰², S. Richter⁸⁰, E. Richter-Was^{40b}, O. Ricken²³, M. Ridel⁸², P. Rieck¹⁷, C.J. Riegel¹⁷⁹, J. Rieger⁵⁶, O. Rifki¹¹⁴, M. Rijssenbeek¹⁵¹, A. Rimoldi^{122a,122b}, M. Rimoldi¹⁸, L. Rinaldi^{22a}, B. Ristic⁵¹, E. Ritsch³², I. Riu¹³, F. Rizatdinova¹¹⁵, E. Rizvi⁷⁸, C. Rizzi¹³, S.H. Robertson^{89,m}, A. Robichaud-Veronneau⁸⁹, D. Robinson³⁰, J.E.M. Robinson⁴⁴, A. Robson⁵⁵, C. Roda^{125a,125b}, Y. Rodina^{87,ak}, A. Rodriguez Perez¹³, D. Rodriguez Rodriguez¹⁷¹, S. Roe³², C.S. Rogan⁵⁸, O. Røhne¹²⁰, A. Romaniouk⁹⁹, M. Romano^{22a,22b}, S.M. Romano Saez³⁶, E. Romero Adam¹⁷¹, N. Rompotis¹³⁹, M. Ronzani⁵⁰, L. Roos⁸², E. Ros¹⁷¹, S. Rosati^{133a}, K. Rosbach⁵⁰, P. Rose¹³⁸, N.-A. Rosien⁵⁶, V. Rossetti^{149a,149b}, E. Rossi^{105a,105b}, L.P. Rossi^{52a}, J.H.N. Rosten³⁰, R. Rosten¹³⁹, M. Rotaru^{28b}, I. Roth¹⁷⁶, J. Rothberg¹³⁹, D. Rousseau¹¹⁸, A. Rozanov⁸⁷, Y. Rozen¹⁵⁵, X. Ruan^{148c}, F. Rubbo¹⁴⁶, M.S. Rudolph¹⁶², F. Rühr⁵⁰, A. Ruiz-Martinez³¹, Z. Rurikova⁵⁰, N.A. Rusakovich⁶⁷, A. Ruschke¹⁰¹, H.L. Russell¹³⁹, J.P. Rutherford⁷, N. Ruthmann³², Y.F. Ryabov¹²⁴, M. Rybar¹⁷⁰, G. Rybkin¹¹⁸, S. Ryu⁶, A. Ryzhov¹³¹, G.F. Rzehorz⁵⁶, A.F. Saavedra¹⁵³, G. Sabato¹⁰⁸, S. Sacerdoti²⁹, H.F.-W. Sadrozinski¹³⁸, R. Sadykov⁶⁷, F. Safai Tehrani^{133a}, P. Saha¹⁰⁹, M. Sahinsoy^{60a}, M. Saimpert¹³⁷, T. Saito¹⁵⁸, H. Sakamoto¹⁵⁸, Y. Sakurai¹⁷⁵, G. Salamanna^{135a,135b}, A. Salamon^{134a,134b}, J.E. Salazar Loyola^{34b}, D. Salek¹⁰⁸, P.H. Sales De Bruin¹³⁹, D. Salihagic¹⁰², A. Salnikov¹⁴⁶, J. Salt¹⁷¹, D. Salvatore^{39a,39b}, F. Salvatore¹⁵², A. Salvucci^{62a,62b,62c}, A. Salzburger³², D. Sammel⁵⁰, D. Sampsonidis¹⁵⁷, J. Sánchez¹⁷¹, V. Sanchez Martinez¹⁷¹, A. Sanchez Pineda^{105a,105b}, H. Sandaker¹²⁰, R.L. Sandbach⁷⁸, H.G. Sander⁸⁵, M. Sandhoff¹⁷⁹, C. Sandoval²¹, D.P.C. Sankey¹³², M. Sannino^{52a,52b}, A. Sansoni⁴⁹, C. Santoni³⁶, R. Santonico^{134a,134b}, H. Santos^{127a}, I. Santoyo Castillo¹⁵², K. Sapp¹²⁶, A. Saprnov⁶⁷, J.G. Saraiva^{127a,127d}, B. Sarrazin²³, O. Sasaki⁶⁸, K. Sato¹⁶⁵, E. Sauvan⁵, G. Savage⁷⁹, P. Savard^{162,d}, N. Savic¹⁰², C. Sawyer¹³², L. Sawyer^{81,r}, J. Saxon³³, C. Sbarra^{22a}, A. Sbrizzi^{22a,22b}, T. Scanlon⁸⁰, D.A. Scannicchio¹⁶⁷, M. Scarcella¹⁵³, V. Scarfone^{39a,39b}, J. Schaarschmidt¹⁷⁶, P. Schacht¹⁰², B.M. Schachtner¹⁰¹, D. Schaefer³², L. Schaefer¹²³, R. Schaefer⁴⁴, J. Schaeffer⁸⁵, S. Schaepe²³, S. Schaezel^{60b}, U. Schäfer⁸⁵, A.C. Schaffer¹¹⁸, D. Schaile¹⁰¹, R.D. Schamberger¹⁵¹, V. Scharf^{60a}, V.A. Schegelsky¹²⁴, D. Scheirich¹³⁰, M. Schernau¹⁶⁷, C. Schiavi^{52a,52b}, S. Schier¹³⁸, C. Schillo⁵⁰, M. Schioppa^{39a,39b}, S. Schlenker³², K.R. Schmidt-Sommerfeld¹⁰², K. Schmieden³², C. Schmitt⁸⁵, S. Schmitt⁴⁴, S. Schmitz⁸⁵, B. Schneider^{164a}, U. Schnoor⁵⁰, L. Schoeffel¹³⁷, A. Schoening^{60b}, B.D. Schoenrock⁹², E. Schopf²³, M. Schott⁸⁵, J.F.P. Schouwenberg¹⁰⁷, J. Schovancova⁸, S. Schramm⁵¹, M. Schreyer¹⁷⁸, N. Schuh⁸⁵, A. Schulte⁸⁵, M.J. Schultens²³, H.-C. Schultz-Coulon^{60a}, H. Schulz¹⁷, M. Schumacher⁵⁰, B.A. Schumm¹³⁸, Ph. Schune¹³⁷, A. Schwartzman¹⁴⁶, T.A. Schwarz⁹¹, H. Schweiger⁸⁶, Ph. Schwemling¹³⁷, R. Schwienhorst⁹², J. Schwindling¹³⁷, T. Schwindt²³, G. Sciolla²⁵, F. Scuri^{125a,125b}, F. Scutti⁹⁰, J. Searcy⁹¹, P. Seema²³, S.C. Seidel¹⁰⁶, A. Seiden¹³⁸, F. Seifert¹²⁹, J.M. Seixas^{26a}, G. Sekhniaidze^{105a}, K. Sekhon⁹¹, S.J. Sekula⁴², D.M. Seliverstov^{124,*}, N. Semprini-Cesari^{22a,22b}, C. Serfon¹²⁰, L. Serin¹¹⁸, L. Serkin^{168a,168b}, M. Sessa^{135a,135b}, R. Seuster¹⁷³, H. Severini¹¹⁴, T. Sfiligoi⁷⁷, F. Sforza³², A. Sfyrla⁵¹, E. Shabalina⁵⁶, N.W. Shaikh^{149a,149b}, L.Y. Shan^{35a}, R. Shang¹⁷⁰, J.T. Shank²⁴, M. Shapiro¹⁶, P.B. Shatalov⁹⁸, K. Shaw^{168a,168b}, S.M. Shaw⁸⁶, A. Shcherbakova^{149a,149b}, C.Y. Shehu¹⁵², P. Sherwood⁸⁰, L. Shi^{154,al}, S. Shimizu⁶⁹, C.O. Shimmmin¹⁶⁷, M. Shimojima¹⁰³, S. Shirabe⁷²,

M. Shiyakova^{67.am}, A. Shmeleva⁹⁷, D. Shoaleh Saadi⁹⁶, M.J. Shochet³³, S. Shojaii^{93a,93b}, D.R. Shope¹¹⁴,
S. Shrestha¹¹², E. Shulga⁹⁹, M.A. Shupe⁷, P. Sicho¹²⁸, A.M. Sickles¹⁷⁰, P.E. Sidebo¹⁵⁰,
O. Sidiropoulou¹⁷⁸, D. Sidorov¹¹⁵, A. Sidoti^{22a,22b}, F. Siegert⁴⁶, Dj. Sijacki¹⁴, J. Silva^{127a,127d},
S.B. Silverstein^{149a}, V. Simak¹²⁹, Lj. Simic¹⁴, S. Simion¹¹⁸, E. Simioni⁸⁵, B. Simmons⁸⁰, D. Simon³⁶,
M. Simon⁸⁵, P. Sinervo¹⁶², N.B. Sinev¹¹⁷, M. Sioli^{22a,22b}, G. Siragusa¹⁷⁸, S.Yu. Sivoklov¹⁰⁰,
J. Sjölin^{149a,149b}, M.B. Skinner⁷⁴, H.P. Skottowe⁵⁸, P. Skubic¹¹⁴, M. Slater¹⁹, T. Slavicek¹²⁹,
M. Slawinska¹⁰⁸, K. Sliwa¹⁶⁶, R. Slovak¹³⁰, V. Smakhtin¹⁷⁶, B.H. Smart⁵, L. Smestad¹⁵, J. Smiesko^{147a},
S.Yu. Smirnov⁹⁹, Y. Smirnov⁹⁹, L.N. Smirnova^{100.an}, O. Smirnova⁸³, M.N.K. Smith³⁷, R.W. Smith³⁷,
M. Smizanska⁷⁴, K. Smolek¹²⁹, A.A. Snesarev⁹⁷, I.M. Snyder¹¹⁷, S. Snyder²⁷, R. Sobie^{173.m},
F. Socher⁴⁶, A. Soffer¹⁵⁶, D.A. Soh¹⁵⁴, G. Sokhrannyi⁷⁷, C.A. Solans Sanchez³², M. Solar¹²⁹,
E.Yu. Soldatov⁹⁹, U. Soldevila¹⁷¹, A.A. Solodkov¹³¹, A. Soloshenko⁶⁷, O.V. Solovyanov¹³¹,
V. Solovyev¹²⁴, P. Sommer⁵⁰, H. Son¹⁶⁶, H.Y. Song^{59.ao}, A. Sood¹⁶, A. Sopczak¹²⁹, V. Sopko¹²⁹,
V. Sorin¹³, D. Sosa^{60b}, C.L. Sotiropoulou^{125a,125b}, R. Soualah^{168a,168c}, A.M. Soukharev^{110.c}, D. South⁴⁴,
B.C. Sowden⁷⁹, S. Spagnolo^{75a,75b}, M. Spalla^{125a,125b}, M. Spangenberg¹⁷⁴, F. Spanò⁷⁹, D. Sperlich¹⁷,
F. Spettel¹⁰², R. Spighi^{22a}, G. Spigo³², L.A. Spiller⁹⁰, M. Spousta¹³⁰, R.D. St. Denis^{55.*}, A. Stabile^{93a},
R. Stamen^{60a}, S. Stamm¹⁷, E. Stanecka⁴¹, R.W. Stanek⁶, C. Stanescu^{135a}, M. Stanescu-Bellu⁴⁴,
M.M. Stanitzki⁴⁴, S. Stapnes¹²⁰, E.A. Starchenko¹³¹, G.H. Stark³³, J. Stark⁵⁷, P. Staroba¹²⁸,
P. Starovoitov^{60a}, S. Stärz³², R. Staszewski⁴¹, P. Steinberg²⁷, B. Stelzer¹⁴⁵, H.J. Stelzer³²,
O. Stelzer-Chilton^{164a}, H. Stenzel⁵⁴, G.A. Stewart⁵⁵, J.A. Stillings²³, M.C. Stockton⁸⁹, M. Stoebe⁸⁹,
G. Stoicea^{28b}, P. Stolte⁵⁶, S. Stonjek¹⁰², A.R. Stradling⁸, A. Straessner⁴⁶, M.E. Stramaglia¹⁸,
J. Strandberg¹⁵⁰, S. Strandberg^{149a,149b}, A. Strandlie¹²⁰, M. Strauss¹¹⁴, P. Strizenc^{147b}, R. Ströhmer¹⁷⁸,
D.M. Strom¹¹⁷, R. Stroynowski⁴², A. Strubig¹⁰⁷, S.A. Stucci²⁷, B. Stugu¹⁵, N.A. Styles⁴⁴, D. Su¹⁴⁶,
J. Su¹²⁶, S. Suchek^{60a}, Y. Sugaya¹¹⁹, M. Suk¹²⁹, V.V. Sulin⁹⁷, S. Sultansoy^{4c}, T. Sumida⁷⁰, S. Sun⁵⁸,
X. Sun^{35a}, J.E. Sundermann⁵⁰, K. Suruliz¹⁵², G. Susinno^{39a,39b}, M.R. Sutton¹⁵², S. Suzuki⁶⁸,
M. Svatos¹²⁸, M. Swiatlowski³³, I. Sykora^{147a}, T. Sykora¹³⁰, D. Ta⁵⁰, C. Taccini^{135a,135b}, K. Tackmann⁴⁴,
J. Taenzer¹⁶², A. Taffard¹⁶⁷, R. Tafirout^{164a}, N. Taiblum¹⁵⁶, H. Takai²⁷, R. Takashima⁷¹, T. Takeshita¹⁴³,
Y. Takubo⁶⁸, M. Talby⁸⁷, A.A. Talyshev^{110.c}, K.G. Tan⁹⁰, J. Tanaka¹⁵⁸, M. Tanaka¹⁶⁰, R. Tanaka¹¹⁸,
S. Tanaka⁶⁸, R. Tanioka⁶⁹, B.B. Tannenwald¹¹², S. Tapia Araya^{34b}, S. Tapprogge⁸⁵, S. Tarem¹⁵⁵,
G.F. Tartarelli^{93a}, P. Tas¹³⁰, M. Tasevsky¹²⁸, T. Tashiro⁷⁰, E. Tassi^{39a,39b}, A. Tavares Delgado^{127a,127b},
Y. Tayalati^{136e}, A.C. Taylor¹⁰⁶, G.N. Taylor⁹⁰, P.T.E. Taylor⁹⁰, W. Taylor^{164b}, F.A. Teischinger³²,
P. Teixeira-Dias⁷⁹, K.K. Temming⁵⁰, D. Temple¹⁴⁵, H. Ten Kate³², P.K. Teng¹⁵⁴, J.J. Teoh¹¹⁹,
F. Tepel¹⁷⁹, S. Terada⁶⁸, K. Terashi¹⁵⁸, J. Terron⁸⁴, S. Terzo¹³, M. Testa⁴⁹, R.J. Teuscher^{162.m},
T. Thevenaux-Pelzer⁸⁷, J.P. Thomas¹⁹, J. Thomas-Wilsker⁷⁹, E.N. Thompson³⁷, P.D. Thompson¹⁹,
A.S. Thompson⁵⁵, L.A. Thomsen¹⁸⁰, E. Thomson¹²³, M. Thomson³⁰, M.J. Tibbetts¹⁶,
R.E. Ticse Torres⁸⁷, V.O. Tikhomirov^{97.ap}, Yu.A. Tikhonov^{110.c}, S. Timoshenko⁹⁹, P. Tipton¹⁸⁰,
S. Tisserant⁸⁷, K. Todome¹⁶⁰, T. Todorov^{5.*}, S. Todorova-Nova¹³⁰, J. Tojo⁷², S. Tokár^{147a},
K. Tokushuku⁶⁸, E. Tolley⁵⁸, L. Tomlinson⁸⁶, M. Tomoto¹⁰⁴, L. Tompkins^{146.aq}, K. Toms¹⁰⁶, B. Tong⁵⁸,
P. Tornambe⁵⁰, E. Torrence¹¹⁷, H. Torres¹⁴⁵, E. Torró Pastor¹³⁹, J. Toth^{87.ar}, F. Touchard⁸⁷,
D.R. Tovey¹⁴², T. Trefzger¹⁷⁸, A. Tricoli²⁷, I.M. Trigger^{164a}, S. Trincaz-Duvoid⁸², M.F. Tripiana¹³,
W. Trischuk¹⁶², B. Trocmé⁵⁷, A. Trofymov⁴⁴, C. Troncon^{93a}, M. Trotter-McDonald¹⁶, M. Trovatelli¹⁷³,
L. Truong^{168a,168c}, M. Trzebinski⁴¹, A. Trzupek⁴¹, J.C-L. Tseng¹²¹, P.V. Tsiarehka⁹⁴, G. Tsipolitis¹⁰,
N. Tsirintanis⁹, S. Tsiskaridze¹³, V. Tsiskaridze⁵⁰, E.G. Tskhadadze^{53a}, K.M. Tsui^{62a}, I.I. Tsukerman⁹⁸,
V. Tsulaia¹⁶, S. Tsuno⁶⁸, D. Tsybychev¹⁵¹, Y. Tu^{62b}, A. Tudorache^{28b}, V. Tudorache^{28b}, A.N. Tuna⁵⁸,
S.A. Tuppiti^{22a,22b}, S. Turchikhin⁶⁷, D. Turecek¹²⁹, D. Turgeman¹⁷⁶, R. Turra^{93a,93b}, P.M. Tuts³⁷,
M. Tyndel¹³², G. Uccielli^{22a,22b}, I. Ueda¹⁵⁸, M. Ughetto^{149a,149b}, F. Ukegawa¹⁶⁵, G. Unal³²,
A. Undrus²⁷, G. Unel¹⁶⁷, F.C. Ungaro⁹⁰, Y. Unno⁶⁸, C. Unverdorben¹⁰¹, J. Urban^{147b}, P. Urquijo⁹⁰,
P. Urrejola⁸⁵, G. Usai⁸, L. Vacavant⁸⁷, V. Vacek¹²⁹, B. Vachon⁸⁹, C. Valderanis¹⁰¹,

E. Valdes Santurio^{149a,149b}, N. Valencic¹⁰⁸, S. Valentinetti^{22a,22b}, A. Valero¹⁷¹, L. Valery¹³, S. Valkar¹³⁰, J.A. Valls Ferrer¹⁷¹, W. Van Den Wollenberg¹⁰⁸, P.C. Van Der Deijl¹⁰⁸, H. van der Graaf¹⁰⁸, N. van Eldik¹⁵⁵, P. van Gemmeren⁶, J. Van Nieuwkoop¹⁴⁵, I. van Vulpen¹⁰⁸, M.C. van Woerden³², M. Vanadia^{133a,133b}, W. Vandelli³², R. Vanguri¹²³, A. Vaniachine¹⁶¹, P. Vankov¹⁰⁸, G. Vardanyan¹⁸¹, R. Vari^{133a}, E.W. Varnes⁷, T. Varol⁴², D. Varouchas⁸², A. Vartapetian⁸, K.E. Varvell¹⁵³, J.G. Vasquez¹⁸⁰, G.A. Vasquez^{34b}, F. Vazeille³⁶, T. Vazquez Schroeder⁸⁹, J. Veatch⁵⁶, V. Veeraraghavan⁷, L.M. Veloce¹⁶², F. Veloso^{127a,127c}, S. Veneziano^{133a}, A. Ventura^{75a,75b}, M. Venturi¹⁷³, N. Venturi¹⁶², A. Venturini²⁵, V. Vercesi^{122a}, M. Verducci^{133a,133b}, W. Verkerke¹⁰⁸, J.C. Vermeulen¹⁰⁸, A. Vest^{46,as}, M.C. Vetterli^{145,d}, O. Viazlo⁸³, I. Vichou^{170,*}, T. Vickey¹⁴², O.E. Vickey Boeriu¹⁴², G.H.A. Viehhauser¹²¹, S. Viel¹⁶, L. Vigani¹²¹, M. Villa^{22a,22b}, M. Villaplana Perez^{93a,93b}, E. Vilucchi⁴⁹, M.G. Vinciter³¹, V.B. Vinogradov⁶⁷, C. Vittori^{22a,22b}, I. Vivarelli¹⁵², S. Vlachos¹⁰, M. Vlasak¹²⁹, M. Vogel¹⁷⁹, P. Vokac¹²⁹, G. Volpi^{125a,125b}, M. Volpi⁹⁰, H. von der Schmitt¹⁰², E. von Toerne²³, V. Vorobel¹³⁰, K. Vorobev⁹⁹, M. Vos¹⁷¹, R. Voss³², J.H. Vosseveld⁷⁶, N. Vranjes¹⁴, M. Vranjes Milosavljevic¹⁴, V. Vrba¹²⁸, M. Vreeswijk¹⁰⁸, R. Vuillermet³², I. Vukotic³³, Z. Vykydal¹²⁹, P. Wagner²³, W. Wagner¹⁷⁹, H. Wahlberg⁷³, S. Wahrmund⁴⁶, J. Wakabayashi¹⁰⁴, J. Walder⁷⁴, R. Walker¹⁰¹, W. Walkowiak¹⁴⁴, V. Wallangen^{149a,149b}, C. Wang^{35b}, C. Wang^{140,87}, F. Wang¹⁷⁷, H. Wang¹⁶, H. Wang⁴², J. Wang⁴⁴, J. Wang¹⁵³, K. Wang⁸⁹, R. Wang⁶, S.M. Wang¹⁵⁴, T. Wang²³, T. Wang³⁷, W. Wang⁵⁹, X. Wang¹⁸⁰, C. Wanotayaraj¹¹⁷, A. Warburton⁸⁹, C.P. Ward³⁰, D.R. Wardrope⁸⁰, A. Washbrook⁴⁸, P.M. Watkins¹⁹, A.T. Watson¹⁹, M.F. Watson¹⁹, G. Watts¹³⁹, S. Watts⁸⁶, B.M. Waugh⁸⁰, S. Webb⁸⁵, M.S. Weber¹⁸, S.W. Weber¹⁷⁸, S.A. Weber³¹, J.S. Webster⁶, A.R. Weidberg¹²¹, B. Weinert⁶³, J. Weingarten⁵⁶, C. Weiser⁵⁰, H. Weits¹⁰⁸, P.S. Wells³², T. Wenaus²⁷, T. Wengler³², S. Wenig³², N. Wermes²³, M. Werner⁵⁰, M.D. Werner⁶⁶, P. Werner³², M. Wessels^{60a}, J. Wetter¹⁶⁶, K. Whalen¹¹⁷, N.L. Whallon¹³⁹, A.M. Wharton⁷⁴, A. White⁸, M.J. White¹, R. White^{34b}, D. Whiteson¹⁶⁷, F.J. Wickens¹³², W. Wiedenmann¹⁷⁷, M. Wielers¹³², C. Wiglesworth³⁸, L.A.M. Wiik-Fuchs²³, A. Wildauer¹⁰², F. Wilk⁸⁶, H.G. Wilkens³², H.H. Williams¹²³, S. Williams¹⁰⁸, C. Willis⁹², S. Willocq⁸⁸, J.A. Wilson¹⁹, I. Wingerter-Seez⁵, F. Winklmeier¹¹⁷, O.J. Winston¹⁵², B.T. Winter²³, M. Wittgen¹⁴⁶, J. Wittkowski¹⁰¹, T.M.H. Wolf¹⁰⁸, M.W. Wolter⁴¹, H. Wolters^{127a,127c}, S.D. Worm¹³², B.K. Wosiek⁴¹, J. Wotschack³², M.J. Woudstra⁸⁶, K.W. Wozniak⁴¹, M. Wu⁵⁷, M. Wu³³, S.L. Wu¹⁷⁷, X. Wu⁵¹, Y. Wu⁹¹, T.R. Wyatt⁸⁶, B.M. Wynne⁴⁸, S. Xella³⁸, D. Xu^{35a}, L. Xu²⁷, B. Yabsley¹⁵³, S. Yacooob^{148a}, D. Yamaguchi¹⁶⁰, Y. Yamaguchi¹¹⁹, A. Yamamoto⁶⁸, S. Yamamoto¹⁵⁸, T. Yamanaka¹⁵⁸, K. Yamauchi¹⁰⁴, Y. Yamazaki⁶⁹, Z. Yan²⁴, H. Yang¹⁴¹, H. Yang¹⁷⁷, Y. Yang¹⁵⁴, Z. Yang¹⁵, W-M. Yao¹⁶, Y.C. Yap⁸², Y. Yasu⁶⁸, E. Yatsenko⁵, K.H. Yau Wong²³, J. Ye⁴², S. Ye²⁷, I. Yeletsikh⁶⁷, A.L. Yen⁵⁸, E. Yildirim⁸⁵, K. Yorita¹⁷⁵, R. Yoshida⁶, K. Yoshihara¹²³, C. Young¹⁴⁶, C.J.S. Young³², S. Youssef²⁴, D.R. Yu¹⁶, J. Yu⁸, J.M. Yu⁹¹, J. Yu⁶⁶, L. Yuan⁶⁹, S.P.Y. Yuen²³, I. Yusuf^{30,at}, B. Zabinski⁴¹, R. Zaidan⁶⁵, A.M. Zaitsev^{131,ae}, N. Zakharchuk⁴⁴, J. Zalieckas¹⁵, A. Zaman¹⁵¹, S. Zambito⁵⁸, L. Zanello^{133a,133b}, D. Zanzi⁹⁰, C. Zeitnitz¹⁷⁹, M. Zeman¹²⁹, A. Zemla^{40a}, J.C. Zeng¹⁷⁰, Q. Zeng¹⁴⁶, K. Zengel²⁵, O. Zenin¹³¹, T. Ženiš^{147a}, D. Zerwas¹¹⁸, D. Zhang⁹¹, F. Zhang¹⁷⁷, G. Zhang^{59,ao}, H. Zhang^{35b}, J. Zhang⁶, L. Zhang⁵⁰, R. Zhang²³, R. Zhang^{59,au}, X. Zhang¹⁴⁰, Z. Zhang¹¹⁸, X. Zhao⁴², Y. Zhao¹⁴⁰, Z. Zhao⁵⁹, A. Zhemchugov⁶⁷, J. Zhong¹²¹, B. Zhou⁹¹, C. Zhou¹⁷⁷, L. Zhou³⁷, L. Zhou⁴², M. Zhou¹⁵¹, N. Zhou^{35c}, C.G. Zhu¹⁴⁰, H. Zhu^{35a}, J. Zhu⁹¹, Y. Zhu⁵⁹, X. Zhuang^{35a}, K. Zhukov⁹⁷, A. Zibell¹⁷⁸, D. Zieminska⁶³, N.I. Zimine⁶⁷, C. Zimmermann⁸⁵, S. Zimmermann⁵⁰, Z. Zinonos⁵⁶, M. Zinser⁸⁵, M. Ziolkowski¹⁴⁴, L. Živković¹⁴, G. Zobernig¹⁷⁷, A. Zoccoli^{22a,22b}, M. zur Nedden¹⁷, L. Zwalinski³².

¹ Department of Physics, University of Adelaide, Adelaide, Australia

² Physics Department, SUNY Albany, Albany NY, United States of America

³ Department of Physics, University of Alberta, Edmonton AB, Canada

⁴ (a) Department of Physics, Ankara University, Ankara; (b) Istanbul Aydin University, Istanbul; (c)

Division of Physics, TOBB University of Economics and Technology, Ankara, Turkey

⁵ LAPP, CNRS/IN2P3 and Université Savoie Mont Blanc, Annecy-le-Vieux, France

⁶ High Energy Physics Division, Argonne National Laboratory, Argonne IL, United States of America

⁷ Department of Physics, University of Arizona, Tucson AZ, United States of America

⁸ Department of Physics, The University of Texas at Arlington, Arlington TX, United States of America

⁹ Physics Department, University of Athens, Athens, Greece

¹⁰ Physics Department, National Technical University of Athens, Zografou, Greece

¹¹ Department of Physics, The University of Texas at Austin, Austin TX, United States of America

¹² Institute of Physics, Azerbaijan Academy of Sciences, Baku, Azerbaijan

¹³ Institut de Física d'Altes Energies (IFAE), The Barcelona Institute of Science and Technology, Barcelona, Spain

¹⁴ Institute of Physics, University of Belgrade, Belgrade, Serbia

¹⁵ Department for Physics and Technology, University of Bergen, Bergen, Norway

¹⁶ Physics Division, Lawrence Berkeley National Laboratory and University of California, Berkeley CA, United States of America

¹⁷ Department of Physics, Humboldt University, Berlin, Germany

¹⁸ Albert Einstein Center for Fundamental Physics and Laboratory for High Energy Physics, University of Bern, Bern, Switzerland

¹⁹ School of Physics and Astronomy, University of Birmingham, Birmingham, United Kingdom

²⁰ ^(a) Department of Physics, Bogazici University, Istanbul; ^(b) Department of Physics Engineering, Gaziantep University, Gaziantep; ^(d) Istanbul Bilgi University, Faculty of Engineering and Natural Sciences, Istanbul, Turkey; ^(e) Bahcesehir University, Faculty of Engineering and Natural Sciences, Istanbul, Turkey, Turkey

²¹ Centro de Investigaciones, Universidad Antonio Narino, Bogota, Colombia

²² ^(a) INFN Sezione di Bologna; ^(b) Dipartimento di Fisica e Astronomia, Università di Bologna, Bologna, Italy

²³ Physikalisches Institut, University of Bonn, Bonn, Germany

²⁴ Department of Physics, Boston University, Boston MA, United States of America

²⁵ Department of Physics, Brandeis University, Waltham MA, United States of America

²⁶ ^(a) Universidade Federal do Rio De Janeiro COPPE/EE/IF, Rio de Janeiro; ^(b) Electrical Circuits Department, Federal University of Juiz de Fora (UFJF), Juiz de Fora; ^(c) Federal University of Sao Joao del Rei (UFSJ), Sao Joao del Rei; ^(d) Instituto de Fisica, Universidade de Sao Paulo, Sao Paulo, Brazil

²⁷ Physics Department, Brookhaven National Laboratory, Upton NY, United States of America

²⁸ ^(a) Transilvania University of Brasov, Brasov, Romania; ^(b) National Institute of Physics and Nuclear Engineering, Bucharest; ^(c) National Institute for Research and Development of Isotopic and Molecular Technologies, Physics Department, Cluj Napoca; ^(d) University Politehnica Bucharest, Bucharest; ^(e) West University in Timisoara, Timisoara, Romania

²⁹ Departamento de Física, Universidad de Buenos Aires, Buenos Aires, Argentina

³⁰ Cavendish Laboratory, University of Cambridge, Cambridge, United Kingdom

³¹ Department of Physics, Carleton University, Ottawa ON, Canada

³² CERN, Geneva, Switzerland

³³ Enrico Fermi Institute, University of Chicago, Chicago IL, United States of America

³⁴ ^(a) Departamento de Física, Pontificia Universidad Católica de Chile, Santiago; ^(b) Departamento de Física, Universidad Técnica Federico Santa María, Valparaíso, Chile

³⁵ ^(a) Institute of High Energy Physics, Chinese Academy of Sciences, Beijing; ^(b) Department of Physics, Nanjing University, Jiangsu; ^(c) Physics Department, Tsinghua University, Beijing 100084, China

- ³⁶ Laboratoire de Physique Corpusculaire, Clermont Université and Université Blaise Pascal and CNRS/IN2P3, Clermont-Ferrand, France
- ³⁷ Nevis Laboratory, Columbia University, Irvington NY, United States of America
- ³⁸ Niels Bohr Institute, University of Copenhagen, Kobenhavn, Denmark
- ³⁹ ^(a) INFN Gruppo Collegato di Cosenza, Laboratori Nazionali di Frascati; ^(b) Dipartimento di Fisica, Università della Calabria, Rende, Italy
- ⁴⁰ ^(a) AGH University of Science and Technology, Faculty of Physics and Applied Computer Science, Krakow; ^(b) Marian Smoluchowski Institute of Physics, Jagiellonian University, Krakow, Poland
- ⁴¹ Institute of Nuclear Physics Polish Academy of Sciences, Krakow, Poland
- ⁴² Physics Department, Southern Methodist University, Dallas TX, United States of America
- ⁴³ Physics Department, University of Texas at Dallas, Richardson TX, United States of America
- ⁴⁴ DESY, Hamburg and Zeuthen, Germany
- ⁴⁵ Lehrstuhl für Experimentelle Physik IV, Technische Universität Dortmund, Dortmund, Germany
- ⁴⁶ Institut für Kern- und Teilchenphysik, Technische Universität Dresden, Dresden, Germany
- ⁴⁷ Department of Physics, Duke University, Durham NC, United States of America
- ⁴⁸ SUPA - School of Physics and Astronomy, University of Edinburgh, Edinburgh, United Kingdom
- ⁴⁹ INFN Laboratori Nazionali di Frascati, Frascati, Italy
- ⁵⁰ Fakultät für Mathematik und Physik, Albert-Ludwigs-Universität, Freiburg, Germany
- ⁵¹ Section de Physique, Université de Genève, Geneva, Switzerland
- ⁵² ^(a) INFN Sezione di Genova; ^(b) Dipartimento di Fisica, Università di Genova, Genova, Italy
- ⁵³ ^(a) E. Andronikashvili Institute of Physics, Iv. Javakhishvili Tbilisi State University, Tbilisi; ^(b) High Energy Physics Institute, Tbilisi State University, Tbilisi, Georgia
- ⁵⁴ II Physikalisches Institut, Justus-Liebig-Universität Giessen, Giessen, Germany
- ⁵⁵ SUPA - School of Physics and Astronomy, University of Glasgow, Glasgow, United Kingdom
- ⁵⁶ II Physikalisches Institut, Georg-August-Universität, Göttingen, Germany
- ⁵⁷ Laboratoire de Physique Subatomique et de Cosmologie, Université Grenoble-Alpes, CNRS/IN2P3, Grenoble, France
- ⁵⁸ Laboratory for Particle Physics and Cosmology, Harvard University, Cambridge MA, United States of America
- ⁵⁹ Department of Modern Physics, University of Science and Technology of China, Anhui, China
- ⁶⁰ ^(a) Kirchhoff-Institut für Physik, Ruprecht-Karls-Universität Heidelberg, Heidelberg; ^(b) Physikalisches Institut, Ruprecht-Karls-Universität Heidelberg, Heidelberg; ^(c) ZITI Institut für technische Informatik, Ruprecht-Karls-Universität Heidelberg, Mannheim, Germany
- ⁶¹ Faculty of Applied Information Science, Hiroshima Institute of Technology, Hiroshima, Japan
- ⁶² ^(a) Department of Physics, The Chinese University of Hong Kong, Shatin, N.T., Hong Kong; ^(b) Department of Physics, The University of Hong Kong, Hong Kong; ^(c) Department of Physics, The Hong Kong University of Science and Technology, Clear Water Bay, Kowloon, Hong Kong, China
- ⁶³ Department of Physics, Indiana University, Bloomington IN, United States of America
- ⁶⁴ Institut für Astro- und Teilchenphysik, Leopold-Franzens-Universität, Innsbruck, Austria
- ⁶⁵ University of Iowa, Iowa City IA, United States of America
- ⁶⁶ Department of Physics and Astronomy, Iowa State University, Ames IA, United States of America
- ⁶⁷ Joint Institute for Nuclear Research, JINR Dubna, Dubna, Russia
- ⁶⁸ KEK, High Energy Accelerator Research Organization, Tsukuba, Japan
- ⁶⁹ Graduate School of Science, Kobe University, Kobe, Japan
- ⁷⁰ Faculty of Science, Kyoto University, Kyoto, Japan
- ⁷¹ Kyoto University of Education, Kyoto, Japan
- ⁷² Department of Physics, Kyushu University, Fukuoka, Japan

- ⁷³ Instituto de Física La Plata, Universidad Nacional de La Plata and CONICET, La Plata, Argentina
- ⁷⁴ Physics Department, Lancaster University, Lancaster, United Kingdom
- ⁷⁵ ^(a) INFN Sezione di Lecce; ^(b) Dipartimento di Matematica e Fisica, Università del Salento, Lecce, Italy
- ⁷⁶ Oliver Lodge Laboratory, University of Liverpool, Liverpool, United Kingdom
- ⁷⁷ Department of Physics, Jožef Stefan Institute and University of Ljubljana, Ljubljana, Slovenia
- ⁷⁸ School of Physics and Astronomy, Queen Mary University of London, London, United Kingdom
- ⁷⁹ Department of Physics, Royal Holloway University of London, Surrey, United Kingdom
- ⁸⁰ Department of Physics and Astronomy, University College London, London, United Kingdom
- ⁸¹ Louisiana Tech University, Ruston LA, United States of America
- ⁸² Laboratoire de Physique Nucléaire et de Hautes Energies, UPMC and Université Paris-Diderot and CNRS/IN2P3, Paris, France
- ⁸³ Fysiska institutionen, Lunds universitet, Lund, Sweden
- ⁸⁴ Departamento de Física Teórica C-15, Universidad Autónoma de Madrid, Madrid, Spain
- ⁸⁵ Institut für Physik, Universität Mainz, Mainz, Germany
- ⁸⁶ School of Physics and Astronomy, University of Manchester, Manchester, United Kingdom
- ⁸⁷ CPPM, Aix-Marseille Université and CNRS/IN2P3, Marseille, France
- ⁸⁸ Department of Physics, University of Massachusetts, Amherst MA, United States of America
- ⁸⁹ Department of Physics, McGill University, Montreal QC, Canada
- ⁹⁰ School of Physics, University of Melbourne, Victoria, Australia
- ⁹¹ Department of Physics, The University of Michigan, Ann Arbor MI, United States of America
- ⁹² Department of Physics and Astronomy, Michigan State University, East Lansing MI, United States of America
- ⁹³ ^(a) INFN Sezione di Milano; ^(b) Dipartimento di Fisica, Università di Milano, Milano, Italy
- ⁹⁴ B.I. Stepanov Institute of Physics, National Academy of Sciences of Belarus, Minsk, Republic of Belarus
- ⁹⁵ National Scientific and Educational Centre for Particle and High Energy Physics, Minsk, Republic of Belarus
- ⁹⁶ Group of Particle Physics, University of Montreal, Montreal QC, Canada
- ⁹⁷ P.N. Lebedev Physical Institute of the Russian Academy of Sciences, Moscow, Russia
- ⁹⁸ Institute for Theoretical and Experimental Physics (ITEP), Moscow, Russia
- ⁹⁹ National Research Nuclear University MEPhI, Moscow, Russia
- ¹⁰⁰ D.V. Skobeltsyn Institute of Nuclear Physics, M.V. Lomonosov Moscow State University, Moscow, Russia
- ¹⁰¹ Fakultät für Physik, Ludwig-Maximilians-Universität München, München, Germany
- ¹⁰² Max-Planck-Institut für Physik (Werner-Heisenberg-Institut), München, Germany
- ¹⁰³ Nagasaki Institute of Applied Science, Nagasaki, Japan
- ¹⁰⁴ Graduate School of Science and Kobayashi-Maskawa Institute, Nagoya University, Nagoya, Japan
- ¹⁰⁵ ^(a) INFN Sezione di Napoli; ^(b) Dipartimento di Fisica, Università di Napoli, Napoli, Italy
- ¹⁰⁶ Department of Physics and Astronomy, University of New Mexico, Albuquerque NM, United States of America
- ¹⁰⁷ Institute for Mathematics, Astrophysics and Particle Physics, Radboud University Nijmegen/Nikhef, Nijmegen, Netherlands
- ¹⁰⁸ Nikhef National Institute for Subatomic Physics and University of Amsterdam, Amsterdam, Netherlands
- ¹⁰⁹ Department of Physics, Northern Illinois University, DeKalb IL, United States of America
- ¹¹⁰ Budker Institute of Nuclear Physics, SB RAS, Novosibirsk, Russia

- ¹¹¹ Department of Physics, New York University, New York NY, United States of America
- ¹¹² Ohio State University, Columbus OH, United States of America
- ¹¹³ Faculty of Science, Okayama University, Okayama, Japan
- ¹¹⁴ Homer L. Dodge Department of Physics and Astronomy, University of Oklahoma, Norman OK, United States of America
- ¹¹⁵ Department of Physics, Oklahoma State University, Stillwater OK, United States of America
- ¹¹⁶ Palacký University, RCPTM, Olomouc, Czech Republic
- ¹¹⁷ Center for High Energy Physics, University of Oregon, Eugene OR, United States of America
- ¹¹⁸ LAL, Univ. Paris-Sud, CNRS/IN2P3, Université Paris-Saclay, Orsay, France
- ¹¹⁹ Graduate School of Science, Osaka University, Osaka, Japan
- ¹²⁰ Department of Physics, University of Oslo, Oslo, Norway
- ¹²¹ Department of Physics, Oxford University, Oxford, United Kingdom
- ¹²² ^(a) INFN Sezione di Pavia; ^(b) Dipartimento di Fisica, Università di Pavia, Pavia, Italy
- ¹²³ Department of Physics, University of Pennsylvania, Philadelphia PA, United States of America
- ¹²⁴ National Research Centre "Kurchatov Institute" B.P.Konstantinov Petersburg Nuclear Physics Institute, St. Petersburg, Russia
- ¹²⁵ ^(a) INFN Sezione di Pisa; ^(b) Dipartimento di Fisica E. Fermi, Università di Pisa, Pisa, Italy
- ¹²⁶ Department of Physics and Astronomy, University of Pittsburgh, Pittsburgh PA, United States of America
- ¹²⁷ ^(a) Laboratório de Instrumentação e Física Experimental de Partículas - LIP, Lisboa; ^(b) Faculdade de Ciências, Universidade de Lisboa, Lisboa; ^(c) Department of Physics, University of Coimbra, Coimbra; ^(d) Centro de Física Nuclear da Universidade de Lisboa, Lisboa; ^(e) Departamento de Física, Universidade do Minho, Braga; ^(f) Departamento de Física Teórica y del Cosmos and CAFPE, Universidad de Granada, Granada (Spain); ^(g) Dep Física and CEFITEC of Faculdade de Ciências e Tecnologia, Universidade Nova de Lisboa, Caparica, Portugal
- ¹²⁸ Institute of Physics, Academy of Sciences of the Czech Republic, Praha, Czech Republic
- ¹²⁹ Czech Technical University in Prague, Praha, Czech Republic
- ¹³⁰ Faculty of Mathematics and Physics, Charles University in Prague, Praha, Czech Republic
- ¹³¹ State Research Center Institute for High Energy Physics (Protvino), NRC KI, Russia
- ¹³² Particle Physics Department, Rutherford Appleton Laboratory, Didcot, United Kingdom
- ¹³³ ^(a) INFN Sezione di Roma; ^(b) Dipartimento di Fisica, Sapienza Università di Roma, Roma, Italy
- ¹³⁴ ^(a) INFN Sezione di Roma Tor Vergata; ^(b) Dipartimento di Fisica, Università di Roma Tor Vergata, Roma, Italy
- ¹³⁵ ^(a) INFN Sezione di Roma Tre; ^(b) Dipartimento di Matematica e Fisica, Università Roma Tre, Roma, Italy
- ¹³⁶ ^(a) Faculté des Sciences Ain Chock, Réseau Universitaire de Physique des Hautes Energies - Université Hassan II, Casablanca; ^(b) Centre National de l'Énergie des Sciences Techniques Nucleaires, Rabat; ^(c) Faculté des Sciences Semlalia, Université Cadi Ayyad, LPHEA-Marrakech; ^(d) Faculté des Sciences, Université Mohamed Premier and LPTPM, Oujda; ^(e) Faculté des sciences, Université Mohammed V, Rabat, Morocco
- ¹³⁷ DSM/IRFU (Institut de Recherches sur les Lois Fondamentales de l'Univers), CEA Saclay (Commissariat à l'Énergie Atomique et aux Énergies Alternatives), Gif-sur-Yvette, France
- ¹³⁸ Santa Cruz Institute for Particle Physics, University of California Santa Cruz, Santa Cruz CA, United States of America
- ¹³⁹ Department of Physics, University of Washington, Seattle WA, United States of America
- ¹⁴⁰ School of Physics, Shandong University, Shandong, China
- ¹⁴¹ Department of Physics and Astronomy, Shanghai Key Laboratory for Particle Physics and

Cosmology, Shanghai Jiao Tong University, Shanghai; (also affiliated with PKU-CHEP), China

¹⁴² Department of Physics and Astronomy, University of Sheffield, Sheffield, United Kingdom

¹⁴³ Department of Physics, Shinshu University, Nagano, Japan

¹⁴⁴ Fachbereich Physik, Universität Siegen, Siegen, Germany

¹⁴⁵ Department of Physics, Simon Fraser University, Burnaby BC, Canada

¹⁴⁶ SLAC National Accelerator Laboratory, Stanford CA, United States of America

¹⁴⁷ ^(a) Faculty of Mathematics, Physics & Informatics, Comenius University, Bratislava; ^(b) Department of Subnuclear Physics, Institute of Experimental Physics of the Slovak Academy of Sciences, Kosice, Slovak Republic

¹⁴⁸ ^(a) Department of Physics, University of Cape Town, Cape Town; ^(b) Department of Physics, University of Johannesburg, Johannesburg; ^(c) School of Physics, University of the Witwatersrand, Johannesburg, South Africa

¹⁴⁹ ^(a) Department of Physics, Stockholm University; ^(b) The Oskar Klein Centre, Stockholm, Sweden

¹⁵⁰ Physics Department, Royal Institute of Technology, Stockholm, Sweden

¹⁵¹ Departments of Physics & Astronomy and Chemistry, Stony Brook University, Stony Brook NY, United States of America

¹⁵² Department of Physics and Astronomy, University of Sussex, Brighton, United Kingdom

¹⁵³ School of Physics, University of Sydney, Sydney, Australia

¹⁵⁴ Institute of Physics, Academia Sinica, Taipei, Taiwan

¹⁵⁵ Department of Physics, Technion: Israel Institute of Technology, Haifa, Israel

¹⁵⁶ Raymond and Beverly Sackler School of Physics and Astronomy, Tel Aviv University, Tel Aviv, Israel

¹⁵⁷ Department of Physics, Aristotle University of Thessaloniki, Thessaloniki, Greece

¹⁵⁸ International Center for Elementary Particle Physics and Department of Physics, The University of Tokyo, Tokyo, Japan

¹⁵⁹ Graduate School of Science and Technology, Tokyo Metropolitan University, Tokyo, Japan

¹⁶⁰ Department of Physics, Tokyo Institute of Technology, Tokyo, Japan

¹⁶¹ Tomsk State University, Tomsk, Russia, Russia

¹⁶² Department of Physics, University of Toronto, Toronto ON, Canada

¹⁶³ ^(a) INFN-TIFPA; ^(b) University of Trento, Trento, Italy, Italy

¹⁶⁴ ^(a) TRIUMF, Vancouver BC; ^(b) Department of Physics and Astronomy, York University, Toronto ON, Canada

¹⁶⁵ Faculty of Pure and Applied Sciences, and Center for Integrated Research in Fundamental Science and Engineering, University of Tsukuba, Tsukuba, Japan

¹⁶⁶ Department of Physics and Astronomy, Tufts University, Medford MA, United States of America

¹⁶⁷ Department of Physics and Astronomy, University of California Irvine, Irvine CA, United States of America

¹⁶⁸ ^(a) INFN Gruppo Collegato di Udine, Sezione di Trieste, Udine; ^(b) ICTP, Trieste; ^(c) Dipartimento di Chimica, Fisica e Ambiente, Università di Udine, Udine, Italy

¹⁶⁹ Department of Physics and Astronomy, University of Uppsala, Uppsala, Sweden

¹⁷⁰ Department of Physics, University of Illinois, Urbana IL, United States of America

¹⁷¹ Instituto de Física Corpuscular (IFIC) and Departamento de Física Atómica, Molecular y Nuclear and Departamento de Ingeniería Electrónica and Instituto de Microelectrónica de Barcelona (IMB-CNM), University of Valencia and CSIC, Valencia, Spain

¹⁷² Department of Physics, University of British Columbia, Vancouver BC, Canada

¹⁷³ Department of Physics and Astronomy, University of Victoria, Victoria BC, Canada

¹⁷⁴ Department of Physics, University of Warwick, Coventry, United Kingdom

- ¹⁷⁵ Waseda University, Tokyo, Japan
- ¹⁷⁶ Department of Particle Physics, The Weizmann Institute of Science, Rehovot, Israel
- ¹⁷⁷ Department of Physics, University of Wisconsin, Madison WI, United States of America
- ¹⁷⁸ Fakultät für Physik und Astronomie, Julius-Maximilians-Universität, Würzburg, Germany
- ¹⁷⁹ Fakultät für Mathematik und Naturwissenschaften, Fachgruppe Physik, Bergische Universität Wuppertal, Wuppertal, Germany
- ¹⁸⁰ Department of Physics, Yale University, New Haven CT, United States of America
- ¹⁸¹ Yerevan Physics Institute, Yerevan, Armenia
- ¹⁸² Centre de Calcul de l'Institut National de Physique Nucléaire et de Physique des Particules (IN2P3), Villeurbanne, France
- ^a Also at Department of Physics, King's College London, London, United Kingdom
- ^b Also at Institute of Physics, Azerbaijan Academy of Sciences, Baku, Azerbaijan
- ^c Also at Novosibirsk State University, Novosibirsk, Russia
- ^d Also at TRIUMF, Vancouver BC, Canada
- ^e Also at Department of Physics & Astronomy, University of Louisville, Louisville, KY, United States of America
- ^f Also at Physics Department, An-Najah National University, Nablus, Palestine
- ^g Also at Department of Physics, California State University, Fresno CA, United States of America
- ^h Also at Department of Physics, University of Fribourg, Fribourg, Switzerland
- ⁱ Also at Departament de Física de la Universitat Autònoma de Barcelona, Barcelona, Spain
- ^j Also at Departamento de Física e Astronomia, Faculdade de Ciências, Universidade do Porto, Portugal
- ^k Also at Tomsk State University, Tomsk, Russia, Russia
- ^l Also at Università di Napoli Parthenope, Napoli, Italy
- ^m Also at Institute of Particle Physics (IPP), Canada
- ⁿ Also at National Institute of Physics and Nuclear Engineering, Bucharest, Romania
- ^o Also at Department of Physics, St. Petersburg State Polytechnical University, St. Petersburg, Russia
- ^p Also at Department of Physics, The University of Michigan, Ann Arbor MI, United States of America
- ^q Also at Centre for High Performance Computing, CSIR Campus, Rosebank, Cape Town, South Africa
- ^r Also at Louisiana Tech University, Ruston LA, United States of America
- ^s Also at Institutio Catalana de Recerca i Estudis Avancats, ICREA, Barcelona, Spain
- ^t Also at Graduate School of Science, Osaka University, Osaka, Japan
- ^u Also at Department of Physics, National Tsing Hua University, Taiwan
- ^v Also at Institute for Mathematics, Astrophysics and Particle Physics, Radboud University Nijmegen/Nikhef, Nijmegen, Netherlands
- ^w Also at Department of Physics, The University of Texas at Austin, Austin TX, United States of America
- ^x Also at CERN, Geneva, Switzerland
- ^y Also at Georgian Technical University (GTU), Tbilisi, Georgia
- ^z Also at O Chadai Academic Production, Ochanomizu University, Tokyo, Japan
- ^{aa} Also at Manhattan College, New York NY, United States of America
- ^{ab} Also at Academia Sinica Grid Computing, Institute of Physics, Academia Sinica, Taipei, Taiwan
- ^{ac} Also at School of Physics, Shandong University, Shandong, China
- ^{ad} Also at Department of Physics, California State University, Sacramento CA, United States of America
- ^{ae} Also at Moscow Institute of Physics and Technology State University, Dolgoprudny, Russia
- ^{af} Also at Section de Physique, Université de Genève, Geneva, Switzerland
- ^{ag} Also at Eotvos Lorand University, Budapest, Hungary
- ^{ah} Also at Departments of Physics & Astronomy and Chemistry, Stony Brook University, Stony Brook

NY, United States of America

^{ai} Also at International School for Advanced Studies (SISSA), Trieste, Italy

^{aj} Also at Department of Physics and Astronomy, University of South Carolina, Columbia SC, United States of America

^{ak} Also at Institut de Física d'Altes Energies (IFAE), The Barcelona Institute of Science and Technology, Barcelona, Spain

^{al} Also at School of Physics and Engineering, Sun Yat-sen University, Guangzhou, China

^{am} Also at Institute for Nuclear Research and Nuclear Energy (INRNE) of the Bulgarian Academy of Sciences, Sofia, Bulgaria

^{an} Also at Faculty of Physics, M.V.Lomonosov Moscow State University, Moscow, Russia

^{ao} Also at Institute of Physics, Academia Sinica, Taipei, Taiwan

^{ap} Also at National Research Nuclear University MEPhI, Moscow, Russia

^{aq} Also at Department of Physics, Stanford University, Stanford CA, United States of America

^{ar} Also at Institute for Particle and Nuclear Physics, Wigner Research Centre for Physics, Budapest, Hungary

^{as} Also at Flensburg University of Applied Sciences, Flensburg, Germany

^{at} Also at University of Malaya, Department of Physics, Kuala Lumpur, Malaysia

^{au} Also at CPPM, Aix-Marseille Université and CNRS/IN2P3, Marseille, France

* Deceased